

Copyright

by

Güner Arslan

2000

**Equalization for  
Discrete Multitone Transceivers**

by

**Güner Arslan, B.S., M.S.**

**Dissertation**

Presented to the Faculty of the Graduate School of

The University of Texas at Austin

in Partial Fulfillment

of the Requirements

for the Degree of

**Doctor of Philosophy**

**The University of Texas at Austin**

December 2000

# Equalization for Discrete Multitone Transceivers

Approved by  
Dissertation Committee:

---

Brian L. Evans, supervisor

---

Ross Baldick

---

Alan C. Bovik

---

Joydeep Ghosh

---

Sayfe Kiaei

---

Edward J. Powers

to my wife and my parents with love

# Acknowledgments

I have a long list of people to thank for their sincere support and help. I would like to start with my parents Selime and Cemal Arslan. They are beautiful parents who supported me through my school years spanning over three countries on three continents. I would like to thank my wife Süeda for her love, support, and understanding. She took care after me during graduate school although I was spending most of my time with my computer instead of her. I also would like to thank my sister Gülay for her patience in dealing with government bureaucracy every month for the past three years to send me my scholarship money.

I would like to thank Dr. Brian L. Evans, my advisor, for his support and guidance in technical, financial, and everyday issues. He helped and supported me in getting in, getting through, and getting out of UT Austin. Without his support, I would not be preparing this dissertation at UT Austin. His success and emphasis on clearly expressing complicated ideas helped me a lot in writing papers and preparing presentations. He has my deepest respect professionally and personally.

I also would like to thank Dr. F. Ayhan Sakarya, my M.S. thesis advisor in Turkey, for her encouragement and support to continue my graduate

education in the US. She guided me through my graduate education in Turkey and taught me the meaning of research.

I would like to thank Dr. Sayfe Kiaei for introducing me to the research topic of this dissertation. He pointed me to key papers defining the problem and answered all of my questions during the reading period of this research. I also would like to thank my dissertation committee– Dr. Baldick, Dr. Bovik, Dr. Evans, Dr. Ghosh, Dr. Kiaei, Dr. Powers– for their useful and constructive feedback.

I would like to thank Biao Lu for her friendship and help especially in university related paperwork issues. She did a terrific job as the manager of the Embedded Signal Processing Laboratory and was like a second advisor. I would like to thank James Monaco for sharing the system administration work load with me. I also would like to thank Jeffrey Wu for the successful project we worked on together which ended up as a section in this dissertation. I would like to thank Niranjan Damera-Venkata, Wade Schwartzkopf, and Magesh Valliappan in Prof. Evans’ group (Embedded Signal Processing Laboratory) for their friendship and our technical discussions. Wade was very helpful and patient in improving and correcting my English and in understanding American culture. I would also like to thank all of the other members of ESPL and Laboratory for Vision Systems (LVS) with whom I worked over the three years I spend at UT – Gregory E. Allen, Serene Banerjee, David M. Brunke, Young H. Cho, Amey A. Deosthali, Ming Ding, Srikanth Gummadi, Zhengting He, Thomas D. Kite, Sanghoon Lee, Shizhong Liu, Tanmoy Mandal, Milos Milosevic, Marios S. Pattichis, Umesh Rajashekar, Hamid R. Sheikh, K. Clint Slatton, Zhou Wang, and Dong Wei for the nice environment they created in ESPL and LVS.

Finally, I would like to thank the Turkish community in Austin for making me feel at home. I am thankful to Murat Torlak and Caner Özdemir who picked me up from the airport the first time I landed in Austin. I am thankful to Süleyman Bahçeci for sheltering me (a stranger for him) in my first few days in Austin. I am thankful to Yetkin Yıldırım for his time we spent searching for an apartment. I am thankful to Aydoğan Ülker and Adnan Kavak for their sincere friendship.

GÜNER ARSLAN

*The University of Texas at Austin*

*December 2000*

# Equalization for Discrete Multitone Transceivers

Publication No. \_\_\_\_\_

Güner Arslan, Ph.D.

The University of Texas at Austin, 2000

Supervisor: Brian L. Evans

G.DMT and G.lite Asymmetric Digital Subscriber Line (ADSL) modems and some Very-high-speed Digital Subscriber Line (VDSL) modems rely on discrete multitone modulation (DMT). In an ADSL discrete multitone receiver, a time-domain equalizer (TEQ) reduces intersymbol interference (ISI) by shortening the effective duration of the channel impulse response. Previous TEQ design methods such as minimum mean-squared error (MMSE), maximum shortening signal-to-noise ratio (MSSNR), and maximum geometric signal-to-noise ratio (MGSNR) do not directly optimize channel capacity.

In this dissertation, I develop a TEQ design method to optimize channel capacity at the output of the TEQ. First, I partition an equalized multicarrier channel into its equivalent signal, noise, and ISI paths to develop a new subchannel signal-to-noise (SNR) definition. Using the new subchannel SNR definition, I derive a nonlinear function of TEQ taps that measures



channel capacity. Based on the nonlinear function, I propose the optimal maximum-channel-capacity (MCC) TEQ that achieves 99.87% of the matched filter bound on ADSL channel capacity with a 17-tap equalizer. I also derive a computationally-efficient, near-optimal minimum-ISI (min-ISI) method that generalizes the MSSNR method by weighting the ISI in the frequency domain. The frequency domain weighting increases computational complexity for higher bit rate. Based on simulations using eight different carrier-serving-area ADSL channels, (1) the proposed methods yield higher bit rates than the MMSE, MSSNR, and MGSNR methods; (2) two-tap TEQs designed with the proposed methods yield higher bit rates than 17-tap MMSE and geometric TEQs; and (3) the min-ISI method achieves 99.99% of the bit rate of the optimal MCC method.

Most state-of-the-art ADSL transceivers use MMSE-based algorithms to design TEQs of 17-32 taps. The min-ISI TEQ gives better performance with a smaller TEQ. For example, a two-tap min-ISI TEQ requires 4 DSP MIPS and outperforms a 20-tap MMSE TEQ which requires 40 DSP MIPS. This reduction in complexity would eliminate the need for hardware acceleration for the TEQ in an ADSL transceiver.

# Contents

<b>Acknowledgments</b>	<b>v</b>
<b>Abstract</b>	<b>viii</b>
<b>List of Tables</b>	<b>xiv</b>
<b>List of Figures</b>	<b>xv</b>
<b>Chapter 1 Introduction</b>	<b>1</b>
1.1 High-speed Wireline Transceivers . . . . .	3
1.1.1 Voiceband transceivers . . . . .	6
1.1.2 Integrated services digital network (ISDN) transceivers	7
1.1.3 Digital subscriber line transceivers . . . . .	9
1.1.4 Cable transceivers . . . . .	11
1.2 Discrete Multitone Modulation . . . . .	12
1.2.1 DMT Transmitter . . . . .	14
1.2.2 DMT Receiver . . . . .	16
1.3 Equalization for Discrete Multitone Modulation . . . . .	17
1.4 Nomenclature . . . . .	18
1.5 Thesis statement and organization of the dissertation . . . . .	21

<b>Chapter 2 Previous Methods for Time Domain Equalizer Design</b>	<b>23</b>
2.1 Introduction . . . . .	24
2.2 Minimum Mean Squared Error (MMSE) Design . . . . .	24
2.3 Maximum Shortening SNR Design . . . . .	32
2.3.1 Divide-and-Conquer TEQ Minimization Design . . . . .	36
2.3.2 Divide-and-Conquer TEQ Cancellation Design . . . . .	37
2.4 Maximum Geometric SNR Design . . . . .	38
2.4.1 Multicarrier Channel Capacity . . . . .	38
2.4.2 The maximum geometric SNR method . . . . .	40
2.5 Conclusion . . . . .	44
<b>Chapter 3 A Model for Subchannel SNR</b>	<b>46</b>
3.1 Introduction . . . . .	46
3.2 Example: Equivalent Impulse Responses for the Signal, ISI, and Noise Paths . . . . .	48
3.3 Generalization of the Equivalent Path Impulse Responses . . . . .	55
3.4 New Definition of Subchannel SNR . . . . .	57
3.5 Conclusion . . . . .	59
<b>Chapter 4 Time Domain Equalizer Design For Maximum Channel Capacity</b>	<b>62</b>
4.1 Introduction . . . . .	63
4.2 The Optimal Maximum Channel Capacity (MCC) Equalizer . . . . .	64
4.3 Optimal Number of Taps in a MCC TEQ . . . . .	67
4.4 Optimal Cyclic Prefix Size for the MCC TEQ . . . . .	72
4.5 Conclusion . . . . .	74

<b>Chapter 5</b>	<b>The Near-Optimal Minimum-ISI Equalizer</b>	<b>76</b>
5.1	Introduction . . . . .	77
5.2	Minimizing ISI . . . . .	78
5.3	The Minimum-ISI Design Method . . . . .	80
5.4	Optimal Number of Taps in a Min-ISI TEQ . . . . .	83
5.5	Optimal Cyclic Prefix Size for the Min-ISI TEQ . . . . .	84
5.6	Fast Min-ISI TEQ Design Methods . . . . .	85
5.6.1	Recursive Min-ISI Method . . . . .	86
5.7	Conclusion . . . . .	90
<b>Chapter 6</b>	<b>Performance Evaluation</b>	<b>93</b>
6.1	Introduction . . . . .	94
6.2	Digital Subscriber Line Characteristics . . . . .	94
6.3	Channel Noise . . . . .	96
6.4	Number of equalizer taps and length of cyclic prefix . . . . .	98
6.5	Achievable bit rates for the CSA loops . . . . .	100
6.6	MATLAB DMTTEQ Toolbox . . . . .	103
6.7	Conclusion . . . . .	107
<b>Chapter 7</b>	<b>Conclusion</b>	<b>113</b>
7.1	Summary . . . . .	113
7.2	Future research . . . . .	120
<b>Appendix A</b>	<b>MATLAB DMTTEQ Toolbox</b>	<b>128</b>
A.1	TEQ Design Functions . . . . .	128
A.2	Performance Evaluation Functions . . . . .	133
A.3	Utility Functions . . . . .	134

<b>Bibliography</b>	<b>139</b>
<b>Vita</b>	<b>153</b>

# List of Tables

1.1	Residential consumer applications . . . . .	2
1.2	Business consumer applications . . . . .	3
1.3	High-speed data communication standards . . . . .	4
2.1	Advantages/disadvantages of TEQ design methods . . . . .	45
4.1	Two-tap MCC TEQ . . . . .	69
5.1	The recursive min-ISI TEQ design algorithm. . . . .	91
6.1	Achievable bit rates for the eight CSA loops . . . . .	100
6.2	Achievable bit rates for the eight CSA loops . . . . .	101
7.1	Advantages/disadvantages of TEQ design methods . . . . .	119
A.1	Global variable names used in the DMTTEQ Toolbox . . . . .	129

# List of Figures

1.1	Typical dial-up connection via a voiceband modem . . . . .	5
1.2	Typical ISDN connection . . . . .	8
1.3	ADSL connection with G.DMT and G.lite . . . . .	10
1.4	Block diagram of a multicarrier modulation system . . . . .	15
2.1	The MMSE time domain equalizer . . . . .	25
2.2	A target and shortened impulse response . . . . .	29
3.1	Example of transmitted symbols . . . . .	48
3.2	Equalized channel impulse response . . . . .	49
3.3	Motivating example . . . . .	49
3.4	Example of transmitted samples . . . . .	50
3.5	Example of a received signal samples . . . . .	51
3.6	Example of the desired signal . . . . .	52
3.7	Example of the signal path impulse response . . . . .	53
3.8	Example of the ISI path impulse response . . . . .	54
3.9	Example of the ISI part . . . . .	55
3.10	Impulse responses . . . . .	57
3.11	Signal, noise, and ISI paths . . . . .	61

4.1	Achievable bit rate vs. number of equalizer taps for MCC TEQ	68
4.2	Pole-zero plot of a CSA loop . . . . .	70
4.3	Impulse response of CSA loop . . . . .	71
4.4	Pole-zero plot of a two-tap MCC TEQ . . . . .	72
4.5	Pole-zero plot of the equalized channel impulse response . . .	73
4.6	Achievable bit rate vs. cyclic prefix length for MCC TEQ . . .	74
4.7	Achievable bit rate vs. cyclic prefix length for MCC TEQ . . .	75
5.1	Achievable bit rate vs. number of equalizer taps for min-ISI TEQ	83
5.2	Achievable bit rate vs. cyclic prefix length for min-ISI TEQ .	84
5.3	Achievable bit rate vs. cyclic prefix length for min-ISI TEQ .	85
6.1	Achievable bit rate vs. the number of equalizer taps . . . . .	109
6.2	achievable bit rate vs. the cyclic prefix length . . . . .	110
6.3	Achievable bit rate vs. cyclic prefix length . . . . .	111
6.4	MATLAB DMTTEQ toolbox window . . . . .	112



# Chapter 1

## Introduction

The advancement in multimedia applications and the development of the Internet have created a demand for high-speed digital communications. Sophisticated audio and video coding methods have reduced the bit rate requirements for audio and video transmission. This in turn motivated the development of communication systems to achieve these requirements. Both technologies enabled high-quality audio and video transmission and introduced a number of new applications for businesses and residential consumers.

Key applications other than voice communications include Internet access, streaming audio, and broadcast video. Table 1.1 and 1.2 list several residential and business applications and their data rate requirements. Downstream (from the service provider to the consumer) and upstream (from the consumer to the service provider) requirements are listed in separate columns because some applications have asymmetric requirements. For example, video broadcasting is an asymmetric application requiring a fast downstream link but no upstream link. Table 1.1 shows that the residential consumer application requirements can be satisfied with a data rate of 3 Mb/s with the exception

Application	downstream data rate (kb/s)	upstream data rate (kb/s)
Voice telephony	16 – 64	16 – 64
Internet access	14 – 3,000	14 – 384
Electronic Mail	9 – 128	9 – 64
High definition TV	12,000 – 24,000	0
Broadcast video	1,500 – 6,000	0
Music on demand	384 – 3,000	9
Videophone	128 – 1,500	128 – 1,500
Distance Learning	384 – 3,000	128 – 3,000
Database Access	14 – 384	9
Software download	384 – 3,000	9
Shop at home	128 – 1,500	9 – 64
Video games	64 – 1,500	64 – 1,500

Table 1.1: Some residential consumer applications and their upstream and downstream data rate requirements [1].

of video and TV applications. Most business applications also require a data rate of 3 Mb/s; however, applications such as supercomputing could require a symmetric data rate of up to 45 Mb/s.

The remainder of this chapter is organized as follows. Section 1.1 describes standards for high-speed wireline transceivers, including digital subscriber lines (DSL) and cable modems. Section 1.2 gives a brief introduction to DMT modulation and Section 1.3 gives a brief introduction to the equalization problems in DMT modulation. Section 1.4 lists the acronyms and abbreviations used in the dissertation. Section 1.5 gives the thesis statement and the organization of this dissertation.

Application	downstream data rate (kb/s)	upstream data rate (kb/s)
Voice telephony	16 – 64	16 – 64
Facsimile	9 – 128	9 – 128
Internet	14 – 3,000	14 – 384
Intranet	64 – 3,000	64 – 1,500
Electronic commerce	28 – 384	28 – 384
Home office	128 – 6,000	64 – 1,500
LAN interconnection	384 – 10,000	384 – 10,000
Electronic Mail	9 – 128	9 – 64
Videophone	128 – 1,500	128 – 1,500
Database Access	14 – 384	9
Software download	384 – 3,000	9
Supercomputing	6,000 – 45,000	6,000 – 45,000
Collaborative design	128 – 1,500	128 – 1,500

Table 1.2: Some business consumer applications and their upstream and downstream data rate requirements [1].

## 1.1 High-speed Wireline Transceivers

Many solutions have been developed for high-speed communications, as shown in Table 1.3. Voiceband modems could be considered to be the first solution. Due to the bandwidth constraint of traditional telephone voice lines, the data rate of voiceband modems cannot achieve the requirements of most of the applications listed in Tables 1.1 and 1.2. Integrated Service Digital Network (ISDN) provides higher bitrates than voiceband modems. Initially, T1/E1 lines offered the only business solution for having higher bitrates than ISDN. However, the installation and maintenance of T1/E1 lines are very high, which motivated service providers to search for cheaper alternatives. DSL technol-

Standard	Data Rates (kb/s)	Description
V.32 (voiceband modem)	9.6	full-duplex using PSK
V.34 (voiceband modem)	33.6	channel precoding
V.90 (voiceband modem)	56 down 33.6 up	pulse code modulation
ISDN (Integrated service digital network)	144	two 64 kb/s and one 16 kb/s channel
HDSL (High-bit-rate DSL)	1,544 / 2,048	two wire pairs, reach of 12,000 feet
HDSL2 (High-bit-rate DSL)	1,544 / 2,048	one wire pair, reach of 12,000 feet
ADSL (Asymmetric DSL)	1,500 – 8,000 down 16 – 640 up	one wire pair, reach of 18,000 feet requires splitters
RADSL (Rate-adaptive ADSL)	1,500 – 8,000 down 16 – 640 up	adaptive rates, one wire pair, requires splitters
G.lite (splitterless ADSL)	up to 1,500 down up to 512 up	no splitter
VDSL (Very high rate DSL)	13,000 – 52,000 down 1,500 – 6,000 up	one wire pair, reach of 4,500 feet
DOCSIS (Data over cable)	27,000 or 36,000 down 320 – 10,240 up	cable TV infrastructure
IEEE 802.14 (Cable Modem)	27,000 or 36,000 down 320 – 20,480 up	cable TV infrastructure

Table 1.3: High-speed data communication standards.

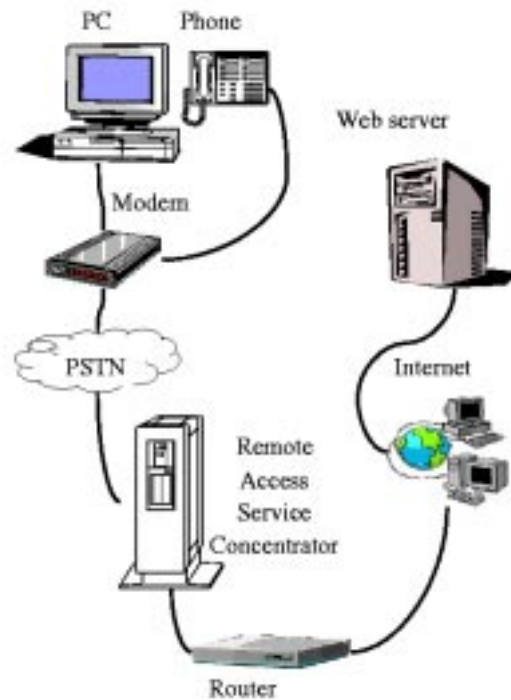


Figure 1.1: Typical dial-up connection via a voiceband modem

ogy offered cheaper alternatives to T1/E1 lines. The first DSL technology was High-bit-rate DSL (HDSL) which was targeted for businesses. The first DSL technology aimed for residential consumers was Asymmetric DSL (ADSL). Initially planned for video-on-demand applications, ADSL evolved into a key Internet access technology. The emerging Very-high-rate DSL (VDSL) standard is intended to be a bridge between fiber and copper communication technology.

### 1.1.1 Voiceband transceivers

Voiceband modems were introduced in the 1950s to transmit data through telephone channels. A typical dial-up connection via a voiceband modem is shown in Fig. 1.1. In Fig. 1.1, a Personal Computer (PC) is connected via the Public Switched Telephone Network (PSTN) to a Remote Access Service (RAS) concentrator which consists of several modems. One of the available modems in the RAS concentrator answers the call from the dial-up modem and directs the call to a router which routes traffic to the desired destination (generally a Web server) over the Internet.

A telephone channel passes only frequencies from about 200 Hz to 3400 Hz. This bandwidth is enough to transmit intelligible voice. A voiceband modem converts the data to be transmitted into a signal which has similar characteristics as a voice signal. Once the data is modulated to fit into the frequency range of the phone channel, it appears as a voice signal to the channel.

One of the first commercial modems featured a speed of 300 b/s and used frequency shift keying (FSK) modulation. It was introduced by AT&T under the name Bell 103. CCITT (now ITU) standardized V.21 modems for the same data rate. Bell 202 was the first modem to achieve 1,200 b/s using half duplex FSK modulation. Vadic Inc. introduced the VA3400 modem in 1973 which was the first modem using phase shift keying (PSK) and featured full duplex 1,200 b/s transmission [1].

V22.bis doubled the bit rate to 2,400 b/s in 1981. The V.32 was the first modem to use trellis coding and featured echo cancellation, which enabled transmission of data in both directions at the same time in the same

frequency bands. V.32 modems achieved a bit rate of 9,600 b/s. Constellation shaping, bandwidth optimization, and channel-dependent coding enabled the V.34 modem to achieve 28.8 kb/s which increased to 33.6 kb/s in 1995.

It was believed that 33.6 kb/s was the highest data rate that could possibly be achieved on a telephone voice channel until 56 kb/s modems were introduced in 1996. The V.90 standard for these modems did not appear until 1998. The V.90 modems, which are also called Pulse Code Modulation (PCM) modems, are asymmetric. They support a downstream bit rate of 56.6 kb/s and an upstream bit rate of 33.6 kb/s. In practice, PCM modems rarely achieve 56.6 kb/s and are generally limited to 50 kb/s [1].

### **1.1.2 Integrated services digital network (ISDN) transceivers**

ISDN was introduced by CCITT in 1976. The first ISDN service in North America was not available until 1986. Initially, ISDN systems were based on time compression multiplexing (TCM) or alternate mark inversion (AMI). However, 2B1Q (2 binary, 1 quaternary) and 4B3T (4 binary, 3 ternary) transmission offered greater loop reach and therefore were adopted in the standard.

Basic rate ISDN supports a bit rate of 160 kb/s symmetric transmission on loops up to 18,000 feet. This rate is divided into two 64 kb/s B channels, one 16 kb/s D channel, and one 16 kb/s framing and control channel; hence, the transmission data rate is 144 kb/s. Basic rate ISDN uses one of the four available signal levels to represent two bits, hence 2B1Q. It supports full duplex communication using echo cancellation. The bandwidth used is about 80 kHz. Provided that the loops are unloaded, basic rate ISDN modems can handle

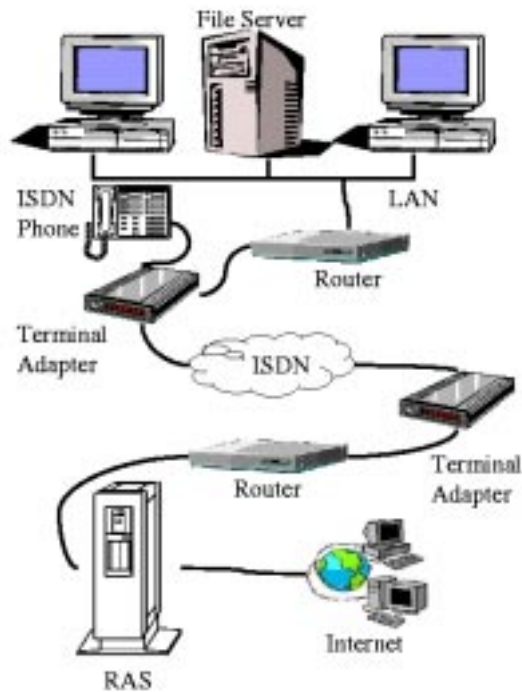


Figure 1.2: Typical ISDN connection

bridge taps by using an adaptive equalizer.

Three methods are used to increase the range of ISDN over 18,000 feet – basic rate ISDN transmission extension (BRITE), mid-span repeater, and extended-range basic rate ISDN. BRITE uses time division multiplexed channels and digital loop carriers to extend the reach of basic rate ISDN. A mid-span repeater can extend the loop reach by a factor of two. Extended range ISDN uses more advanced digital communication methods to extend the range of basic rate ISDN; e.g., trellis coding enables transmission of 160 kb/s for up to 28,000 feet without a repeater.



### 1.1.3 Digital subscriber line transceivers

In the 1960s, T1/E1 lines became an efficient way to interconnect two central telephone offices. Voice became digital at a rate of 64 kb/s. In North America, 24 voice channels each consisting of 8 bits were grouped to form frames of 193 bits including the framing bit. One T1 line carried these frames at a rate of 8 kHz resulting in a bit rate of 1.544 Mb/s. In Europe, 30 voice channels were grouped in addition with two framing and signaling channels which results in 32 64 kb/s channels to be transmitted over one E1 line. Hence, the bit rate of an E1 line is 2.048 Mb/s.

In the 1980s, T1/E1 lines became available to businesses for voice and data transmission. T1/E1 lines required repeaters every 3,000 to 5,000 feet, and all bridged taps had to be removed for proper use of these lines. Therefore, a T1/E1 line was expensive to install (on the order of \$10,000) and the installation as well as maintenance was time consuming. This motivated the search for transmission techniques that would be easy to install, would not need repeaters every 5,000 feet, and could support bridge taps. This search led to the development of the first member of the DSL family: HDSL.

HDSL is based on ISDN. HDSL uses 2B1Q transmission which supported repeaterless transmission up to 12,000 feet. HDSL splits T1 transmission rate of 1.544 Mb/s into two 784 kb/s signals which require a signal rate of 392 kHz with 2B1Q transmission. In Europe, the E1 transmission rate of 2.048 Mb/s rate was initially split into two three-wire pairs which later was reduced to two pairs each transmitting 1.168 Mb/s.

The acceptance of HDSL led to the exploration of whether or not a T1/E1 line could be replaced by only one wire pair instead of two wire pairs as

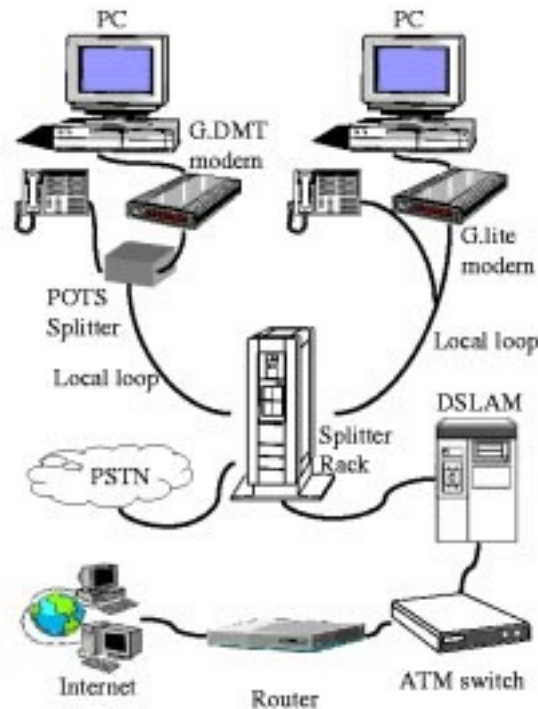


Figure 1.3: ADSL connection with G.DMT and G.lite

in the HDSL standard. This is achieved with the second generation of HDSL or HDSL 2. HDSL 2 uses sophisticated coding and modulation techniques to achieve the required bit rate and reach on a single wire pair.

DSL technology is not limited to businesses and communication between central offices. Consumer applications such as video-on-demand required high throughput in the downstream and smaller throughput in the upstream. ADSL was originally proposed for video-on-demand applications to transmit MPEG-1 video streams. Before the standardization, the bit rate requirements changed due to the development of MPEG-2.

Internet browsing is another example of asymmetric communication.

Unlike video-on-demand applications, Internet browsing does not have a fixed bit rate requirement that needs to be supported. Rate-adaptive ADSL automatically determines the highest rate it can provide over a given loop. Rate-adaptive ADSL (RADSL) supports downstream rates up to 7 – 10 Mb/s and upstream rates up to 512 – 900 kb/s. To separate the data band from the Plain Old Telephone System (POTS) band, a splitter has to be installed at the consumer side. This expensive process motivated a low rate ADSL standard which does not require a splitter to be installed. Splitterless ADSL or G.lite targets a data rate of 1.5 Mb/s downstream primarily for Internet applications.

ADSL was the first DSL standard to adopt multicarrier modulation. The emerging Very High Bit Rate DSL (VDSL) standards will likely support two line codes – multicarrier modulation and carrierless amplitude/phase (CAP) modulation. Multicarrier modulated VDSL will likely be an extension of ADSL. The goal for VDSL is to achieve up to 52 Mb/s downstream for distances up to 1,000 feet and 13 Mb/s downstream for distances up to 3,750 feet. VDSL is proposed as a way to connect a consumer to a fiber optical communication network in the consumer’s neighborhood.

#### **1.1.4 Cable transceivers**

In the 1990s, the demand for high-speed communication motivated cable companies to search for ways to use their cable infrastructure for high-speed communications. Initially, cable TV systems could not support two-way communication. One ad-hoc solution uses POTS voice band modems for the upstream and the cable channel for the downstream. In 1994, the IEEE formed the 802.14 Cable TV Media Access Control and Physical Protocol Working Group

to form a standard [2]. Their standard was not released until 1997.

Because of the delay of the IEEE standard, several vendors formed their own group to decide on a standard for cable modems. They released the Data Over Cable System Interface Specification (DOCSIS) in early 1996. Both the DOCSIS and IEEE standards are similar in the physical layer but have differences in the media access control layer. The IEEE standard is based on Asynchronous Transfer Mode (ATM) whereas the DOCSIS standard supports variable length packets for the delivery of Internet Protocol (IP) traffic. Although better in some aspects, the IEEE ATM approach has a higher implementation cost than DOCSIS. Therefore, nearly all of the major cable modem vendors use the DOCSIS standard [1].

According to the DOCSIS standard, the downstream channel uses 64 or 256 Quadrature Amplitude Modulation (QAM) on a carrier of 6 MHz. The data rate is either 27 or 36 Mb/s. The upstream modulation method is Quadrature Phase Shift Keying (QPSK) and 16 QAM on a variable carrier between 200 kHz and 3.2 MHz. Data rate is between 320 kb/s and 10 Mb/s [3]. This data rate is shared by all cable users on the same local area cable network.

## 1.2 Discrete Multitone Modulation

High-speed communication standards mentioned in the previous section require broadband channels. Inter-symbol interference (ISI) is a major problem associated with broadband channels. This undesirable effect is caused by the spectral shaping of the channel. In other words, variation of magnitude and phase responses of the channel over frequency causes neighboring symbols to

interfere with each other at the receiver. Two approaches to combat ISI are full channel equalization and multicarrier modulation (MCM).

Full channel equalization undoes the spectral shaping effect of a channel using a filter which is called an equalizer. Although linear equalizers are easy to implement, they enhance noise and thus degrade the performance of the system. Therefore, more complicated nonlinear equalizers, such as the decision feedback equalizer, have been proposed. One of the drawbacks of nonlinear equalizers is their computational complexity, especially under high sampling rates.

Multicarrier modulation is one possible solution for high-speed digital communications. In contrast to single carrier modulation, multicarrier modulation,

- avoids full equalization of a channel,
- uses available bandwidth efficiently by controlling the power and number of bits in each subchannel,
- is robust against impulsive noise and fast fading due to its long symbol duration, and
- avoids narrowband distortion by simply disabling one or more subchannels.

Multicarrier modulation has been standardized for G.DMT and G.lite ADSL [4] as well as digital audio/video broadcasting [5, 6].

In multicarrier modulation, the channel is partitioned into a large number of small bandwidth channels called subchannels. If a subchannel were narrow enough so that the channel gain in the subchannel is approximately a

complex constant, then no ISI would occur in this subchannel. Thus, information can be transmitted over these narrowband subchannels without ISI, and the total number of bits transmitted is the sum of the number of bits transmitted in each subchannel. If the available power were distributed over the subchannels using the SNR of each subchannel, then high spectral efficiency could be achieved. This principle dates back to Shannon's 1948 paper [7] and has been applied in practical systems as early as the late 1950s [8].

Efficiently dividing the channel into hundreds of subchannels became tractable only in the 1990s with the cost vs. performance provided by programmable digital signal processors and the advancement in digital signal processing methods [8]. One of the most efficient ways to partition a channel into large number of narrowband channels is the fast Fourier transform (FFT) [8]. Multicarrier modulation implemented via a FFT is called Discrete Multitone (DMT) modulation or Orthogonal Frequency Division Multiplexing (OFDM). DMT is more common in wireline applications, whereas OFDM is more common for wireless applications. In transmission, the key difference between the two methods is in the assignment of bits to each subchannel.

### **1.2.1 DMT Transmitter**

A block diagram of a DMT (or OFDM) transceiver is shown in Fig. 1.4. In the transmitter,  $M$  bits of the input bit stream are buffered. These bits are then assigned to each of the  $N/2$  subchannels using a bit loading algorithm [8]. In DMT systems, bit loading algorithms assign the bits and available power to each subchannel according to the SNR in each subchannel, such that high SNR subchannels receive more bits than low SNR subchannels. Extremely

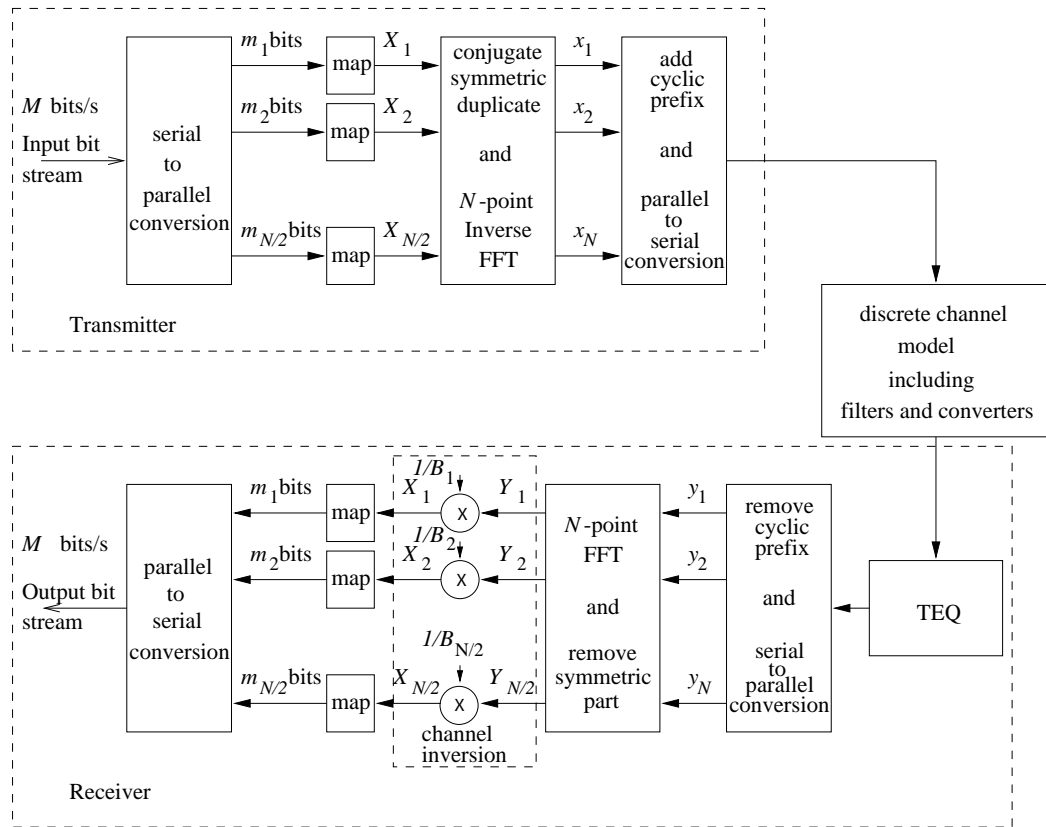


Figure 1.4: Block diagram of a multicarrier modulation system. The transmit filter, D/A converter, channel, A/D converter, and receive filter are combined into one block.

low SNR subchannels are not used. In OFDM systems, the number of bits in each channel is equal and constant. Thus, there is no need for a bit loading algorithm.

The second step is the mapping of the assigned bits to subsymbols using a modulation method, such as QAM in ADSL modems. These subsymbols are complex-valued in general and can be thought of being in the frequency domain. The efficiency of DMT and OFDM lies in the modulation of the subcarriers. Instead of having  $N/2$  independent modulators, the modulators

are implemented with an  $N$ -point inverse FFT (IFFT). In order to obtain real samples after IFFT, the  $N/2$  subsymbols are duplicated with their conjugate symmetric counterparts. The obtained time domain samples are called a DMT symbol.

A guard period between DMT symbols is used to prevent ISI. It is implemented by prepending a symbol with its last  $v$  samples, which is called a cyclic prefix. Thus, one block consists of  $N + v$  samples instead of  $N$  samples, which reduces the channel throughput by a factor of  $\frac{N + v}{N}$ . ISI is completely eliminated for channels with impulse responses of length less than or equal to  $v + 1$ . The prefix is selected as the last  $v$  samples of the symbol in order to convert the linear convolution effect of the channel into circular convolution and help the receiver perform symbol synchronization. Circular convolution can be implemented in the DFT domain by using the FFT. After the FFT in the receiver, the subsymbols are the product of the  $N$ -point FFT of the channel impulse response and the  $N$ -point FFT of the transmitted subsymbols.

### 1.2.2 DMT Receiver

The receiver is basically the dual of the transmitter with the exception of the addition of time-domain and frequency domain equalizers. The time-domain equalizer ensures that the equalized channel impulse response is shortened to be less than the length of the cyclic prefix. If the TEQ is successful, then the received complex subsymbols after the FFT are the multiplication of the transmitted subsymbols with the FFT of the shortened (equalized) channel impulse response. The frequency domain equalizer (also called a one-tap equalizer) divides the received subsymbols by the FFT coefficients of the shortened channel



impulse response. After mapping the subsymbols back to the corresponding bits using the QAM constellation, they are converted to serial bits.

### 1.3 Equalization for Discrete Multitone Modulation

With DMT, the problem of fully equalizing a channel is converted into partitioning the channel into small subchannels which is more efficient to implement in high-speed transmission. However, this does not imply that equalization is not required in an DMT system. The spectra of each inverse FFT (IFFT) modulated subchannel is a sampled sinc function which is not bandlimited. Demodulation is still possible due to the orthogonality between the sinc functions. An ISI causing channel, however, destroys orthogonality between subchannels so that they cannot be separated at the receiver.

One way to prevent ISI is to use a guard period between two successive DMT symbols (one DMT symbol consists of  $N$  samples where  $N/2 + 1$  is the number of subchannels). This guard period has to be at least as long as the channel impulse response. Since no new information is transmitted in this guard period, the channel throughput reduces proportionally to the length of it. If the channel impulse response is relatively long compared to the symbol length, then this performance loss can be prohibitive.

One way to reduce ISI with a shorter cyclic prefix is to use an equalizer. Since the length of a DMT symbol is longer than a symbol in single carrier modulation, equalization is simpler. Also, noise enhancement by the equalizer is not an issue because the equalizer does not affect the SNR in each

subchannel, which are the primary parameters to determine the performance of a DMT system.

The ADSL standard uses a guard period, time-domain equalization, and frequency-domain equalization. The Time-Domain Equalizer (TEQ) shortens the channel to a length of a predetermined but short guard period. The TEQ can be implemented as an FIR filter whose filter coefficients are trained during initialization. Although this combination has been standardized and is implemented in practical systems, on-going research seeks to improve the performance of DMT transceivers. TEQ design is one of the topics promising improvement for DMT transceivers and is the topic of this dissertation.

The major challenge in designing a TEQ is to combine channel capacity optimization into the design procedure. Optimizing channel capacity requires solving a nonlinear optimization problem, which raises serious questions about the computational complexity for a real-time solution. A successful TEQ design method must, therefore, not only optimize channel capacity but also must do this with acceptable implementation complexity. The goal of this research is to find such a design method.

## 1.4 Nomenclature

ADSL	: Asymmetric Digital Subscriber Lines
AMI	: Alternate Mark Inversion
ATM	: Asynchronous Transfer Mode
AWGN	: Additive White Gaussian Noise
BRITE	: Basic Rate ISDN Transmission Extension
CAP	: Carrierless Amplitude/Phase

CCITT	: Comite Consultatif Internationale de Telegraphie et Telephonie
CP	: Cyclic Prefix
CSA	: Carrier Serving Area
DC	: Divide And Conquer
DFT	: Discrete Fourier Transform
DMT	: Discrete Multitone Modulation
DOCSIS	: Data Over Cable Service Interface Specifications
DSL	: Digital Subscriber Line
FEXT	: Far-End Crosstalk
FFT	: Fast Fourier Transform
FIR	: Finite Impulse Response
FSK	: Frequency Shift Keying
GSNR	: Geometric Signal-to-Noise Ratio
GUI	: Graphical User Interface
HDSL	: High-bit-rate Digital Subscriber Line
ICI	: Interchannel Interference
IEEE	: Institute of Electrical and Electronics Engineers
IFFT	: Inverse Fast Fourier Transform
IP	: Internet Protocol
ISDN	: Integrated Service Digital Network
ISI	: Intersymbol Interference
ITU	: International Telecommunication Union
LAN	: Local Area Network
LMS	: Least Mean Squared
LU	: Lower Upper
MAC	: Multiply and Accumulate

MCC	: Maximum Channel Capacity
MFB	: Matched Filter Bound
MGSNR	: Maximum Geometric Signal-to-Noise Ratio
min-ISI	: Minimum Intersymbol Interference
MIPS	: Million Instructions per Second
ML	: Maximum Likelihood
MMSE	: Minimum Mean Squared Error
MPEG	: Moving Picture Experts Group
MSE	: Mean Squared Error
MSSNR	: Maximum Shortening Signal-to-noise Ratio
NEXT	: Near-End Crosstalk
OFDM	: Orthogonal Frequency Division Multiplexing
PCM	: Pulse Code Modulation
POTS	: Plain Old Telephone System
PSK	: Phase Shift Keying
PSTN	: Public Switched Telephone Network
QAM	: Quadrature Amplitude Modulation
QPSK	: Quadrature Phase Shift Keying
RADSL	: Rate-adaptive Asymmetric Digital Subscriber Line
RAS	: Remote Access Service
SIR	: Shortened Impulse Response
SNR	: Signal-to-noise Ratio
SSNR	: Shortening Signal-to-noise Ratio
TCM	: Time Compression Multiplexing
TEQ	: Time-Domain Equalizer
TIR	: Target Impulse Response

UEC	: Unit-Energy Constraint
UTC	: Unit-Tap Constraint
VDSL	: Very-high-speed Digital Subscriber Lines

## 1.5 Thesis statement and organization of the dissertation

In this dissertation, I defend the following thesis statement:

DMT TEQ design that minimizes frequency weighted ISI power to push ISI into low SNR frequency bands gives equivalent performance to optimal DMT TEQ design that maximizes channel capacity.

Showing this statement to be true would enable the design of optimal TEQs without directly optimizing channel capacity. Channel capacity optimization generally involves nonlinear programming which is not suitable for real-time implementation due to its computational complexity.

This dissertation is organized as follows. Chapter 2 summarizes previous work on TEQ design. It describes MMSE TEQ design which is currently the most commonly used approach in commercial ADSL modems. The MSSNR design method is followed by a suboptimal but computationally efficient alternative to the MSSNR design method called the divide-and-conquer design method. The MGSNR method follows with the multicarrier channel capacity definition.

Chapter 3 proposes a new subchannel SNR definition. I first motivate the definition by an example and then generalize the example to define equivalent signal, noise, and ISI paths in DMT transceivers. These equivalent paths allow me to write SNR in a subchannel as a function of signal, noise, and ISI power.

Chapter 4 proposes the optimal maximum channel capacity (MCC) TEQ design method. I derive an objective function for channel capacity that is a nonlinear function of TEQ taps based on the SNR definition in Chapter 3. This objective function defines the nonlinear optimization problem for optimizing TEQ design in terms of maximizing channel capacity. The MCC TEQ can be calculated by a unconstrained nonlinear optimization method.

Chapter 5 proposes the near-optimal minimum-ISI (min-ISI) TEQ design method. It is based on the thesis that minimizing the total ISI power maximizes channel capacity. I show that this method generalizes the MSSNR method by adding a frequency domain weighting of the ISI power. Fast iterative and recursive algorithms are presented to reduce the computation complexity of the min-ISI method.

Chapter 6 details the simulation environment and its parameters used in the comparative performance analysis of all of the TEQ design methods. Simulation results show that the min-ISI method gives equivalent performance to the optimal MCC method as claimed in the thesis statement.

Chapter 7 summarizes this dissertation and points out possible areas for further research. Appendix A presents details of the MATLAB DMTTEQ toolbox for TEQ design which we developed during the course of this research.

## Chapter 2

# Previous Methods for Time Domain Equalizer Design

Communication subsystems should ideally be designed to enable the overall system to achieve data rates that are as close as possible to the channel capacity. In the design of time domain equalizers, optimizing objective functions such as the mean squared error (MSE) or shortening signal-to-noise ratio (SSNR) might increase channel capacity. However, as explained in this chapter, it is possible that a TEQ with worse MSE or SSNR can give better channel capacity than a system with better MSE or SSNR. Among the many TEQ design methods available, however, only one method – maximum geometric SNR (MGSNR) – attempts to maximize channel capacity directly. The MGSNR method has limited success due to inappropriate assumptions and inaccurate approximations.

## 2.1 Introduction

Time domain equalizer design methods can be categorized into three major approaches: minimizing Mean Squared Error (MSE), maximizing Shortening SNR (SSNR), and maximizing channel capacity. The Minimum MSE (MMSE) approach is the first application of channel shortening to multicarrier systems [9]. Adaptive MMSE design methods [10, 11] are commonly used in practical systems. Maximizing SSNR is equivalent to minimize the energy of the component of the channel impulse response that cause ISI [12, 13, 14]. Melsa, Younce and Rohrs introduced this approach and the optimal solution. Neither the MMSE nor the Maximum SSNR (MSSNR) methods attempt to maximize channel capacity directly. Al-Dhahir and Cioffi [15, 16] propose the Maximum Geometric SNR (MGSNR) method to shorten the channel impulse response while maximizing an approximation to the channel capacity.

This chapter summarizes research in the three major approaches to time domain equalizer design. Section 2.2 summarizes MMSE design methods. Section 2.3 derives the MSSNR TEQ design methods and presents two suboptimal divide-and-conquer TEQ design methods. Section 2.4 defines channel capacity for DMT systems and summarizes the MGSNR design method. Section 2.5 concludes this chapter.

## 2.2 Minimum Mean Squared Error (MMSE) Design

Falconer and Magee [17] introduce the MMSE design method to shorten a channel impulse response for maximum likelihood (ML) receivers. Their goal



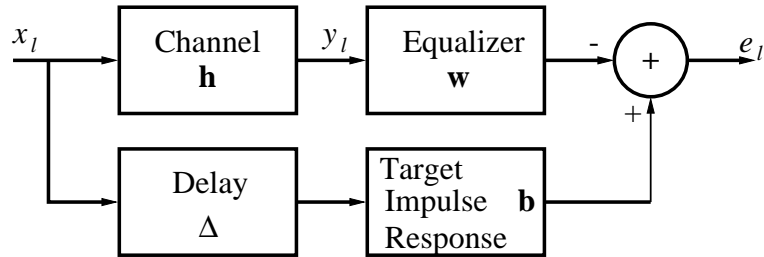


Figure 2.1: Block diagram of the minimum mean-squared error (MMSE) equalizer. The equalizer is an FIR filter with impulse response  $\mathbf{w}$ . The bottom path does not physically exist, but is part of the design method.

is to design a prefilter to the Viterbi algorithm, which is one of the most popular solutions for maximum likelihood data sequence estimation. The prefilter shortens the channel impulse response, which dramatically reduces the computational complexity of the Viterbi algorithm. The Viterbi algorithm requires a number of computations that is exponential in the length of the channel impulse response [18].

Chow and Cioffi [9] are the first to apply channel shortening equalization to multicarrier modulation. They use the MMSE design method to shorten a given channel to the length of the cyclic prefix. Compared to Falconer and Magee’s approach, they use a training sequence instead of decision directed equalization, and apply a unit-tap constraint (UTC) instead of a unit-energy constraint (UEC) to prevent an all-zero trivial solution for the equalizer taps during minimization.

The idea behind the MMSE TEQ design method may be explained by Fig. 2.1. The structure consists of an FIR equalizer in cascade with the channel and a parallel branch that consists of a delay and an FIR filter with a target impulse response (TIR). The goal in the MMSE design of the vector of TEQ taps  $\mathbf{w}$  is to minimize the mean square of the error between the output of the

equalizer and the output of the TIR. Assume that the error is zero for any given input signal. That means the impulse response of both branches are equal. In other words, the equalized channel impulse response (upper branch) would be equal to a delayed version of the TIR. Setting the number of taps of the TIR to a desired length forces the equalizer channel impulse response to have the same length.

Al-Dhahir and Cioffi [19] generalize the idea of [9] and [17]. They show that a unit-energy constraint on the target impulse response gives a lower mean squared error than a unit-tap constraint on the target impulse response. I use their derivations to introduce the MMSE design method below.

Assuming an oversampling factor of  $S$  at the receiver, the  $L$ -tap FIR channel output over a block of  $N_w$  symbols (each consisting of  $S$  samples) can be written as

$$\begin{bmatrix} y_{k+N_w-1} \\ y_{k+N_w-2} \\ \vdots \\ y_k \end{bmatrix} = \begin{bmatrix} h_0 & \cdots & h_L & 0 & \cdots & 0 \\ 0 & h_0 & \cdots & h_L & 0 & \cdots \\ \vdots & \ddots & \ddots & & \ddots & \vdots \\ 0 & \cdots & 0 & h_0 & \cdots & h_L \end{bmatrix} \begin{bmatrix} x_{k+N_w-1} \\ x_{k+N_w-2} \\ \vdots \\ x_{k-L} \end{bmatrix} + \begin{bmatrix} n_{k+N_w-1} \\ n_{k+N_w-2} \\ \vdots \\ n_{k-L} \end{bmatrix} \quad (2.1)$$

where

$$\mathbf{y}_k = \begin{bmatrix} y_{k0} \\ \vdots \\ y_{kS} \end{bmatrix}, \mathbf{x}_k = \begin{bmatrix} x_{k0} \\ \vdots \\ x_{kS} \end{bmatrix}, \mathbf{n}_k = \begin{bmatrix} n_{k0} \\ \vdots \\ n_{kS} \end{bmatrix} \quad (2.2)$$

Writing (2.1) in a more compact form,

$$\mathbf{y}_k = \mathbf{H}\mathbf{x}_k + \mathbf{n}_k \quad (2.3)$$

Again the objective is to minimize the MSE which is given as

$$\text{MSE} = \mathcal{E}\{e_k^2\} = \mathbf{b}^T \mathbf{R}_{\mathbf{xx}} \mathbf{b} - \mathbf{b}^T \mathbf{R}_{\mathbf{xy}} \mathbf{w} - \mathbf{w}^T \mathbf{R}_{\mathbf{yx}} \mathbf{b} + \mathbf{w}^T \mathbf{R}_{\mathbf{xx}} \mathbf{w} \quad (2.4)$$

where  $\mathbf{R}_{xx} = \mathcal{E}\{\mathbf{x}_k \mathbf{x}_k^T\}$ ,  $\mathbf{R}_{xy} = \mathcal{E}\{\mathbf{x}_k \mathbf{y}_k^T\}$ ,  $\mathbf{R}_{yx} = \mathcal{E}\{\mathbf{y}_k \mathbf{x}_k^T\}$ ,  $\mathbf{R}_{yy} = \mathcal{E}\{\mathbf{y}_k \mathbf{y}_k^T\}$ .

Taking the gradient with respect to  $\mathbf{w}$  and setting it to zero yields

$$\mathbf{b}^T \mathbf{R}_{xy} = \mathbf{w}^T \mathbf{R}_{yy} \quad (2.5)$$

By substituting (2.5) into (2.4),

$$\text{MSE} = \mathbf{b}^T \left[ \mathbf{R}_{xx} - \mathbf{R}_{xy} \mathbf{R}_{yy}^{-1} \mathbf{R}_{yx} \right] \mathbf{b} = \mathbf{b}^T \mathbf{R}_{x|y} \mathbf{b} \quad (2.6)$$

Define

$$\mathbf{S} = \left[ \mathbf{0}_{(\nu+1) \times \Delta} \quad \mathbf{I}_{(\nu+1) \times (\nu+1)} \quad \mathbf{0}_{(\nu+1) \times (N_w + L - \Delta - \nu - 1)} \right]^T \quad (2.7)$$

where  $\mathbf{0}_{m \times n}$  is a  $m \times n$  matrix of zeros,  $\mathbf{I}_{n \times n}$  is an  $n \times n$  identity matrix, and  $\nu + 1$  is the number of elements in  $\mathbf{b}$ . By defining

$$\mathbf{R}_{\Delta} = \mathbf{S}^T \mathbf{R}_{x|y} \mathbf{S} \quad (2.8)$$

the MSE can be written as

$$\text{MSE} = \mathbf{b}^T \mathbf{R}_{\Delta} \mathbf{b} \quad (2.9)$$

To obtain the unit-tap constraint solution, Al-Dhahir and Cioffi [19] define  $\mathbf{e}_i$  as the  $i^{\text{th}}$  unit vector and form the Lagrangian

$$L^{UTC}(\mathbf{b}, \lambda) = \mathbf{b}^T \mathbf{R}_{\Delta} \mathbf{b} + \lambda(\mathbf{b}^T \mathbf{e}_i - 1) \quad (2.10)$$

Taking the gradient with respect to  $\mathbf{b}$  and setting it to zero

$$\frac{\partial L^{UTC}}{\partial \mathbf{b}} = 2\mathbf{R}_{\Delta} \mathbf{b} + \lambda \mathbf{e}_i = 0 \quad (2.11)$$

which has the solution

$$\mathbf{b} = \frac{\mathbf{R}_{\Delta}^{-1} \mathbf{e}_i}{\mathbf{R}_{\Delta}^{-1}(i, i)} \quad (2.12)$$

where  $i \in [0, \nu]$  and  $\mathbf{R}_\Delta^{-1}(i, i)$  is the  $i^{\text{th}}$  element in the diagonal of the matrix  $\mathbf{R}_\Delta^{-1}$ . The solution for  $\mathbf{b}$  given by (2.12) yields an MSE of

$$\text{MSE} = \frac{1}{\mathbf{R}_\Delta^{-1}(i, i)} \quad (2.13)$$

The value of  $i$  that minimizes the MSE can be found from

$$i_{opt} = \arg \max_{0 \leq i \leq \nu} \{\mathbf{R}_\Delta^{-1}(i, i)\} \quad (2.14)$$

and the optimal  $\mathbf{b}$  is given as

$$\mathbf{b}_{opt} = \frac{\mathbf{R}_\Delta^{-1} \mathbf{e}_{i_{opt}}}{\mathbf{R}_\Delta^{-1}(i_{opt}, i_{opt})} \quad (2.15)$$

and  $\mathbf{w}_{opt}$  can be obtained from (2.5) by using  $\mathbf{b} = \mathbf{b}_{opt}$ .

If the unit-energy constraint on  $\mathbf{b}$  were used instead of the unit-tap constraint, then the Lagrangian would become

$$L^{UEC} = \mathbf{b}^T \mathbf{R}_\Delta \mathbf{b} + \lambda(\mathbf{b}^T \mathbf{b} - 1) \quad (2.16)$$

After setting the gradient of (2.16) with respect to  $\mathbf{b}$  to zero,

$$\mathbf{R}_\Delta \mathbf{b} = \lambda \mathbf{b} \quad (2.17)$$

which shows that  $\mathbf{b}$  is an eigenvector of  $\mathbf{R}_\Delta$ . Since  $\text{MSE} = \mathbf{b}^T \mathbf{R}_\Delta \mathbf{b} = \mathbf{b}^T \lambda \mathbf{b} = \lambda$ ,  $\mathbf{b}$  should be chosen as the eigenvector corresponding to the minimum eigenvalue of  $\mathbf{R}_\Delta$  to minimize the MSE. Thus,

$$\mathbf{b}_{opt} = \text{eigenvector of } \mathbf{R}_\Delta \text{ corresponding to the minimum eigenvalue} \quad (2.18)$$

Fig. 2.2 shows a TIR and SIR. The MMSE design method formulates the square of the difference between the TIR and SIR as the error and minimizes it. The method minimizes the difference between the TIR and SIR both inside

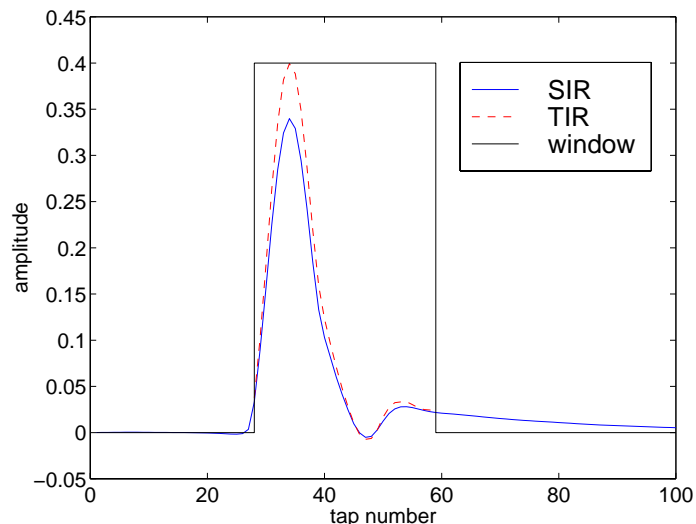


Figure 2.2: A target impulse response (TIR) and shortened impulse response (SIR).

and outside the target window. In fact, the difference between the TIR and SIR inside the target window does not cause ISI. Both the TIR and SIR inside the target window have higher amplitudes, which means that difference inside the target window might contribute more to the MSE than the difference outside.

The MMSE design method maximizes the SNR at the TEQ output. The equalizer frequency response, therefore, tends to be a narrow bandpass filter placed at a center frequency, which has high SNR. The equalizer increases the output SNR by filtering out the low SNR regions of the channel frequency response. Webster and Roberts [20] mention this problem and suggest to exclude the channel noise from the design procedure. This would ensure that only the ISI is minimized instead of the combination of noise and ISI. However, they do not give an algorithm to accomplish this task.

Since the MMSE method in general cannot force the error to become exactly zero, some residual ISI will remain. To maximize channel capacity, the residual ISI should be placed in frequency bands with high channel noise. This ensures that the residual ISI would be small compared to the noise and the effect on the SNR would be negligible. The MMSE design method does not have a mechanism to shape the residual ISI in frequency. Therefore, it is not optimal in the sense of maximizing channel capacity.

Wang and Adalı [21, 22, 23, 24] propose to weight the error in the frequency domain. They use the weighting function to prevent the optimization of unused subchannels by setting the weight to zero. They do not propose a way to calculate weights so that the residual ISI is shaped to increase channel capacity. Wang, Lu, and Antoniou [25] propose a new constraint for the MMSE design method. Instead of constraining the total energy of the TIR, they constrain the energy of the TIR only in the used subchannels to unity. Their method still minimizes an MSE measure which is not directly related to channel capacity.

Kerckhove and Spruyt [26] add the gain of the TIR in the unused frequency bands to the error term. By minimizing the error, the TIR energy in unused bands is also minimized. Acker, Leus, Moonen, Wiel, and Pollet [27, 28] map the TEQ to the frequency domain equalizer. They remove the TEQ from the system and instead add more taps to the frequency domain equalizer. Having an equalizer for each tone makes it possible to optimize the ISI location in frequency.

The unit-energy constrained MMSE solution requires an eigenvalue decomposition and the unit-tap constrained solution has an additional search direction for the optimal index. Decreasing the computational complexity of

MMSE design methods is an active area of research. Falconer and Magee [17] along with the original MMSE design method propose an adaptive algorithm to calculate the TIR and TEQ. The algorithm is based on the least mean squared (LMS) algorithm. The TIR and the TEQ are separately adapted with standard LMS with an addition to satisfy the unit-energy constraint. After every iteration, the TIR is normalized so that its energy is equal to one.

Chow, Cioffi, and Bingham [10, 11] propose a different iterative method to calculate the MMSE TIR and TEQ. They propose two methods to update the TIR and TEQ: frequency domain LMS and frequency domain division. To ensure that the updated TIR and TEQ have the desired lengths, they transform the TIR back to time domain and window it. The combination of these methods generates four different MMSE design algorithms. Slow convergence is a major problem with all four methods.

Strait [29] combines the two separate LMS algorithms into a single LMS by forming a new vector with the TEQ and TIR coefficients. Slow convergence is again a major problem. To solve this problem, Strait transforms the input signal by using a unitary transform. He shows that transform domain adaptation converges faster but requires higher computational complexity per iteration.

Nafie and Gatherer [30] compute the minimum eigenvalue by using the iterative power method [31]. They also propose to use the LU decomposition and run a pair of iterations that are more stable and faster to implement. In the same paper, they also propose an off-line LMS algorithm. Assuming that they have an estimate of the channel impulse response, they use the estimate as the input vector to the TEQ. The TIR is the desired response and the error is the difference between the TIR and the output of the equalizer.

Lashkarian and Kiaei [32] propose an iterative algorithm to solve the MMSE design problem. It is based on the asymptotic equivalence of Toeplitz and circulant matrices to estimate the Hessian of a quadratic form. The proposed algorithm is computationally less complex than the iterative power method and may be parallelized for efficient implementation in hardware.

Another drawback of the MMSE design method is the deep notches in the frequency response of the designed TEQ. The subchannels in which a notch appears cannot be used for data transmission because the gain in the subchannel is too small. Farhang-Boroujeny and Ding [33, 34] propose an eigen-approach based sub-optimum solution to overcome this problem. Instead of using only the eigenvector of the minimum eigenvalue as derived in (2.18), they use a weighted sum of all eigenvectors as the TEQ. This solution gives higher MSE but equal bit rate to the original MMSE method.

## 2.3 Maximum Shortening SNR Design

Seeing the TEQ design problem as a channel shortening problem rather than an equalization problem, Melsa, Younce, and Rohrs [12] propose a different solution. The goal is to find a TEQ that minimizes the energy of the SIR outside the target window, while keeping the energy inside constant. They have a reasonable assumption that the channel impulse response is known. In DMT applications such as ADSL, the channel FFT coefficients are estimated for bit loading [8]. The channel impulse response can be estimated from the FFT coefficients.

The samples of the SIR inside the target window can be written in



matrix form as

$$\mathbf{h}_{win} = \begin{bmatrix} h_{\Delta+1} & h_{\Delta} & \cdots & h_{\Delta-N_w+2} \\ h_{\Delta+2} & h_{\Delta+1} & \cdots & h_{\Delta-N_w+3} \\ \vdots & & \ddots & \vdots \\ h_{\Delta+\nu+1} & h_{\Delta+\nu} & \cdots & h_{\Delta-N_w+\nu+2} \end{bmatrix} \begin{bmatrix} w_0 \\ w_1 \\ \vdots \\ w_{N_w-1} \end{bmatrix} = \mathbf{H}_{win} \mathbf{w}$$

and the samples outside the target window as

$$\mathbf{h}_{wall} = \begin{bmatrix} h_0 & 0 & \cdots & 0 \\ h_1 & h_0 & \cdots & 0 \\ \vdots & \vdots & & \vdots \\ h_{\Delta} & h_{\Delta-1} & \cdots & h_{\Delta-N_w+1} \\ h_{\Delta+\nu+2} & h_{\Delta+\nu+1} & \cdots & h_{\Delta-N_w+\nu+3} \\ \vdots & \vdots & & \vdots \\ h_{L-1} & h_{L-2} & \cdots & h_{L-N_w+1} \\ 0 & h_{L-1} & \cdots & h_{L-N_w+2} \\ \vdots & \vdots & & \vdots \\ 0 & 0 & \cdots & h_{L-1} \end{bmatrix} \begin{bmatrix} w_0 \\ w_1 \\ \vdots \\ w_{N_w-1} \end{bmatrix} = \mathbf{H}_{wall} \mathbf{w}$$

The energy inside and outside the target window is

$$\begin{aligned} \mathbf{h}_{win}^T \mathbf{h}_{win} &= \mathbf{w}^T \mathbf{H}_{win}^T \mathbf{H}_{win} \mathbf{w} = \mathbf{w}^T \mathbf{B} \mathbf{w} \\ \mathbf{h}_{wall}^T \mathbf{h}_{wall} &= \mathbf{w}^T \mathbf{H}_{wall}^T \mathbf{H}_{wall} \mathbf{w} = \mathbf{w}^T \mathbf{A} \mathbf{w} \end{aligned} \quad (2.19)$$

The problem is formulated as

$$\min_{\mathbf{w}} \mathbf{w}^T \mathbf{A} \mathbf{w} \quad \text{s.t.} \quad \mathbf{w}^T \mathbf{B} \mathbf{w} = 1 \quad (2.20)$$

This is equivalent to maximizing the SSNR defined as

$$\text{SSNR} = \frac{\mathbf{w}^T \mathbf{B} \mathbf{w}}{\mathbf{w}^T \mathbf{A} \mathbf{w}} \quad (2.21)$$

The solution is

$$\mathbf{w}_{opt} = (\sqrt{\mathbf{B}})^{-1} \mathbf{p}_{min} \quad (2.22)$$

where  $\sqrt{\mathbf{B}}$  is the Cholesky decomposition of  $\mathbf{B}$  and  $\mathbf{p}_{min}$  is the eigenvector corresponding to the minimum eigenvalue of a composite matrix

$$(\sqrt{\mathbf{B}})^{-1} \mathbf{A} (\sqrt{\mathbf{B}^T})^{-1}$$

The matrix  $\mathbf{B}$  has to be positive definite in order to have a Cholesky decomposition. It is also assumed that  $\mathbf{B}$  is invertible which is true only if  $N_w < \nu$ . The solution when  $\mathbf{B}$  is singular is more complicated [12]. Yin and Yue [35] maximize  $\mathbf{w}^T \mathbf{A} \mathbf{w}$  while constraining  $\mathbf{w}^T \mathbf{B} \mathbf{w} = 1$ . In this case,  $\mathbf{A}$  needs to be positive definite and invertible, which is true for most physical channels.

The MSSNR method minimizes the part of the SIR that causes ISI. If the energy outside the target window were zero, then the channel would be perfectly shortened and ISI would be totally eliminated. The solution which gives zero energy outside the target window is optimum also in the sense of maximum channel capacity since this is the case where ISI is totally canceled. In practice, however, this optimum solution cannot be achieved. For this case, the MSSNR solution is not guaranteed to yield maximum channel capacity solution. The reason is similar to that of the MMSE design method; i.e., the residual ISI power cannot be placed in high noise regions in the frequency domain. The method only minimizes the energy outside the target window and does not care where the residual ISI lies in frequency.

Wang, Adalı, Liu, and Vlahjnic [36] not only minimize the energy outside the target window but also add another term to be minimized. This term is a frequency weighted energy of the equalizer. Using the weighting function, it is

possible to shape the equalizer frequency response. This is useful to prevent large equalizer gains in unused subchannels. However, it does not optimize the residual ISI.

A second problem with the MSSNR design approach is the computation complexity due to the eigenvalue and Cholesky decompositions. Chiu, Tsai, Liau, and Troulis [37] propose an inverse power method. This method needs neither Cholesky decomposition nor matrix inversion. It directly iterates on two matrices to obtain the optimal TEQ in the sense of MSSNR.

The divide-and-conquer design method [38] is a faster implementation of the MSSNR method [12]. The idea is to divide the equalizer design problem into smaller problems that are easier to solve and then combine the results together. An FIR filter of length  $N$  can be represented as a convolution of  $N - 1$  two-tap filters. In this TEQ design method, the equalizer is divided into a number of two-tap equalizers. Each two-tap equalizer has only one unknown tap since the first tap is set to one. This can be considered as a unit-tap constraint that is similar to that used in the MMSE design approach. Designing an  $N_w$ -tap filter requires the design of  $N_w - 1$  two-tap filters. For the  $i^{th}$  two-tap filter, the method optimizes the two-tap filter  $\mathbf{w}_i$ , and convolves the optimized filter with the current channel impulse response to obtain the new channel impulse response to be used at stage  $i + 1$ . Once the  $N_w - 1$  two-tap filters have been computed, they are convolved together to form one  $N_w$ -tap equalizer. Two different versions of the divide-and-conquer (DC) design method are DC TEQ Minimization and DC TEQ Cancellation.

### 2.3.1 Divide-and-Conquer TEQ Minimization Design

Each TEQ stage in DC TEQ Minimization maximizes the SSNR defined in (2.21) or equivalently minimizes the inverse of it with a two-tap filter defined as

$$\mathbf{w}_i = [1, g_i]^T \quad (2.23)$$

Since  $\mathbf{w}_i$  consists of two taps, the matrices  $\mathbf{A}_i$  and  $\mathbf{B}_i$  are  $2 \times 2$  Toeplitz matrices. For the  $i^{\text{th}}$  filter, the SSNR becomes

$$\frac{\mathbf{w}_i^T \mathbf{A}_i \mathbf{w}_i}{\mathbf{w}_i^T \mathbf{B}_i \mathbf{w}_i} = \frac{\begin{bmatrix} 1 & g_i \end{bmatrix} \begin{bmatrix} a_{1,i} & a_{2,i} \\ a_{2,i} & a_{3,i} \end{bmatrix} \begin{bmatrix} 1 \\ g_i \end{bmatrix}}{\begin{bmatrix} 1 & g_i \end{bmatrix} \begin{bmatrix} b_{1,i} & b_{2,i} \\ b_{2,i} & b_{3,i} \end{bmatrix} \begin{bmatrix} 1 \\ g_i \end{bmatrix}} = \frac{a_{1,i} + 2a_{2,i}g_i + a_{3,i}g_i^2}{b_{1,i} + 2b_{2,i}g_i + b_{3,i}g_i^2} \quad (2.24)$$

The matrices  $\mathbf{A}_i$  and  $\mathbf{B}_i$  are also indexed with  $i$  because at every iteration, a new channel impulse response is calculated which changes  $\mathbf{A}_i$  and  $\mathbf{B}_i$ . The denominator in (2.24) does not become zero for any  $g_i$  [38].

The optimal  $g_i$  is calculated by differentiating (2.24) with respect to  $g_i$  and setting the result to zero. The solutions are

$$g_i = \frac{-(a_{3,i}b_{1,i} - a_{1,i}b_{3,i}) \pm c_i}{2(a_{3,i}b_{2,i} - a_{2,i}b_{3,i})} \quad (2.25)$$

where

$$c_i = \sqrt{(a_{3,i}b_{1,i} - a_{1,i}b_{3,i})^2 - 4(a_{3,i}b_{2,i} - a_{2,i}b_{3,i})(a_{2,i}b_{1,i} - a_{1,i}b_{2,i})}$$

From (2.25) the best solution for  $g_i$  with respect to (2.24) is chosen. The solution is always real-valued [38].

### 2.3.2 Divide-and-Conquer TEQ Cancellation Design

The DC TEQ Cancellation method avoids the computationally expensive calculation of  $\mathbf{A}_i$  and  $\mathbf{B}_i$  at every stage. Instead of maximizing the SSNR only, the energy outside the target window is minimized. Since unit-tap constraints are used for each two-tap filter, constraining the energy of the SIR inside the target window is not necessary. The following derivation is one of the contributions of this thesis.

Define  $\mathbf{h}_i$  as the new channel impulse response and  $\mathbf{h}_i^{\text{wall}}$  as the new  $\mathbf{h}^{\text{wall}}$  at stage  $i$ , so that  $\mathbf{h}_0$  is the channel impulse response and  $\mathbf{h}_i$  is the convolution of  $\mathbf{h}_{i-1}$  with  $\mathbf{w}_i$ . Note that the length of  $\mathbf{h}_i$  increases with  $i$  due to the convolution. At stage  $i$ ,

$$\mathbf{h}_i^{\text{wall}} = \begin{bmatrix} h_{i-1}(1) & 0 \\ h_{i-1}(2) & h_{i-1}(1) \\ \vdots & \vdots \\ h_{i-1}(\Delta) & h_{i-1}(\Delta - 1) \\ h_{i-1}(\Delta + \nu + 2) & h_{i-1}(\Delta + \nu + 1) \\ \vdots & \vdots \\ h_{i-1}(L_{h_{i-1}}) & h_{i-1}(L_{h_{i-1}} - 1) \end{bmatrix} \begin{bmatrix} 1 \\ g_i \end{bmatrix} \quad (2.26)$$

$$\mathbf{h}_i^{\text{wall}} = \begin{bmatrix} h_{i-1}(1) + 0 \\ h_{i-1}(2) + h_{i-1}(1)g \\ \vdots \\ h_{i-1}(\Delta) + h_{i-1}(\Delta - 1)g \\ h_{i-1}(\Delta + \nu + 2) + h_{i-1}(\Delta + \nu + 1)g \\ \vdots \\ h_{i-1}(L_{h_{i-1}}) + h_{i-1}(L_{h_{i-1}} - 1)g \end{bmatrix} \quad (2.27)$$

where  $L_{h_{i-1}}$  is the length of  $\mathbf{h}_{i-1}$ . The energy to be minimized is

$$\mathbf{h}_i^{\text{wall}T} \mathbf{h}_i^{\text{wall}} = \sum_{k \in S} (h_{i-1}(k) + g_i h_{i-1}(k-1))^2, \quad (2.28)$$

where

$$S = \{1, 2, \dots, \Delta, \Delta + \nu + 2, \dots, L_{h_{i-1}}\}$$

The minimum of (2.28) can again be found by taking the derivative with respect to  $g_i$  and setting it to zero. The solution is

$$g_i = - \frac{\sum_{k \in S} h_{i-1}(k-1)h_{i-1}(k)}{\sum_{k \in S} h_{i-1}^2(k-1)} \quad (2.29)$$

The TEQ is calculated by convolving  $N_w - 1$  two-tap filters. This DC design method does not use any matrix decompositions or matrix inversions; hence, it is suitable for real-time implementation. Although it is efficient in terms of computation complexity, it retains all of the drawbacks of the MSSNR method.

## 2.4 Maximum Geometric SNR Design

In a communication system, the ultimate goal is to reach optimum channel capacity. Al-Dhahir and Cioffi [15] introduced the idea of a TEQ design method to optimize channel capacity. Section 2.4.1 gives the channel capacity for multicarrier channels. Section 2.4.2 introduces the maximum geometric SNR method.

### 2.4.1 Multicarrier Channel Capacity

If the number of subchannels  $N/2 + 1$  (i.e.  $N/2 - 1$  two-dimensional and two one-dimensional) is large, then it is reasonable to assume that the channel

noise power spectrum in the subchannels are flat. In this case, each subchannel can be modeled as an independent AWGN channel. The achievable capacity of a multicarrier channel can be written as the sum of the capacities of AWGN channels

$$b_{DMT} = \sum_{i \in \mathcal{S}} \log_2 \left( 1 + \frac{\text{SNR}_i^{MFB}}{\gamma} \right) \text{ bits/symbol} \quad (2.30)$$

where  $i$  is the subchannel index,  $\mathcal{S}$  is the set of the indices of the used  $\bar{N}$  subchannels out of the  $N/2 + 1$  subchannels,  $\text{SNR}_i^{MFB}$  is the matched filter bound of the SNR in the  $i^{\text{th}}$  subchannel as defined below in (2.31), and  $\gamma$  is the SNR gap for achieving Shannon channel capacity and is assumed to be constant over all subchannels. The SNR gap is a function of several factors including the modulation method, allowable probability of error  $P_e$ , coding gain  $\gamma_{eff}$ , and desired system margin  $\gamma_m$ .

The system margin accounts for modeling error and is generally 6 dB in ADSL systems [1]. If one needs a channel with an SNR of  $x$  dB to transmit a certain amount of bits at the rate of the theoretical bound, then in practice an SNR of  $x + 6$  dB is actually used. The system margin of 6 dB ensures that with the unaccounted errors, the desired bit rate can be supported.

The SNR gap can be approximated in the case of QAM as [39]

$$\gamma \approx \frac{\gamma_m}{3\gamma_{eff}} \left( Q^{-1} \left( \frac{P_e}{2} \right) \right)^2$$

Assuming that the input signal and noise are wide sense stationary, the SNR in the  $i^{\text{th}}$  subchannel can be defined as

$$\text{SNR}_i^{MFB} = \frac{S_{x,i} |H_i|^2}{S_{n,i}} \quad (2.31)$$

where  $S_{x,i}$  and  $S_{n,i}$  are the transmitted signal and channel noise power, respectively, and  $H_i$  is the gain of the channel spectrum in the  $i^{\text{th}}$  subchannel. Here

the assumption is that the subchannels are narrow enough so that the channel frequency response and transmitted signal power spectrum can be considered constant in each subchannel. The definition in (2.31) does not include the effect of ISI and any equalizers. It is the maximum achievable SNR or the matched filter bound (MFB). If the channel causes ISI or an equalizer has been used, then the definition has to be modified.

### 2.4.2 The maximum geometric SNR method

The maximum geometric SNR (MGSNR) method maximizes a channel capacity cost function that is based on a geometric SNR definition, as

$$\text{GSNR} = \left( \left[ \prod_{i \in \mathcal{S}} \left( 1 + \frac{\text{SNR}_i^{EQ}}{\phantom{,}} \right) \right]^{1/\bar{N}} - 1 \right) \quad (2.32)$$

which is related to channel capacity. By using (2.32), we rewrite (2.30) as

$$b_{\text{DMT}} = \bar{N} \log_2 \left( 1 + \frac{\text{GSNR}}{\phantom{,}} \right) \text{ bits/symbol}$$

This means that all of the subchannels act together like  $\bar{N}$  AWGN channels, with each channel having an SNR equal to the GSNR. Therefore, maximizing the GSNR is equivalent to maximizing the channel capacity. In (2.32), the subchannel SNR in (2.31) is modified to include the effect of the equalizer [15]

$$\text{SNR}_i^{EQ} = \frac{S_{x,i} |B_i|^2}{S_{n,i} |W_i|^2} \quad (2.33)$$

where  $S_{x,i}$  is signal power,  $S_{n,i}$  is the noise power, and  $B_i$  and  $W_i$  are the gains of  $\mathbf{b}$  and  $\mathbf{w}$  in the  $i^{\text{th}}$  subchannel, respectively. This definition is discussed in detail later in this section.



The derivation [15] proceeds with the following approximation of the GSNR, which is obtained by ignoring the +1 and -1 terms in (2.32):

$$\text{GSNR} \approx \left[ \prod_{i \in \mathcal{S}} \text{SNR}_i^{EQ} \right]^{1/\bar{N}} \quad (2.34)$$

This approximation is valid if the SNR in each subchannel is larger than one, so that the “1” terms can be ignored. This assumption may be reasonable only if bandwidth optimization is used. That is, the channels without sufficient SNR to carry bits are not used [40]. In this case, the problem of maximizing (2.34) can be converted to the maximization of

$$L(\mathbf{b}) = \frac{1}{\bar{N}} \sum_{i \in \mathcal{S}} \ln |B_i|^2 \quad (2.35)$$

which can be obtained by substituting (2.33) into (2.34) and taking the natural logarithm, based on the assumption that  $\mathbf{b}$  and  $\mathbf{w}$  do not depend on each other.  $B_i$  is the  $i^{\text{th}}$  FFT coefficient of  $\mathbf{b}$  defined as

$$B_i = \sum_{k=0}^{N-1} b_k e^{-j \frac{2\pi}{N} ki}$$

The assumption that  $\mathbf{b}$  and  $\mathbf{w}$  do not depend on each other is not accurate because once  $\mathbf{b}_{opt}$  is calculated by maximizing (2.35), the optimum (in the MMSE sense) TIR  $\mathbf{w}_{opt}$  is found using

$$\mathbf{w}_{opt}^T = \mathbf{b}_{opt}^T \mathbf{R}_{xy} \mathbf{R}_{yy}^{-1} \quad (2.36)$$

where  $\mathbf{R}_{xy}$  and  $\mathbf{R}_{yy}$  are the channel input-output cross-correlation and channel output autocorrelation matrices, respectively. This choice of TEQ taps ensures that the MSE is minimum for the given TIR [15].

When maximizing (2.35), a unit-energy constraint is placed on  $\mathbf{b}$  to prevent an infinite gain in the TEQ. This constraint maximizes the cost function for  $|B_i|^2 = 1 \forall i$ , which implies a zero forcing equalization of the channel.

The goal is not to equalize the channel fully since in fact one of the primary reasons for the application of multicarrier modulation is to avoid full equalization because it requires high-order equalizers. Furthermore, full equalization with a short equalizer, as is typical for TEQs, would cause large MSE. Therefore, an additional constraint is required to keep the MSE below a threshold  $\text{MSE}_{max}$ . This threshold has to be tuned if the channel, noise level, or signal power changes. Setting the threshold to the correct value for a given channel is crucial for good performance [37]. Including the above constraints, Al-Dhahir and Cioffi state the optimum TIR problem as

$$\max_{\mathbf{b}} \sum_{i \in \mathcal{S}} \ln |B_i|^2 \text{ s.t. } \|\mathbf{b}\|^2 = 1 \text{ and } \mathbf{b}^T \mathbf{R}_{\Delta} \mathbf{b} \leq \text{MSE}_{max} \quad (2.37)$$

where

$$\mathbf{R}_{\Delta} = [\mathbf{0}_{(\nu+1) \times \Delta} \quad \mathbf{I}_{\nu+1} \quad \mathbf{0}_{(\nu+1) \times P}] \left( \frac{1}{S_x} \mathbf{I}_{N_w+L-1} + \mathbf{H}^T \mathbf{R}_{nn}^{-1} \mathbf{H} \right)^{-1} \begin{bmatrix} \mathbf{0}_{\Delta \times (\nu+1)} \\ \mathbf{I}_{\nu+1} \\ \mathbf{0}_{P \times (\nu+1)} \end{bmatrix}$$

Here,  $P = N_w + L - \Delta - \nu - 2$ ,  $\mathbf{0}_{m \times n}$  is an  $m \times n$  matrix of zeros,  $\mathbf{I}_m$  is the  $m \times m$  identity matrix,  $S_x$  is the average energy of the input symbols,  $\mathbf{R}_{nn}$  is the  $N_w \times N_w$  noise correlation matrix, and  $\mathbf{H}$  is the  $N_w \times (N_w + L - 1)$  channel convolution matrix. This nonlinear constrained optimization problem does not have a closed-form solution [15], but it may be solved by numerical methods [41].

The MGSNR TEQ design method is based on the maximization of the approximate GSNR. Due to several inaccurate approximations, it is not optimum in the sense of maximizing channel capacity. The most important approximation is in the definition of the subchannel SNR,  $\text{SNR}_i^{EQ}$ , in (2.33). This definition includes the equalizer effect but not the ISI effect even though

the objective of the TEQ is to minimize ISI. A later modification [40] includes an ISI term:

$$\text{SNR}_i^{ISI} = \frac{S_{x,i}|B_i|^2}{S_{x,i}|B_i - W_i H_i|^2 + S_{n,i}|W_i|^2} \quad (2.38)$$

However, this modified definition is only used to evaluate the performance of the MGSNR TEQ method, which is still based on the definition given in (2.33).

The modified definition in (2.38) represents ISI in the  $i^{\text{th}}$  subchannel as  $S_{x,i}|B_i - H_i W_i|^2$ . Assume that the SIR fits perfectly in the target window and there is no energy outside this window. However, the SIR differs from the TIR inside the window. Although there is no ISI in the system, the definition measures the difference as ISI. Therefore, this definition is only accurate if the difference between the SIR and TIR is small so that its contribution to ISI is negligible. Furthermore, both the subchannel SNR definition without an ISI term  $\text{SNR}_i^{EQ}$  in (2.33) and the one with an ISI term  $\text{SNR}_i^{ISI}$  in (2.38) are only useful if the structure in Fig. 2.1 is used. In general, a TIR is not available. Then, these definitions are not suitable and a new definition is necessary.

In summary the drawbacks of the MGSNR TEQ method are that

- its derivation is based on a subchannel SNR definition  $\text{SNR}_i^{EQ}$  that does not include the effect of ISI;
- it depends on the parameter  $\text{MSE}_{max}$  which has to be tuned for different channels;
- its objective function (2.37) assumes that  $\mathbf{b}$  and  $\mathbf{w}$  are independent;
- it requires a constrained nonlinear optimization method; and
- it assumes that the SNR in each subchannel is much greater than one.

Considerable effort has been spent to overcome the last issue. Lashkarian and Kiaei [42] propose a projection onto convex sets method to solve the constrained nonlinear optimization problem iteratively with lower computational complexity. Milisavljević and Verriest [43] propose simulated annealing and genetic algorithms to solve the nonlinear optimization problem, which have high complexity.

## 2.5 Conclusion

This chapter summarizes several approaches to design DMT TEQs. Table 2.1 summarizes the advantages and disadvantages of all the methods mentioned in this chapter. As shown in Table 2.1 MMSE and MGSNR methods have more disadvantages compared to MSSNR methods. The only method with no disadvantage is the DC TEQ Cancellation method of Section 2.3.2. However, none of the MMSE and MSSNR methods optimize channel capacity and the MGSNR methods optimize only an approximation to the channel capacity.

Maximizing channel capacity is the primary goal in designing a TEQ. However, only the MGSNR method in Section 2.4 attempts to optimize the channel capacity. As discussed in that section, the MGSNR method is not optimum in the sense of maximizing channel capacity due to many inaccurate approximations and assumptions. A design method that is not only computationally efficient enough for cost-effective real-time implementations but also truly maximizes the channel capacity is not available. My goal in this dissertation is to write the channel capacity as a function of TEQ taps with minimal assumptions and approximations. By maximizing this function the optimal TEQ coefficients can be calculated.

Advantages							Disadvantages						
1. Adaptive or iterative 2. Off-line (initialization) 3. Maximizes channel capacity 4. Minimizes directly ISI causing tail 5. Frequency weighting 6. Optimize subchannels							1. Deep notches in frequency 2. SIR-TIR difference inside window 3. Slow or uncertain convergence 4. Requires eigendecomposition 5. Requires nonlinear optimization 6. Narrowband frequency response 7. Numerical instabilities possible						
		Advantages					Disadvantages						
	1	2	3	4	5	6	1	2	3	4	5	6	7
<i>MMSE methods</i>													
Chow <i>et al.</i> [9]		✓					✓	✓				✓	✓
Chow <i>et al.</i> [10, 11]	✓						✓	✓	✓			✓	✓
Al-Dhahir <i>et al.</i> [19]		✓					✓	✓		✓		✓	✓
Kerckhove <i>et al.</i> [26]		✓			✓		✓	✓		✓		✓	✓
Nafe <i>et al.</i> [30]	✓	✓		✓			✓						
Strait [29]	✓						✓	✓				✓	
Wang <i>et al.</i> [21, 22]		✓			✓		✓	✓		✓		✓	✓
Lashkarian <i>et al.</i> [32]	✓	✓					✓	✓		✓		✓	
Acker <i>et al.</i> [27, 28]	✓	✓			✓	✓			✓				
Boroujeny <i>et al.</i> [33]		✓						✓		✓		✓	✓
Wang <i>et al.</i> [25]		✓			✓					✓			✓
<i>MSSNR methods</i>													
Melsa <i>et al.</i> [12]		✓		✓						✓			✓
Yin <i>et al.</i> [35]		✓		✓						✓			✓
Chiu <i>et al.</i> [37]	✓	✓		✓					✓				
Wang <i>et al.</i> [36]		✓		✓	✓					✓			✓
Lu <i>et al.</i> [38]	✓	✓		✓									
<i>MGSNR methods</i>													
Al-Dhahir <i>et al.</i> [15]		✓	✓ <sup>†</sup>			✓	✓	✓			✓	✓	✓
Lashkarian <i>et al.</i> [42]	✓	✓	✓ <sup>†</sup>			✓	✓		✓			✓	✓
Milisavljević <i>et al.</i> [43]	✓	✓	✓ <sup>†</sup>			✓			✓		✓		

<sup>†</sup> Maximizes an approximate GSNR not the true channel capacity.

Table 2.1: Advantage/disadvantages of TEQ design methods mentioned in this chapter.

# Chapter 3

## A Model for Subchannel SNR

A TEQ increases the capacity of a DMT system by minimizing ISI. Although intuitive, there is no model available which represents this fact mathematically. The purpose of this chapter is to provide such a mathematical model. With the proposed model, I define subchannel SNR as the ratio of a desired signal power to channel noise power plus ISI power. The model suggests a way to decompose a received DMT modulated signal into a desired signal, channel noise, and ISI components. Using this partitioning, I write subchannel SNR in terms of the TEQ taps to prove that capacity is a function of the TEQ taps.

### 3.1 Introduction

The first problem one comes across in optimal TEQ design is the lack of a mathematical foundation of the effect of a TEQ on channel capacity. Ideally, one would like to have the channel capacity as a function of the TEQ taps. The only parameter of channel capacity that might be affected by a TEQ is the SNR in each subchannel. The conventional definition of SNR as the ratio

of signal power to channel noise power does not provide a relationship between the SNR and TEQ taps since both the signal power and channel noise power are filtered by the same filter. The SNR distribution cannot be changed by a TEQ unless the TEQ has zeros in its frequency response. If the TEQ gain were zero, then there would be neither signal nor noise which makes the definition of SNR meaningless. Therefore, a new definition of subchannel SNR is necessary.

With the assumption that the received samples consist of a desired signal, channel noise, and ISI, I define SNR as the ratio of the desired signal power to the channel noise plus ISI power. Only with such a definition can the effect of a TEQ on subchannel SNR, hence channel capacity, be written mathematically. To understand the effect of a TEQ on subchannel SNR, I classify each received sample in order to formulate the definition of a signal, noise, and ISI path in a DMT system. The input to the signal and ISI paths is the transmitted DMT signal, and the outputs are the signal and ISI power at the receiver. The input to the noise path is the channel noise and the output gives the TEQ filtered noise at the receiver.

My model suggests that the signal path impulse response is a windowed version of the equalized channel impulse response. The ISI path impulse response is the rest of the equalized channel impulse response, i.e. the part lying outside of the window. So, the desired signal and ISI at the receiver are filtered versions of the transmitted DMT signal. The TEQ shapes these filters.

Section 3.2 motivates the derivation of the equivalent signal, noise, and ISI paths by an example. Section 3.3 generalizes the example of Section 3.2. Section 3.4 introduces the proposed subchannel SNR definition. Section 3.5 concludes this chapter.

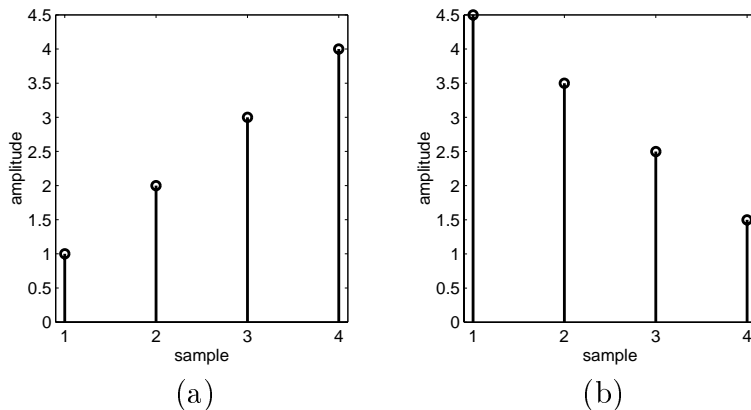


Figure 3.1: Example of transmitted symbols (a) **a** and (b) **b**.

### 3.2 Example: Equivalent Impulse Responses for the Signal, ISI, and Noise Paths

Consider a DMT system with an FFT size of  $N = 4$ , and a cyclic prefix length of  $\nu = 1$ . Consider the transmission of two DMT symbols  $\mathbf{a} = [a_1 a_2 a_3 a_4]$  and  $\mathbf{b} = [b_1 b_2 b_3 b_4]$  over an equalized channel with impulse response  $\tilde{\mathbf{h}} = \mathbf{h} * \mathbf{w}$ , as shown in Fig. 3.3. To visualize the example, I assign numbers for the transmitted symbol samples shown in Fig. 3.1 as well as the equalized channel impulse response as shown in Fig. 3.2. The length of the equalized channel  $\tilde{\mathbf{h}} = [\tilde{h}_1 \tilde{h}_2 \tilde{h}_3 \tilde{h}_4]$  is four, and its delay is assumed to be  $\Delta = 1$ . Since the length of the equalized channel is longer than  $\nu + 1$ , ISI and interchannel interference (ICI) will occur. ICI is defined as leaking signal power from one subchannel to the adjacent ones. Distorted orthogonality causes ICI as well as ISI.

By adding the cyclic prefix, the symbols become  $\hat{\mathbf{a}} = [a_4 a_1 a_2 a_3 a_4]$  and  $\hat{\mathbf{b}} = [b_4 b_1 b_2 b_3 b_4]$  which form the transmitted sequence  $\mathbf{x} = [\hat{\mathbf{a}} \hat{\mathbf{b}}]$  as shown in



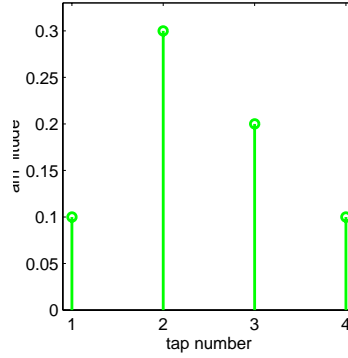


Figure 3.2: Impulse response of an equalized channel  $\mathbf{h}$

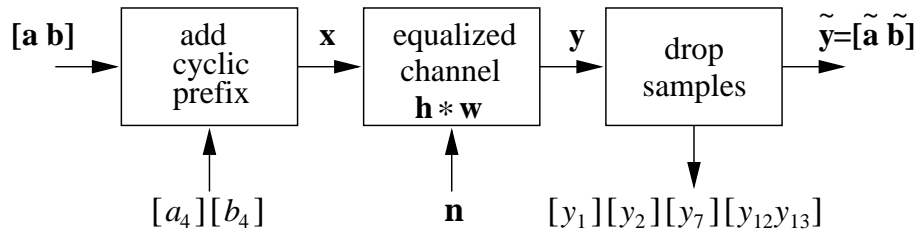


Figure 3.3: Example: Two DMT symbols  $\mathbf{a}$  and  $\mathbf{b}$  are transmitted over an equalized channel  $\tilde{\mathbf{h}} = \mathbf{h} * \mathbf{w}$ . After dropping the ISI/ICI and cyclic prefix samples, the two symbols are received as  $\tilde{\mathbf{a}}$  and  $\tilde{\mathbf{b}}$ .

Fig 3.4.

The received signal

$$\mathbf{y} = \mathbf{x} * \tilde{\mathbf{h}} + \tilde{\mathbf{n}} \quad (3.1)$$

is a vector of size  $2(N + \nu) + L - 1 = 2(4 + 1) + 4 - 1 = 13$ , as shown in Fig 3.5 for the case of no channel noise. Expanding (3.1),

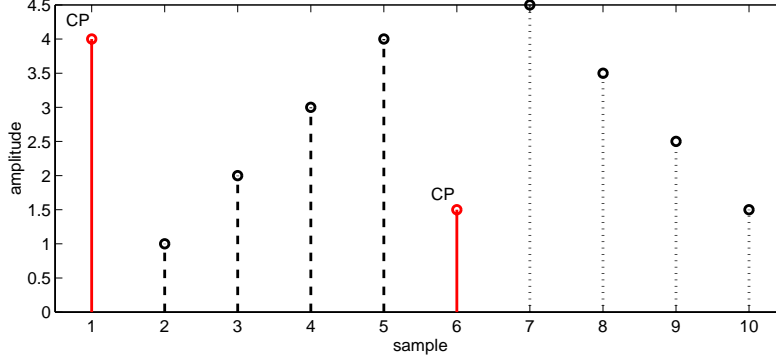


Figure 3.4: Example of transmitted samples  $\mathbf{x}$ .

$$\begin{array}{l}
 \text{delay} \rightarrow \\
 \text{CP} \rightarrow \\
 \\
 \\
 \\
 \text{CP} \rightarrow \\
 \\
 \\
 \\
 \text{tail} \rightarrow
 \end{array}
 \begin{array}{c}
 \boxed{y_1} \\
 \boxed{y_2} \\
 y_3 \\
 y_4 \\
 y_5 \\
 y_6 \\
 \boxed{y_7} \\
 y_8 \\
 y_9 \\
 y_{10} \\
 y_{11} \\
 \boxed{y_{12}} \\
 \boxed{y_{13}}
 \end{array}
 =
 \begin{array}{c}
 \boxed{\tilde{h}_1 a_4} \\
 \boxed{\tilde{h}_1 a_1 + \tilde{h}_2 a_4} \\
 \tilde{h}_1 a_2 + \tilde{h}_2 a_1 + \tilde{h}_3 a_4 \\
 \tilde{h}_1 a_3 + \tilde{h}_2 a_2 + \tilde{h}_3 a_1 + \tilde{h}_4 a_4 \\
 \tilde{h}_1 a_4 + \tilde{h}_2 a_3 + \tilde{h}_3 a_2 + \tilde{h}_4 a_1 \\
 \tilde{h}_1 b_4 + \tilde{h}_2 a_4 + \tilde{h}_3 a_3 + \tilde{h}_4 a_2 \\
 \boxed{\tilde{h}_1 b_1 + \tilde{h}_2 b_4 + \tilde{h}_3 a_4 + \tilde{h}_4 a_3} \\
 \tilde{h}_1 b_2 + \tilde{h}_2 b_1 + \tilde{h}_3 b_4 + \tilde{h}_4 a_4 \\
 \tilde{h}_1 b_3 + \tilde{h}_2 b_2 + \tilde{h}_3 b_1 + \tilde{h}_4 b_4 \\
 \tilde{h}_1 b_4 + \tilde{h}_2 b_3 + \tilde{h}_3 b_2 + \tilde{h}_4 b_1 \\
 \tilde{h}_2 b_4 + \tilde{h}_3 b_3 + \tilde{h}_4 b_2 \\
 \boxed{\tilde{h}_3 b_4 + \tilde{h}_4 b_3} \\
 \boxed{\tilde{h}_4 b_4}
 \end{array}
 +
 \begin{array}{c}
 \boxed{\tilde{n}_1} \\
 \boxed{\tilde{n}_2} \\
 \tilde{n}_3 \\
 \tilde{n}_4 \\
 \tilde{n}_5 \\
 \tilde{n}_6 \\
 \boxed{\tilde{n}_7} \\
 \tilde{n}_8 \\
 \tilde{n}_9 \\
 \tilde{n}_{10} \\
 \tilde{n}_{11} \\
 \boxed{\tilde{n}_{12}} \\
 \boxed{\tilde{n}_{13}}
 \end{array}
 \quad (3.2)$$

where  $\tilde{\mathbf{n}}$  is the additive channel noise at the output of the equalizer.

The received samples can be classified as follows:

- $y_1$ : The equalized channel has a delay of one, so the first received sample

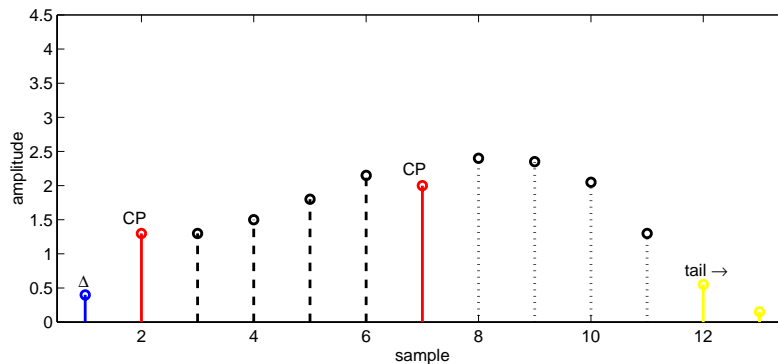


Figure 3.5: Example of a received signal samples  $\mathbf{y}$ .

is invalid.

- $y_2$ : The first transmitted sample is the cyclic prefix and is ignored.
- $y_3 - y_6$ : These samples correspond to the first received DMT symbol  $\tilde{\mathbf{a}}$ .
- $y_7$ : This sample is the cyclic prefix for the second symbol and is dropped.
- $y_8 - y_{11}$ : These samples correspond to the second received DMT symbol  $\tilde{\mathbf{b}}$ .
- $y_{12} - y_{13}$ : All transmitted symbols have been received, so the remaining samples are invalid. They are caused by the duration of the channel impulse response.

In order to demodulate the received DMT symbols  $\tilde{\mathbf{a}}$  and  $\tilde{\mathbf{b}}$  correctly, the channel length has to be at most  $\nu + 1 = 2$ . Since the channel impulse response length in this example is four, the received symbols have an ISI component in addition to the desired signal component and noise component.

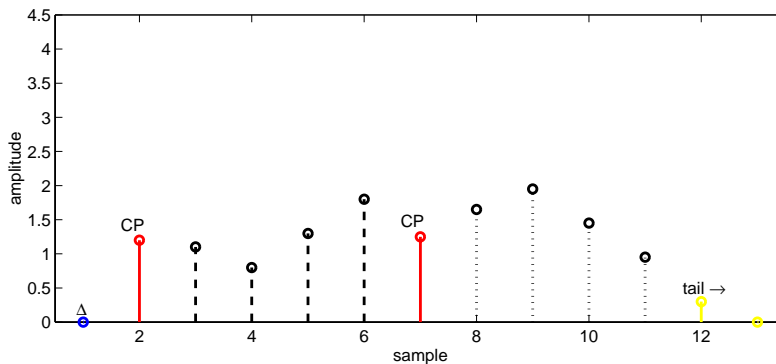


Figure 3.6: Example of the desired part of the received signal samples  $\mathbf{y}$  which is equal to  $\mathbf{h}^{signal} * \mathbf{x}$  and shown as dashed lines. Here, CP means cyclic prefix and  $\Delta$  is the channel delay.

- *The Desired Signal Component:* A cyclic prefix length of  $\nu = 1$  sample prevents ISI for channels up to length  $\nu + 1 = 2$ . In the ideal case where the channel is shortened to this length, the received symbols are the 4-point circular convolution of the transmitted symbols and the channel impulse response. Then, the transmitted subsymbols can be recovered by dividing the received subsymbols with the channel frequency response (frequency domain equalizer as one-tap equalizer). Therefore, the desired component of  $\mathbf{y}$  is

$$\mathbf{y}^{signal} = [0 \tilde{h}_2 \tilde{h}_3 0] * \mathbf{x} = \mathbf{h}^{signal} * \mathbf{x}$$

and is shown in (3.2) inside the oval box and numerically in Fig 3.6. The symbol  $*$  represents linear convolution, and  $\mathbf{h}^{signal}$  is the equivalent signal path impulse response which has two ( $\nu + 1 = 2$ ) nonzero taps starting after a delay of one ( $\Delta = 1$ ) sample. The equivalent signal impulse response  $\mathbf{h}^{signal}$  is shown in Fig. 3.7. In fact, only samples 3 – 6

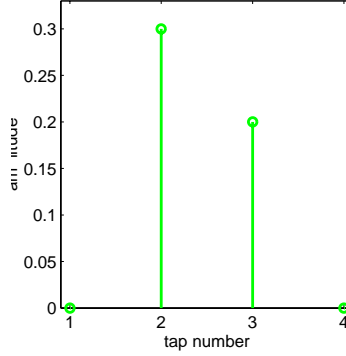


Figure 3.7: Example of the signal path impulse response  $\mathbf{h}^{signal}$  for Fig. 3.2

(shown as dashed lines in Fig. 3.6) and samples 8 – 11 (also shown as dotted lines in Fig. 3.6) of  $\mathbf{y}^{signal}$  are of interest since the remaining samples are being dropped. The samples 3 – 6 of  $\mathbf{y}^{signal}$  are the desired part of symbol  $\mathbf{a}$  represented with  $\tilde{\mathbf{a}}^{signal}$  and similarly samples 8 – 11 of  $\mathbf{y}^{signal}$  are the desired part of symbol  $\mathbf{b}$  represented with  $\tilde{\mathbf{b}}^{signal}$ .

- *The ISI Component:* All additional components outside the oval box in (3.2) are considered ISI and ICI terms, which are due to the extra nonzero taps in the channel impulse response. For each DMT symbol, these ISI/ICI terms can be written as

$$\mathbf{y}^{ISI} = [\tilde{h}_1 \ 0 \ 0 \ \tilde{h}_4] * \mathbf{x} = \mathbf{h}^{ISI} * \mathbf{x} \quad (3.3)$$

Here  $\mathbf{h}^{ISI}$  represents the equivalent ISI path impulse response, which is shown in Fig. 3.8. The ISI/ICI part  $\mathbf{y}^{ISI}$  of the received samples is shown in Fig. 3.9. Similar to the desired part of  $\mathbf{y}$ , only samples 3 – 6 represented with  $\tilde{\mathbf{a}}^{ISI}$  (shown as dashed lines in Fig. 3.9) and samples 8 – 11 represented with  $\tilde{\mathbf{b}}^{ISI}$  (shown as dashed lines in Fig. 3.9) are of

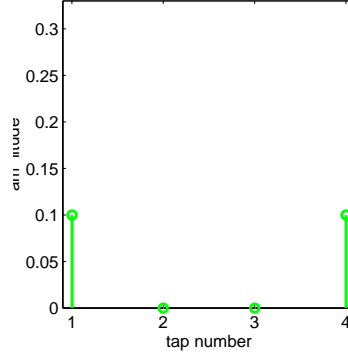


Figure 3.8: Example of the ISI path impulse response  $\mathbf{h}^{ISI}$  for Fig. 3.2.

interest.

- *The Output Noise Component:* The last component in the received symbols corresponds to the additive noise  $\tilde{\mathbf{n}}$  which is the filtered version of the channel noise by the equalizer. Therefore, the equivalent path for the noise consists only of the equalizer. That is,

$$\tilde{\mathbf{n}} = \mathbf{w} * \mathbf{n} = \mathbf{h}^{noise} * \mathbf{n}$$

In summary, the received samples consist of three components – the desired signal, the ISI, and the noise components

$$\begin{aligned} \mathbf{y} &= \mathbf{y}^{desired} + \mathbf{y}^{ISI} + \tilde{\mathbf{n}} \\ &= \mathbf{h}^{signal} * \mathbf{x} + \mathbf{h}^{ISI} * \mathbf{x} + \mathbf{h}^{noise} * \mathbf{n} \end{aligned}$$

The equivalent signal path impulse response  $\mathbf{h}^{signal}$  and the equivalent ISI path impulse response  $\mathbf{h}^{ISI}$  can be obtained from the equalized impulse response using a window function  $\mathbf{g}$  as follows:

$$\mathbf{h}^{signal} = \tilde{\mathbf{h}} \odot \mathbf{g} = [\tilde{h}_1 \tilde{h}_2 \tilde{h}_3 \tilde{h}_4] \odot [0 \ 1 \ 1 \ 0] = [0 \ \tilde{h}_2 \ \tilde{h}_3 \ 0]$$

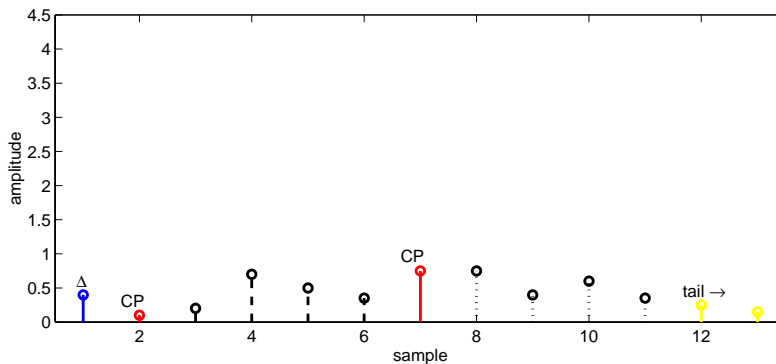


Figure 3.9: Example of the ISI part of the received signal samples  $\mathbf{y}$  which is equal to  $\mathbf{h}^{ISI} * \mathbf{x}$ .

$$\mathbf{h}^{ISI} = \tilde{\mathbf{h}} \odot (\mathbf{1} - \mathbf{g}) = [\tilde{h}_1 \tilde{h}_2 \tilde{h}_3 \tilde{h}_4] \odot [1 0 0 1] = [\tilde{h}_1 0 0 \tilde{h}_4]$$

where  $\odot$  represents element by element multiplication,  $\mathbf{g}$  is a zero vector everywhere except that it is one for the  $\nu + 1 = 2$  elements starting at index  $\Delta + 1 = 2$ , and  $\mathbf{1}$  is a vector of all ones.

### 3.3 Generalization of the Equivalent Path Impulse Responses

The example in Section 3.2 can be generalized such that any received signal can be partitioned into the desired signal, ISI, and noise components. The signal and ISI components are linear filtered versions of the same transmitted signal. The filters can be obtained by partitioning the equalized channel impulse response. One of the filters is formed from the samples of the equalized channel inside the target window, which is called the equivalent signal path impulse response  $h_k^{signal}$ . The second filter is formed from the remaining sam-

ples of the equalized channel impulse response, which is called the equivalent ISI path impulse response  $h_k^{ISI}$ .

In general, the two equivalent paths can be represented as

$$\begin{aligned} h_k^{signal} &= \tilde{h}_k g_k \\ h_k^{ISI} &= \tilde{h}_k (1 - g_k) \end{aligned} \quad (3.4)$$

Here,  $\tilde{h}_k = h_k * w_k$  such that  $h_k$  and  $w_k$  are the channel impulse response and TEQ, respectively, and

$$g_k = \begin{cases} 1 & \Delta + 1 \leq k \leq \Delta + \nu + 1 \\ 0 & \text{otherwise} \end{cases}$$

represents the target window.

Figs. 3.10(a)–(c) show a simulated channel, equalizer, and equalized channel. Figs. 3.10(d)–(f) show the signal path, ISI path and the sum of both paths which is equal to the equalized channel. The equalizer cannot shorten the channel to fit in the target window. Therefore, a small part of the equalized channel acts as the equivalent ISI path impulse response.

The portion of the received signal corresponding to the additive noise of the channel is filtered by the equalizer. The equivalent noise impulse response is equal to the equalizer taps

$$h_k^{noise} = w_k$$

The original channel and equalizer along with all three equivalent paths block diagrams are shown in Fig. 3.11.



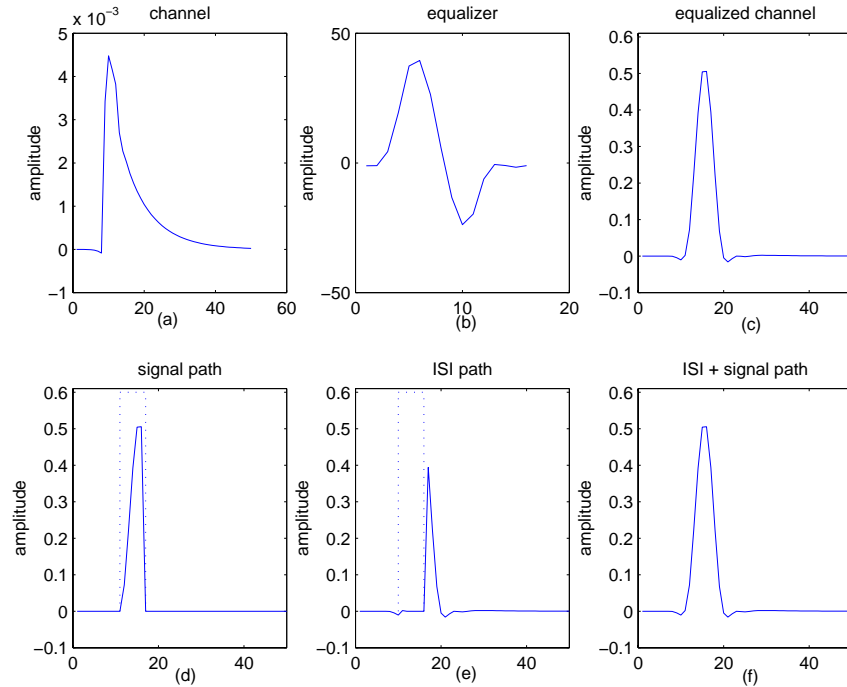


Figure 3.10: Impulse responses: (a) channel, (b) equalizer, (c) equalized channel, (d) signal path, (e) ISI path, and (f) ISI + signal path. The sum of the signal and ISI paths is equal to the equalized channel impulse response.

### 3.4 New Definition of Subchannel SNR

As described in the previous section, the received signal consists of three components: the desired signal component, the ISI component, and the output noise component. The SNR can be defined as

$$\text{SNR} = \frac{\text{signal power}}{\text{noise power} + \text{ISI power}}$$

Using the equivalent path definitions, I define a new subchannel SNR to incorporate both types of distortion as

$$\text{SNR}_i^{NEW} = \frac{S_{x,i}|H_i^{signal}|^2}{S_{n,i}|H_i^{noise}|^2 + S_{x,i}|H_i^{ISI}|^2} \quad (3.5)$$

where  $S_{x,i}$ ,  $S_{n,i}$ ,  $H_i^{signal}$ ,  $H_i^{noise}$ , and  $H_i^{ISI}$  are the transmitted signal power, channel noise power (before the equalizer), signal path gain, noise path gain, and the ISI path gain in the  $i^{th}$  subchannel, respectively. The equivalent path gains in subchannel  $i$  are the  $i^{th}$  FFT coefficients of the equivalent path impulse responses.

When the channel is perfectly equalized to the desired length, the ISI path impulse response is equal to zero. In this case,

$$\begin{aligned} h_k^{signal} = \tilde{h}_k = h_k * w_k &\rightarrow H_i^{signal} = W_i H_i \\ h_k^{noise} = w_k &\rightarrow H_i^{noise} = W_i \\ h_k^{ISI} = 0 &\rightarrow H_i^{ISI} = 0 \end{aligned}$$

and the subchannel SNR ( $\text{SNR}_i^{No\ ISI}$ ) can be written as

$$\text{SNR}_i^{No\ ISI} = \frac{S_{x,i}|W_i|^2|H_i|^2}{S_{n,i}|W_i|^2} = \frac{S_{x,i}|H_i|^2}{S_{n,i}} \text{ if } |W_i| \neq 0 \quad (3.6)$$

Equation (3.6) is equal to the MFB,  $\text{SNR}_i^{MFB}$ , given in (2.31) and is the maximum achievable SNR. This is expected since the SNR should be maximum when there is no ISI. The second equality in (3.6) is valid only if  $|W_i|$  is nonzero. For the subchannels in which  $|W_i|$  is equal to zero, the equalizer zeros out the signal and noise which makes the definition of SNR meaningless.

To substitute  $H_i^{signal}$ ,  $H_i^{ISI}$ , and  $H_i^{noise}$  in (3.5),  $N$ -point FFTs of  $h_k^{signal}$ ,  $h_k^{ISI}$ , and  $h_k^{noise}$  are required. As a result of the convolution of the channel of length  $L$  and the equalizer of length  $N_w$ , the length of  $h_k^{signal}$  and  $h_k^{ISI}$  is

$L + N_w - 1$ . Furthermore, the length of  $h_k^{noise}$  is equal to that of  $w_k$ , which is  $N_w$ . To obtain length- $N$  sequences, I either pad zeros (if the sequence is shorter than  $N$ ) or drop the last few samples (if the sequence is longer than  $N$ ).

In general, the TEQ is shorter than  $N$  ( $N_w < N$ ) and the length of the SIR is longer than  $N$  ( $L + N_w - 1 > N$ ). Therefore, I need to pad zeros to the noise path impulse response and drop samples of the signal and ISI path impulse responses. This process does not introduce any error for the signal path impulse response since the target window is placed near the energy concentration of the SIR and the samples near the tail are already zeroed out. In the ISI path case, however, a small error is introduced by dropping the samples between indices  $N + 1$  to  $L + N_w - 1$ . Since the SIR has most of its energy at the beginning of the response, this error is small and can be ignored. For example, in the eight standard CSA test loops the ratio of the energy in the ignored part to the energy in the used part is on the order of  $10^{-6}$ .

### 3.5 Conclusion

This chapter proposes a new definition for subchannel SNR that incorporates channel noise as well as the distortion caused by ISI and ICI. The definition is based on partitioning of a multicarrier channel into signal, ISI, and noise paths. The output of the signal path is the desired part of the signal, and the output of the ISI path is ISI and ICI caused by the channel. The signal and ISI path impulse responses are obtained by windowing the equalized channel impulse response. The part of the equalized impulse response inside the window is defined as the signal path while the part outside is defined as

the ISI path impulse response. If the equalized channel length were shorter than the cyclic prefix, then the entire channel would fit into the window and the ISI path impulse response becomes zero. The noise path impulse response is the equalizer impulse response because the noise passes only through the equalizer. By using this model, any received signal can be partitioned into signal, ISI, and noise parts.

The model proposed in this chapter is the basis of the TEQ design method proposed in Chapters 4 and 5. The optimal Maximum Channel Capacity (MCC) method in Chapter 4 directly follows from the model by placing the proposed SNR definition into the channel capacity equation and rewriting it in matrix form. The near-optimal min-ISI method of Chapter 5 minimizes a frequency weighted ISI, which is defined as the output of the ISI path impulse response given by the model. In addition to being a basis for the proposed TEQ design methods, the proposed model can be used to compare the performance of different TEQ design methods. It allows the direct calculation of channel capacity without extensive simulations in which millions of symbols would have needed to be transmitted to obtain an accurate estimate of the channel capacity.

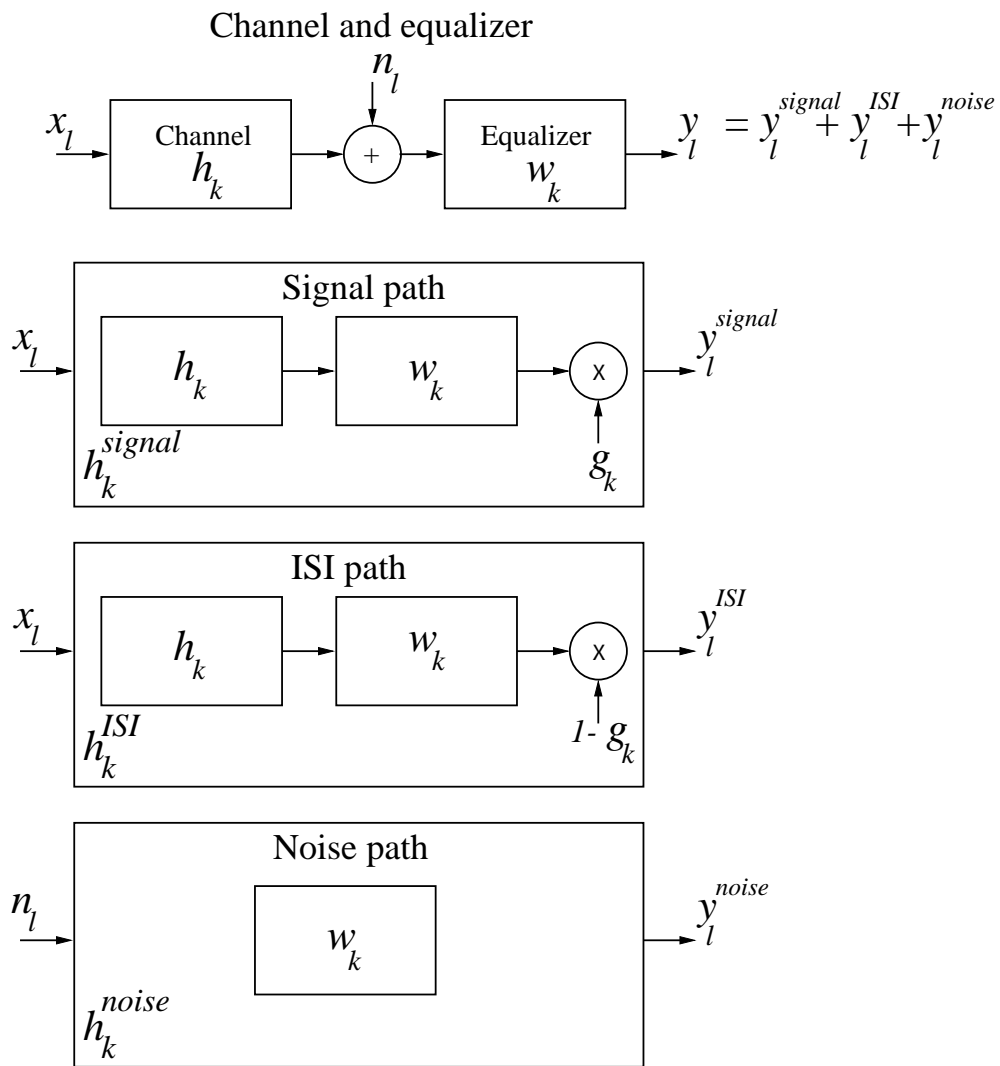


Figure 3.11: Block diagrams for the (a) equalized channel, and the corresponding (b) signal, (c) noise, and (d) ISI paths in a DMT system.

# Chapter 4

## Time Domain Equalizer Design For Maximum Channel Capacity

The subchannel SNR model in Chapter 3 is the first model that expresses channel capacity directly in terms of equalizer taps. With a matrix-vector representation of all filters, windows, and transforms in the model, I write the channel capacity as nonlinear function of a vector containing the TEQ taps. The channel capacity can then be maximized with unconstrained nonlinear programming methods to find the optimal Maximum Channel Capacity (MCC) TEQ. Compared to the MGSNR method, the proposed MCC method takes into account the ISI in the SNR, does not need any constraints in the optimization, does not have any ad-hoc parameters, and does not require any postprocessing to obtain the TEQ taps. The MCC-TEQ design method outperforms the MGSNR-TEQ design method by achieving in the worst case

98.5% of upper bound on channel capacity for the eight standard carrier-serving-area (CSA) ADSL loops. For some of the CSA ADSL loops, a two-tap MCC-TEQ achieves more than 99% of the upper bound on channel capacity.

## 4.1 Introduction

In this chapter, I develop a method for optimizing TEQ designs for channel capacity. A straightforward substitution of (3.5) into channel capacity given by (2.30) yields channel capacity in terms of the frequency response of the signal, noise, and ISI paths of a DMT system. The key idea is to represent these frequency responses in matrix-vector form so that the TEQ taps are in a separate vector. I achieve this by writing the equalized channel impulse response as a matrix-vector product of the channel convolution matrix and TEQ tap vector. Then, I represent the windowing operation with a diagonal matrix multiplication. To convert these impulse responses into frequency responses, I multiply them with a DFT vector of size  $N$ .

Section 4.2 derives the MCC-TEQ. I analyze the performance of the MCC-TEQ with respect to the number of TEQ taps in Section 4.3 and with respect to the target length of the equalized channel impulse response in Section 4.4. Section 4.5 concludes this chapter.

## 4.2 The Optimal Maximum Channel Capacity (MCC) Equalizer

To write the achievable channel capacity in terms of the TEQ tap values, I derive the subchannel SNRs as a function of the TEQ taps. Including the zero padding and sample dropping mentioned in Section 3.4, I rewrite the equivalent signal, ISI, and noise path impulse responses in matrix form as

$$\begin{aligned}
 \mathbf{h}^{signal} &= \mathbf{G}\mathbf{H}\mathbf{w} \\
 \mathbf{h}^{ISI} &= \mathbf{D}\mathbf{H}\mathbf{w} \\
 \mathbf{h}^{noise} &= \mathbf{F}\mathbf{w}
 \end{aligned} \tag{4.1}$$

where  $\mathbf{h}^{signal}$ ,  $\mathbf{h}^{ISI}$ , and  $\mathbf{h}^{noise}$  are length- $N$  vectors representing the equivalent signal, ISI, and noise path impulse responses, respectively. The  $N \times N_w$  matrix  $\mathbf{H}$  is defined as the first  $N$  rows of the convolution matrix of the channel,

$$\mathbf{H} = \begin{bmatrix}
 h_0 & 0 & 0 & \cdots & 0 \\
 h_1 & h_0 & 0 & \cdots & 0 \\
 \vdots & \vdots & \vdots & \ddots & \vdots \\
 h_{N_w-1} & h_{N_w-2} & h_{N_w-3} & \cdots & h_0 \\
 h_{N_w} & h_{N_w-1} & h_{N_w-2} & \cdots & h_1 \\
 \vdots & \vdots & \vdots & \ddots & \vdots \\
 h_{N-1} & h_{N-2} & h_{N-3} & \cdots & h_{N-N_w}
 \end{bmatrix}$$

$\mathbf{G}$  and  $\mathbf{D}$  are  $N \times N$  diagonal matrices representing the window function  $g_k$  and  $1 - g_k$ , respectively, which are defined as

$$\mathbf{G} = \text{diag}(\underbrace{0, \dots, 0}_{\Delta \text{ zeros}}, \underbrace{1, \dots, 1}_{\nu+1 \text{ ones}}, 0, \dots, 0)$$

N elements



and

$$\mathbf{D} = \text{diag}(\overbrace{1, \dots, 1}^{\Delta \text{ ones}}, \overbrace{0, \dots, 0}^{\nu+1 \text{ zeros}}, 1, \dots, 1)$$

where  $\text{diag}(\cdot)$  forms a diagonal matrix from its vector argument. The  $N \times N_w$  matrix  $\mathbf{F}$  is defined as

$$\mathbf{F} = \begin{bmatrix} \mathbf{I}_{N_w \times N_w} \\ \mathbf{0}_{(N-N_w) \times N_w} \end{bmatrix}$$

Here,  $\mathbf{I}_{N_w \times N_w}$  represents an  $N_w \times N_w$  identity matrix and  $\mathbf{0}_{(N-N_w) \times N_w}$  represents an  $(N - N_w) \times N_w$  matrix consisting of zeros. Define the FFT vector as

$$\mathbf{q}_i = \left[ 1 \quad e^{j2\pi i/N} \quad e^{j2\pi 2i/N} \quad \dots \quad e^{j2\pi(N-1)i/N} \right]^T \quad (4.2)$$

so that the inner product of  $\mathbf{q}_i^H$  with a  $N$ -point vector gives the  $i^{\text{th}}$  FFT coefficient of that vector. Using (4.1) and (4.2), the FFTs of (4.1) can be written as

$$\begin{aligned} H_i^{\text{signal}} &= \mathbf{q}_i^H \mathbf{G} \mathbf{H} \mathbf{w} \\ H_i^{\text{ISI}} &= \mathbf{q}_i^H \mathbf{D} \mathbf{H} \mathbf{w} \\ H_i^{\text{noise}} &= \mathbf{q}_i^H \mathbf{F} \mathbf{w} \end{aligned} \quad (4.3)$$

Finally, by substituting (4.3) into (3.5),

$$\text{SNR}_i^{\text{NEW}} = \frac{S_{x,i} |\mathbf{q}_i^H \mathbf{G} \mathbf{H} \mathbf{w}|^2}{S_{n,i} |\mathbf{q}_i^H \mathbf{F} \mathbf{w}|^2 + S_{x,i} |\mathbf{q}_i^H \mathbf{D} \mathbf{H} \mathbf{w}|^2} \quad (4.4)$$

This definition includes the effect of both ISI and a TEQ.

To find the optimal TEQ which maximizes  $b_{DMT}$  given by (2.30), I expand the absolute value quantities in (4.4)

$$\text{SNR}_i^{\text{NEW}} = \frac{\mathbf{w}^T \mathbf{H}^T \mathbf{G}^T \mathbf{q}_i S_{x,i} \mathbf{q}_i^H \mathbf{G} \mathbf{H} \mathbf{w}}{\mathbf{w}^T \mathbf{F}^T \mathbf{q}_i S_{n,i} \mathbf{q}_i^H \mathbf{F} \mathbf{w} + \mathbf{w}^T \mathbf{H}^T \mathbf{D}^T \mathbf{q}_i S_{x,i} \mathbf{q}_i^H \mathbf{D} \mathbf{H} \mathbf{w}} \quad (4.5)$$

$$= \frac{\mathbf{w}^T \mathbf{A}_i \mathbf{w}}{\mathbf{w}^T \mathbf{B}_i \mathbf{w}}$$

where

$$\mathbf{A}_i = \mathbf{H}^T \mathbf{G}^T \mathbf{q}_i S_{x,i} \mathbf{q}_i^H \mathbf{G} \mathbf{H} \quad (4.6)$$

$$\mathbf{B}_i = \mathbf{F}^T \mathbf{q}_i S_{n,i} \mathbf{q}_i^H \mathbf{F} + \mathbf{H}^T \mathbf{D}^T \mathbf{q}_i S_{x,i} \mathbf{q}_i^H \mathbf{D} \mathbf{H} \quad (4.7)$$

Substituting this result into (2.30),

$$b_{DMT} = \sum_{i \in \mathcal{S}} \log_2 \left( 1 + \frac{1}{\gamma} \frac{\mathbf{w}^T \mathbf{A}_i \mathbf{w}}{\mathbf{w}^T \mathbf{B}_i \mathbf{w}} \right) \text{ bits/symbol} \quad (4.8)$$

which gives the achievable capacity as a function of the TEQ taps  $\mathbf{w}$ .

No constraint is required during optimization to prevent a trivial solution [19] or an infinite gain equalizer [15]. The only constraint that might be placed on the denominator is to prevent a division by zero. This is not necessary in practice because the denominator represents channel noise plus ISI power. Even if the equalizer were perfect and there were no ISI, some channel noise would be present.

Thus, I can find the maximum channel capacity (MCC) TEQ that maximizes  $b_{DMT}$  by applying an unconstrained nonlinear programming method such as the quasi-Newton, conjugate gradient, or simplex algorithms [41] to maximize (4.8). I use the Broyden-Fletcher-Goldfarb-Shanno quasi-Newton algorithm [41] (fminu) in the MATLAB optimization toolbox to find the MCC-TEQ.

The model proposed in Chapter 3 leads to a nonlinear optimization problem of maximizing (4.8) to find the optimal MCC-TEQ as does the geometric TEQ method [15], but the MCC-TEQ design method

- includes the effect of ISI as part of the proposed subchannel SNR model;
- does not make unrealistic assumptions to obtain the achievable capacity as a function of equalizer taps;
- does not require constraints for the optimization problem, which enables the use of faster optimization methods;
- does not have ad-hoc parameters, such as  $\text{MSE}_{max}$ , which would need to be adjusted for different channels; and
- obtains the TEQ taps directly from the optimization, unlike the geometric TEQ method which calculates the equalizer by using (2.36) after the TIR is obtained from the optimization.

### 4.3 Optimal Number of Taps in a MCC TEQ

This section studies the achievable bit rate for different number of taps in the equalizer. More taps in the TEQ means higher computation complexity in the design procedure as well as the TEQ implementation. More taps also generally means higher channel capacity. I compare the achievable bit rate with the upper bound (MFB) bit rate via simulations.

For the simulations, I start with the CSA loop 4 ADSL channel which is one of the hardest to equalize. Given a cyclic prefix length of 32, coding gain of 4.2 dB, system margin of 6 dB, input power of 14 dBm, AWGN power of  $-113$  dBm/Hz, and 10 ADSL disturbers causing NEXT noise, the achievable and upper bound bit rates vs. number of taps is shown in Fig. 4.1. The upper bound performance does not depend on the number taps hence is constant in

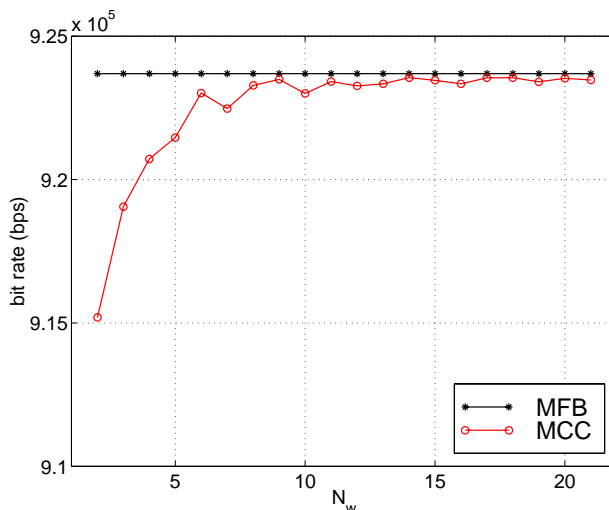


Figure 4.1: Achievable bit rate vs. the number of equalizer taps for CSA loop 4,  $\nu = 32$ ,  $N = 512$ , coding gain = 4.2 dB, margin = 6 dB, input power = 14 dBm, and AWGN power  $-113$  dBm/Hz. NEXT noise modeled as 10 ADSL disturbers.

Fig. 4.1. With a two-tap TEQ, a bit rate of 915 kb/s can be achieved while the upper bound bit rate is 924 kb/s. This means more than 99% of the MFB bit rate is achieved with a two-tap TEQ.

I repeat the experiment for the other seven CSA loops to see whether or not a two-tap equalizer performs similarly in each case. Table 4.1 lists the achievable bit rate with a two-tap TEQ, the MFB bit rate, and the optimal two-tap TEQ coefficients. For easier comparison, I normalize the TEQ coefficients so that the first coefficient is always one. This normalization does not change the value of  $b_{DMT}$  given by (4.8). As seen from Table 4.1 a two-tap TEQ achieves at worst 98.5% of the MFB bit rate. The complexity-performance tradeoff suggests that a two-tap equalizer is the best solution for

CSA loop number	Achievable bit rate (bps)	MFB bit rate (bps)	optimal coefficients	achievable MFB percentage
1	1,050,872	1,063,134	[1 -0.9644]	98.8%
2	1,122,817	1,132,436	[1 -0.9630]	99.2%
3	1,116,426	1,121,972	[1 -0.9691]	99.5%
4	915,191	923,695	[1 -0.9630]	99.1%
5	1,093,785	1,098,939	[1 -0.9670]	99.5%
6	988,353	1,000,247	[1 -0.9697]	98.8%
7	1,059,027	1,069,303	[1 -0.9701]	99.0%
8	1,043,288	1,059,479	[1 -0.9742]	98.5%

Table 4.1: Two-tap TEQ designed with the MCC method for the eight CSA loops.

the optimal TEQ design problem using the MCC TEQ.

### The Two-tap MCC TEQ

This section explains how a two-tap MCC TEQ can shorten a channel and optimize channel capacity. Based on two-port network model a channel frequency response can be approximated with an all-pole model [44]. An ADSL channel can generally be modeled with 7–9 poles [45]. The pole-zero plot of a nine-pole model for CSA loop 1 is shown in Fig 4.2.

Subscriber loop impulse responses generally have a tail which dies out exponentially. This tail can be approximated as the impulse response of a pole that is close to the unit circle. Fig. 4.3 shows the CSA loop 1 impulse response and the impulse response of the pole causing the tail. Although the other poles are affecting the shape of the tail, the primary reason for the tail is the pole close to the unit circle.

A two-tap equalizer has one zero (see Fig. 4.4) which is used to cancel

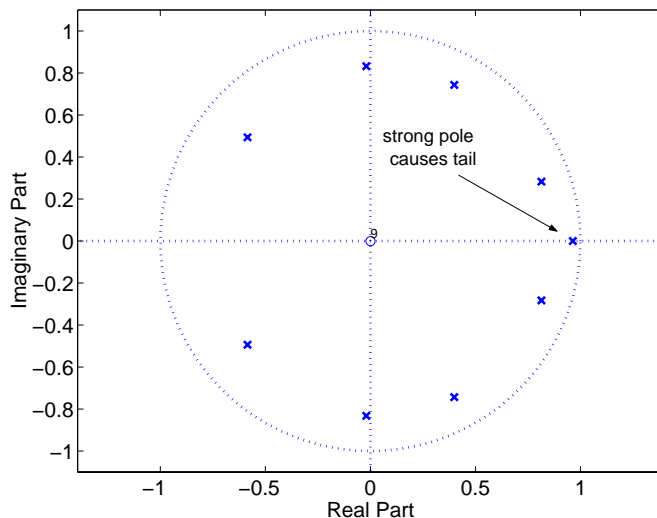


Figure 4.2: Pole-zero plot of a nine-pole model of CSA loop 1. The marked pole is close to the unit circle causing a long tail.

the pole causing the tail. In other words, the optimization in the MCC design method ensures that the zero of the TEQ is as close as possible to the pole causing the tail. Hence, the effect of the pole is cancelled by the zero.

Fig. 4.5 shows the nine-pole model of the equalized channel impulse response. The two-tap TEQ shifts the tail causing pole from  $z = 0.96$  to  $z = 0.41$ , which weakens the effect of the pole and makes the tail die out more quickly. The pole does not vanish because the zero cannot exactly be located on the pole using numeric optimization. A pole at  $z = 0.96$  would cause a long tail, whereas a pole at  $z = 0.41$  would die out more quickly.

Mathematically, a one-pole transfer function can be written as

$$H(z) = \frac{1}{1 - a z^{-1}} \quad (4.9)$$

where  $a$  determines the pole location. Using the inverse  $z$ -transform, with the

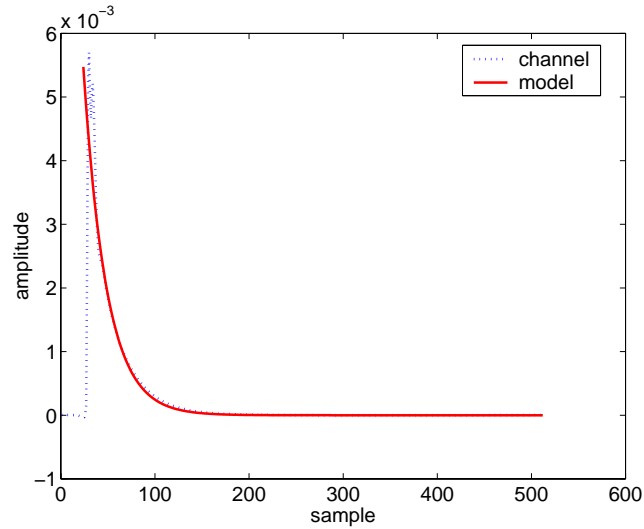


Figure 4.3: Impulse response of CSA loop 1 and the impulse response of the pole causing the tail shown in Fig 4.2.

assumption that the system is causal and stable, the impulse response is

$$h[n] = a^n u[n] \quad (4.10)$$

For a pole at  $a = 0.96$ , the impulse response is

$$h_{0.96}[n] = 0.96^n u[n] \quad (4.11)$$

which dies off with increasing  $n$  more slowly than

$$h_{0.41}[n] = 0.41^n u[n] \quad (4.12)$$

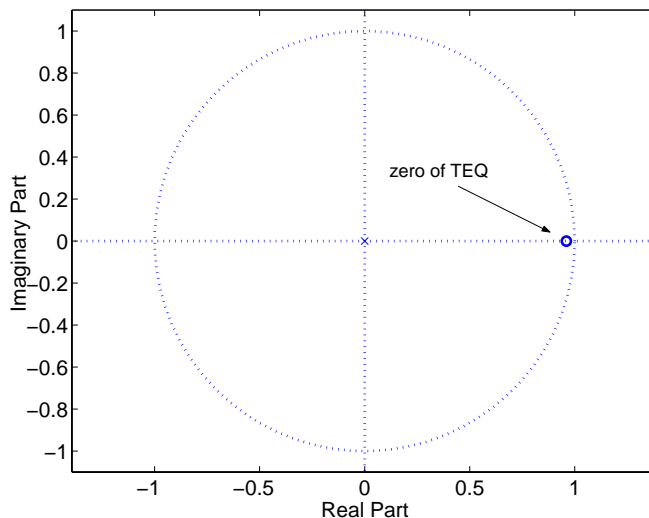


Figure 4.4: Pole-zero plot of a two-tap TEQ designed with the MCC method. The zero location is close to the tail causing pole location.

## 4.4 Optimal Cyclic Prefix Size for the MCC TEQ

The goal of this section is to analyze the performance of the MCC TEQ under different cyclic prefix sizes. As mentioned in Sec. 1.2.1, a cyclic prefix reduces the throughput of the channel proportional to its length. Hence, the cyclic prefix should be as short as possible. Fig. 4.6 shows how the performance for a two-tap MCC TEQ changes with respect to the cyclic prefix size.

As shown in Fig. 4.6, the MFB bit-rate drops with an increasing cyclic prefix size. The performance of the two-tap MCC TEQ becomes close to MFB for a cyclic prefix length of 16 or greater. The highest bitrate is achieved with a cyclic prefix length of 25. The achievable performance of the two-tap MCC TEQ is within the range of 920 kb/s to 923 kb/s for cyclic prefix sizes between



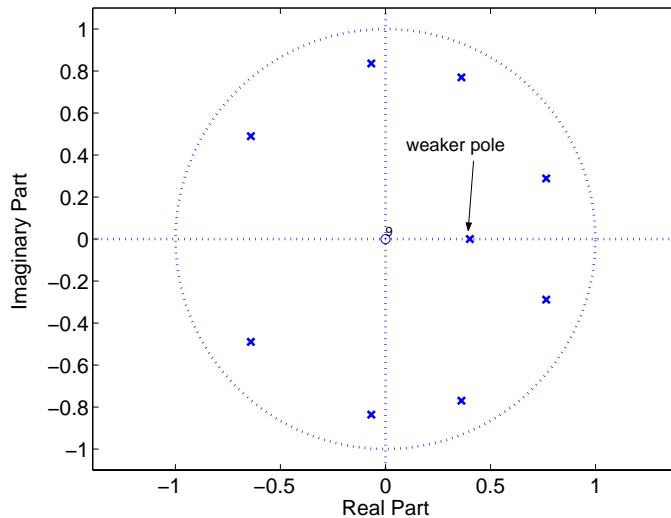


Figure 4.5: Pole-zero plot of the equalized channel impulse response. The two-tap TEQ shifted the tail causing pole away from the unit circle which weakens the effect of the pole hence shortens the tail.

17 and 32 samples. This means that the MCC design method obtains within 1% of channel capacity for a two-tap TEQ for a cyclic prefix length of 16 or higher.

Fig. 4.7 shows how the performance changes with respect to cyclic prefix size if a 17-tap MCC TEQ were used. Compared to the two-tap case in Fig. 4.6, the 17-tap performance of MCC TEQ reaches the MFB performance with a cyclic prefix of length 3. As expected, a shorter TEQ requires a longer cyclic prefix for acceptable performance whereas longer TEQ requires a shorter cyclic prefix to obtain similar performance.

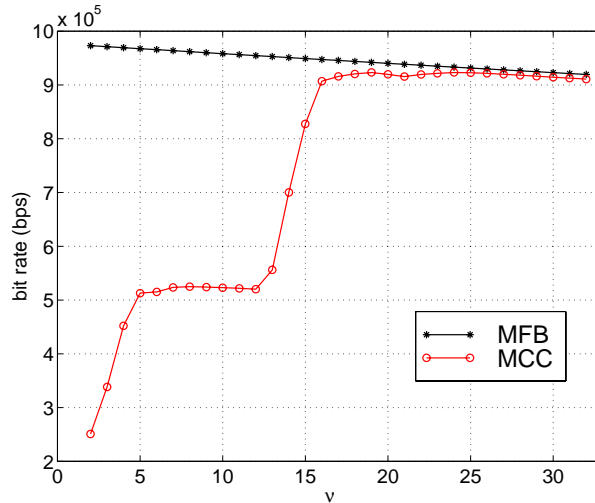


Figure 4.6: Achievable bit rate vs. cyclic prefix length  $\nu$  for CSA loop 4,  $N_w = 2$ ,  $N = 512$ , coding gain = 4.2 dB, margin = 6 dB, input power = 14 dBm, and AWGN power  $-113$  dBm/Hz. NEXT noise modeled as 10 ADSL disturbers.

## 4.5 Conclusion

Using the subchannel SNR model of Chapter 3, I write the achievable channel capacity as a nonlinear function of the TEQ taps. Maximizing this function gives the optimal MCC TEQ which performs close to the upper bound (MFB) performance. Simulation results show that a two-tap MCC TEQ can effectively shorten a channel and achieve close to upper bound performance given that the cyclic prefix size is greater than 15. In the case of a longer 17-tap MCC TEQ, the cyclic prefix size can be as small as 3 to achieve the desired upper bound performance. Most state-of-the-art ADSL systems use MMSE-based TEQ design algorithms which would require 17-21 taps for a cyclic prefix size of 32 samples. Taking into account the sampling rate for the G.DMT standard,

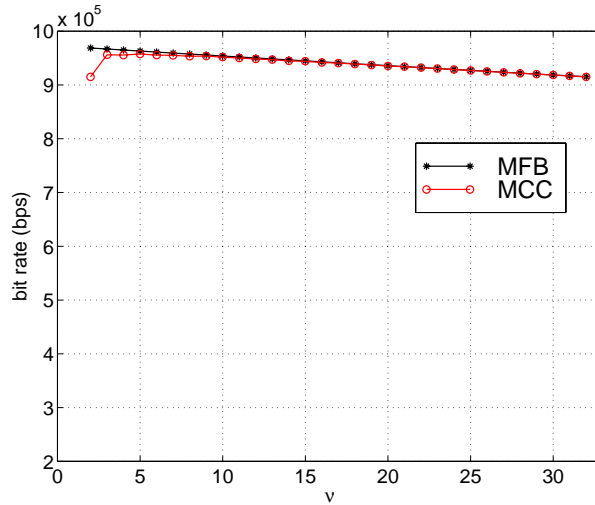


Figure 4.7: Achievable bit rate vs. cyclic prefix length  $\nu$  for CSA loop 4,  $N_w = 17$ ,  $N = 512$ , coding gain = 4.2 dB, margin = 6 dB, input power = 14 dBm, and AWGN power  $-113$  dBm/Hz. NEXT noise modeled as 10 ADSL disturbers.

the computation complexity of a 20-tap MMSE TEQ is 40 MIPS compared to only 4 MIPS for a two-tap MCC TEQ. The shorter MCC TEQ can be moved from hardware, which is a common choice for G.DMT ADSL transceivers, to software, which would reduce the cost of the modem. The MCC TEQ requires lower computational complexity yet it outperforms the MMSE TEQ in bit rate.

# Chapter 5

## The Near-Optimal Minimum-ISI Equalizer

The MCC TEQ given in Chapter 4 is optimum in the sense of channel capacity. However, a nonlinear optimization method is required to calculate the optimum TEQ which makes the MCC design method impractical for a low-cost real-time implementation. In this chapter, I propose a near-optimum minimum-ISI method for TEQ design. The minimum-ISI TEQ reaches 99% of the channel capacity of the optimum method but does not require a nonlinear optimization method. I develop fast algorithms for the minimum-ISI method.

The minimum-ISI method is based on my observation that the only effect that TEQ has on channel capacity is the way it distributes ISI power over frequency. Minimizing the sum of the ISI power over all of the subchannels would reduce ISI but does not optimize the distribution of ISI power over frequency. In high noise regions, ISI is dominated by the noise and its effect on SNR can be ignored. If the same amount of ISI were placed in low

noise frequency bands, then ISI would be reduced dramatically. Although the mathematical derivation suggests a weighting of ISI with the inverse of the channel noise, I instead incorporate the channel gain into the frequency weighting which gives better results.

## 5.1 Introduction

Calculating the MCC TEQ taps requires solving a nonlinear optimization problem. Even if a fast optimization algorithm were used, finding the global optimum can be a computationally expensive process. Avoiding nonlinear optimization methods is key in developing cost-effective equalizers for real-time applications. In this section, I propose the minimum-ISI equalizer which can be calculated without using a globally optimal nonlinear programming method.

The capacity of a multicarrier channel is the sum of capacities of the AWGN subchannels. The capacity of AWGN channel is a logarithm function of its SNR. Therefore, the capacity of the multicarrier channel is a sum of logarithms which is a nonlinear function. To avoid nonlinearity, hence nonlinear optimization, I avoid using capacity as the objective function.

The key observation behind the minimum-ISI equalizer is that both the signal and channel noise are filtered by the equalizer; hence, they are both shaped with the same frequency response. In other words, the change in SNR before and after equalization is due to the effect on the ISI and not on the signal or the noise. The MCC design method tends to push the residual ISI (if any remains) into frequency bands with lowest SNR or equivalently the highest amount of noise. ISI in low SNR frequency bands is dominated by channel noise and therefore does not affect the SNR. This motivates the proposed

method which minimizes a weighted ISI so that the residual ISI is primarily in low SNR frequency bands.

This chapter is organized as follows. Section 5.2 derives the objective function and constraint for minimizing ISI. Section 5.3 derives the min-ISI TEQ design method. Section 5.4 evaluates the performance of the min-ISI design method with respect to the number of taps in the TEQ. Section 5.5 evaluates it with respect to the cyclic prefix size. Section 5.6 presents recursive algorithms for fast implementation. Section 5.7 concludes this chapter.

## 5.2 Minimizing ISI

The idea behind the min-ISI method can be explained from (4.5). In (4.5), both the numerator and the denominator contain power terms. Since a power term is always nonnegative, minimizing the distortion power in each subchannel (the denominator of  $\text{SNR}_i^{NEW}$ ) is equivalent to minimizing the sum of the distortion power of all subchannels

$$\sum_{i \in \mathcal{S}} \left( \mathbf{w}^T \mathbf{F}^T \mathbf{q}_i S_{n,i} \mathbf{q}_i^H \mathbf{F} \mathbf{w} + \mathbf{w}^T \mathbf{H}^T \mathbf{D}^T \mathbf{q}_i S_{x,i} \mathbf{q}_i^H \mathbf{D} \mathbf{H} \mathbf{w} \right)$$

where  $\mathcal{S}$  is the set of used subchannels and  $\mathbf{q}_i^H \mathbf{F} \mathbf{w}$  is the  $i^{\text{th}}$   $N$ -point FFT coefficient of  $\mathbf{w}$ . Normalizing with  $S_{n,i}$ ,

$$\sum_{i \in \mathcal{S}} \mathbf{w}^T \mathbf{F}^T \mathbf{q}_i \mathbf{q}_i^H \mathbf{F} \mathbf{w} + \sum_{i \in \mathcal{S}} \mathbf{w}^T \mathbf{H}^T \mathbf{D}^T \mathbf{q}_i (S_{x,i}/S_{n,i}) \mathbf{q}_i^H \mathbf{D} \mathbf{H} \mathbf{w} \quad (5.1)$$

The first term in (5.1) is the squared sum of the  $N$ -point FFT coefficients of  $\mathbf{w}$ , which is equal to the squared sum of the coefficients of  $\mathbf{w}$  due to Parseval's Theorem:

$$\mathbf{w}^T \mathbf{w} + \mathbf{w}^T \mathbf{H}^T \mathbf{D}^T \sum_{i \in \mathcal{S}} \left( \mathbf{q}_i \frac{S_{x,i}}{S_{n,i}} \mathbf{q}_i^H \right) \mathbf{D} \mathbf{H} \mathbf{w} \quad (5.2)$$

The first term does not affect the minimization of (5.2) for a constant norm  $\mathbf{w}$ . Directly minimizing the second term

$$\mathbf{w}^T \mathbf{H}^T \mathbf{D}^T \sum_{i \in \mathcal{S}} \left( \mathbf{q}_i (S_{x,i}/S_{n,i}) \mathbf{q}_i^H \right) \mathbf{D} \mathbf{H} \mathbf{w} = \mathbf{w}^T \hat{\mathbf{X}} \mathbf{w} \quad (5.3)$$

can also minimize the total signal power. To prevent this, I use the constraint

$$\|\mathbf{h}^{signal}\|^2 = \mathbf{w}^T \mathbf{H}^T \mathbf{G}^T \mathbf{G} \mathbf{H} \mathbf{w} = \mathbf{w}^T \mathbf{Y} \mathbf{w} = 1$$

This ensures that the norm of the signal path impulse response is one. Hence, the output signal power is equal to the input signal power. Finally, the optimization problem for minimum ISI becomes

$$\min_{\mathbf{w}} \mathbf{w}^T \hat{\mathbf{X}} \mathbf{w} \quad \text{s.t.} \quad \mathbf{w}^T \mathbf{Y} \mathbf{w} = 1 \quad (5.4)$$

Solving (5.4) minimizes ISI and generalizes the MSSNR method [12]. The constraints in both methods are equivalent in that they set the norm of the signal path impulse response to one. The MSSNR method minimizes the norm of the ISI path impulse response. The above derivation for minimizing ISI first maps the ISI path impulse response to the FFT domain, then weights the FFT coefficients with the signal power to noise power ratio ( $S_{x,i}/S_{n,i}$ ), and finally minimizes the norm of the weighted ISI path impulse response. The product of  $S_{x,i}$  with the ISI path power spectrum gives the ISI power. The ISI power is weighted with the inverse of the noise power.

The MSSNR method minimizes the energy in the ISI path impulse response while the minimizing ISI approach minimizes the power at the output of the ISI path impulse response. This is a significant difference. The MSSNR method overspecifies the problem by minimizing the ISI path over the entire bandwidth whereas the min-ISI method has an additional degree of freedom

to improve the performance by *not* minimizing the ISI path impulse response at unused frequency bands (subchannels). Both methods are equivalent if the ratio of the signal power to the noise power is one for all subchannels.

The weighting function emphasizes the placement of ISI in the frequencies with high SNR (low noise power). A small amount of ISI power in subchannels with low noise power can reduce the SNR dramatically. In subchannels with low SNR, however, the noise power is large enough to dominate the ISI power such that the effect of ISI power on the SNR is negligible. This explains why the MSSNR method is not optimal in the sense of maximum channel capacity – it treats ISI in low and high SNR subchannels equally.

### 5.3 The Minimum-ISI Design Method

Simulation results show that equalizers designed with the frequency weighting function  $(S_{x,i}/S_{n,i})$  still allow considerable ISI power in high SNR frequency bands. Weighting by  $(|H_i|^2 S_{x,i}/S_{n,i})$  gives considerable improvement where  $|H_i|^2$  is the channel gain in the  $i^{th}$  subchannel. Therefore, I propose the min-ISI method to be

$$\min_{\mathbf{w}} \mathbf{w}^T \mathbf{X} \mathbf{w} \quad \text{s.t.} \quad \mathbf{w}^T \mathbf{Y} \mathbf{w} = 1 \quad (5.5)$$

where

$$\mathbf{X} = \mathbf{H}^T \mathbf{D}^T \sum_{i \in \mathcal{S}} \left( \mathbf{q}_i (|H_i|^2 S_{x,i}/S_{n,i}) \mathbf{q}_i^H \right) \mathbf{D} \mathbf{H} \quad (5.6)$$

$$\mathbf{Y} = \mathbf{H}^T \mathbf{G}^T \mathbf{G} \mathbf{H} \quad (5.7)$$

Other weighting functions could be applied. For example, if some subchannels were not used in data transmission, then maximizing the SNR in those subchannels is not necessary. A weighting function which is zero at these



subchannels could relax the minimization problem in (5.5) and lead to better solutions.

Next, I propose an alternative solution for the problem in (5.4) and (5.5) which can also be applied to solve the MSSNR problem in (2.20). Given  $\mathbf{X}$  and  $\mathbf{Y}$ , I form the Lagrangian

$$L(\mathbf{w}, \lambda) = \mathbf{w}^T \mathbf{X} \mathbf{w} + \lambda(\mathbf{w}^T \mathbf{Y} \mathbf{w} - 1) \quad (5.8)$$

where  $\lambda$  is the Lagrange multiplier. By taking the gradient of (5.8) with respect to  $\mathbf{w}$  and setting the result to zero,

$$\frac{\partial L(\mathbf{w}, \lambda)}{\partial \mathbf{w}} = 2\mathbf{X} \mathbf{w} + 2\lambda \mathbf{Y} \mathbf{w} = 0$$

The solution for  $\mathbf{w}$  is the optimal solution  $\mathbf{w}^*$  for (5.4) and has to satisfy

$$\mathbf{X} \mathbf{w}^* = \hat{\lambda} \mathbf{Y} \mathbf{w}^* \quad (5.9)$$

where  $\hat{\lambda} = -\lambda$ . This implies that  $\mathbf{w}^*$  is one of the generalized eigenvectors of the matrix pencil  $(\mathbf{X}, \mathbf{Y})$  and  $\hat{\lambda}$  is the corresponding generalized eigenvalue. Substituting (5.9) into (5.3), the minimum value for (5.3) is

$$\mathbf{w}^{*T} \mathbf{X} \mathbf{w}^* = \hat{\lambda} \mathbf{w}^{*T} \mathbf{Y} \mathbf{w}^*$$

Since the minimum is proportional to the generalized eigenvalue, the minimum generalized eigenvalue and corresponding eigenvector should be chosen as the solution of (5.4).

The generalized eigenvalue problem can be converted to a regular eigenvalue problem as follows:

$$\begin{aligned} \mathbf{X} \mathbf{w}^* &= \hat{\lambda} \mathbf{Y} \mathbf{w}^* \\ \frac{1}{\hat{\lambda}} \mathbf{w}^* &= (\mathbf{X}^{-1} \mathbf{Y}) \mathbf{w}^* \\ \tilde{\lambda} \mathbf{w}^* &= \mathbf{Z} \mathbf{w}^* \end{aligned}$$

The minimum generalized eigenvalue ( $\hat{\lambda}$ ) of the matrix pair  $\mathbf{X}$  and  $\mathbf{Y}$  is equivalent to the maximum eigenvalue ( $\tilde{\lambda}$ ) of the matrix  $\mathbf{Z}$ . Since  $\mathbf{w}^T \mathbf{X} \mathbf{w}$  is the total distortion power,  $\mathbf{w}^T \mathbf{X} \mathbf{w} \geq 0 \forall \mathbf{w} \neq \mathbf{0}$ . In practice, the total distortion power would always be non-zero; hence,  $\mathbf{X}$  is positive definite and invertible.

Only the maximum eigenvalue and corresponding eigenvector of  $\mathbf{Z}$  needs to be calculated. One approach could be to use the power method [31] which is a simple iterative algorithm to find the dominant (maximum) eigenvalue and its corresponding eigenvector. The  $k^{th}$  iteration of the power method is

$$\begin{aligned} \mathbf{z}^{(k)} &= \mathbf{Z} \mathbf{w}^{(k-1)} \\ \mathbf{w}^{(k)} &= \mathbf{z}^{(k)} / \|\mathbf{z}^{(k)}\| \\ \tilde{\lambda}^{(k)} &= \mathbf{w}^{(k)T} \mathbf{Z} \mathbf{w}^{(k)} \end{aligned}$$

Note that  $\tilde{\lambda}^{(k)}$  does not have to be calculated since we only care about  $\mathbf{w}$ . The convergence rate of this algorithm depends on the ratio of the dominant eigenvalue to the second largest eigenvalue [31]. To avoid computing the inverse of  $\mathbf{X}$ , the following modification of the power method could be used:

$$\begin{aligned} \mathbf{y}^{(k)} &= \mathbf{Y} \mathbf{w}^{(k-1)} \\ \text{solve for } \mathbf{z}^{(k)} \text{ in } \mathbf{X} \mathbf{z}^{(k)} &= \mathbf{y}^{(k)} \\ \mathbf{w}^{(k)} &= \mathbf{z}^{(k)} / \|\mathbf{z}^{(k)}\| \end{aligned}$$

Since  $\mathbf{X}$  does not change, one could perform LU decomposition once on  $\mathbf{X}$  before the iteration begins to simplify the second step.

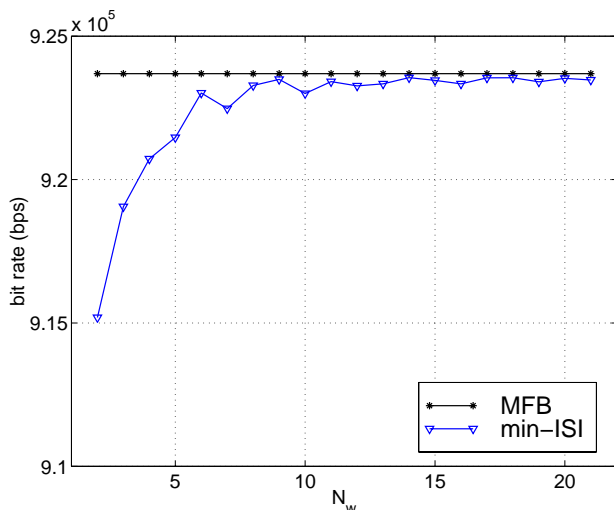


Figure 5.1: Achievable bit rate vs. the number of equalizer taps for CSA loop 4,  $\nu = 32$ ,  $N = 512$ , coding gain = 4.2 dB, margin = 6 dB, input power = 14 dBm, AWGN power  $-113$  dBm/Hz, NEXT noise modeled as 10 ADSL disturbers.

## 5.4 Optimal Number of Taps in a Min-ISI TEQ

As in the case of the MCC-TEQ in Chapter 4, I analyze the effect of the number of TEQ taps on the performance. All simulations use CSA loop 4 for the channel model. For a cyclic prefix length of 32, coding gain of 4.2 dB, system margin of 6 dB, input power of 14 dBm, AWGN power of  $-113$  dBm/Hz, and 10 ADSL disturbers causing NEXT noise, the bitrate vs. TEQ length is plotted in Fig. 5.1. The performance of the min-ISI TEQ follows the same trend as the MCC TEQ with respect to the number of taps. A two-tap TEQ delivers 99% of the upper bound performance. The min-ISI design method does not require a nonlinear optimization method, hence is computationally less complex than the MCC design method.

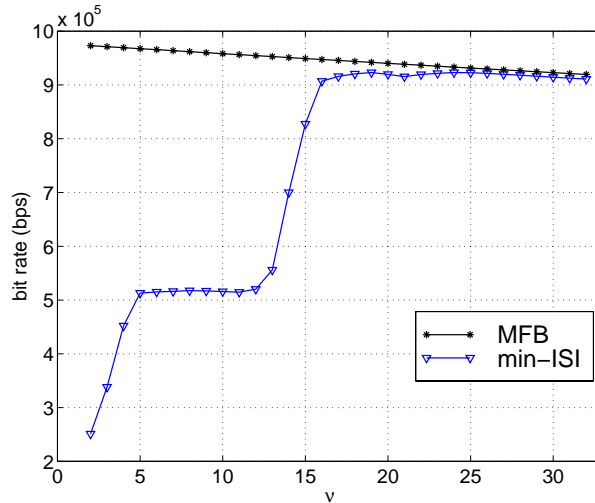


Figure 5.2: Achievable bit rate vs. cyclic prefix length  $\nu$  for CSA loop 4,  $N_w = 2$ ,  $N = 512$ , coding gain = 4.2 dB, margin = 6 dB, input power = 14 dBm, AWGN power  $-113$  dBm/Hz, NEXT noise modeled as 10 ADSL disturbers.

## 5.5 Optimal Cyclic Prefix Size for the Min-ISI TEQ

The goal of this section is to analyze the performance of the min-ISI TEQ under different cyclic prefix sizes. Fig. 5.2 shows the performance of a two-tap min-ISI TEQ with respect to cyclic prefix size. Again the min-ISI TEQ performs virtually equally to the optimal MCC TEQ. Given a two-tap min-ISI TEQ, a cyclic prefix of 16-17 samples is required to achieve upper bound performance.

Fig. 5.3 shows how the performance changes with respect to cyclic prefix size of a 17-tap min-ISI TEQ. Compared to the two-tap case in Fig. 5.2, the 17-tap performance of MCC-TEQ reaches the MFB performance with a

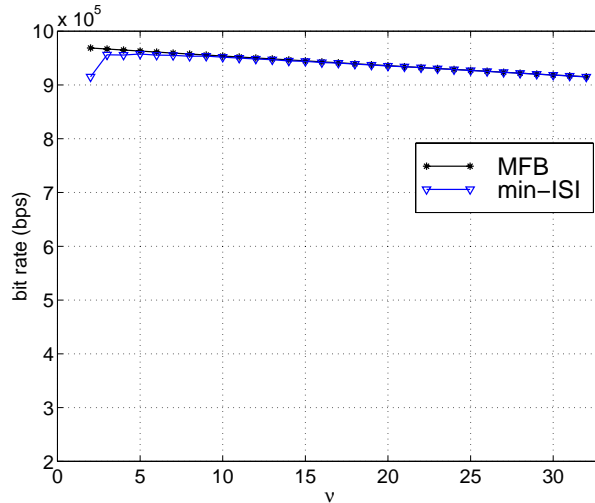


Figure 5.3: Achievable bit rate vs. cyclic prefix length  $\nu$  for CSA loop 4,  $N_w = 17$ ,  $N = 512$ , coding gain = 4.2 dB, margin = 6 dB, input power = 14 dBm, AWGN power  $-113$  dBm/Hz, NEXT noise modeled as 10 ADSL disturbers.

cyclic prefix of three samples. In general, the number of TEQ taps plus the cyclic prefix length should be 20 to exceed 98% of the matched filter bound. As expected, a smaller TEQ requires a larger cyclic prefix for acceptable performance while a large TEQ requires a small cyclic prefix to obtain similar performance.

## 5.6 Fast Min-ISI TEQ Design Methods

The problem in (5.4) is equivalent to (2.20) with the only difference being that  $\mathbf{A}$  is replaced with  $\mathbf{X}$ . The constraint matrices  $\mathbf{Y}$  and  $\mathbf{B}$  are equal. The solution to (5.4) is equivalent to that of (2.20) given by (2.22) with the only difference being that  $\mathbf{A}$  is replaced with  $\mathbf{X}$ . The computational complexity of

the two methods differ only in the calculation of  $\mathbf{X}$  and  $\mathbf{A}$ . Using symmetry properties of  $\mathbf{H}_{wall}$  and  $\mathbf{H}_{win}$ , the calculation of  $\mathbf{A}$  requires  $\mathcal{O}(N N_w)$  multiplications and additions for a channel length  $L_h$  equal to  $N$ . I assume that the channel length does not exceed the symbol length. In general,  $N > N_w$ , e.g,  $N = 512$  and  $N_w = 17$ . The frequency domain weighting of the  $\mathbf{X}$  matrix destroys some of the symmetry properties, which results in a higher computational complexity of  $\mathcal{O}(N^2 N_w)$ .

### 5.6.1 Recursive Min-ISI Method

#### Calculating Matrix $\mathbf{Y}$

The  $n^{\text{th}}$  column of the convolution matrix  $\mathbf{H}$  can be written as

$$\mathbf{H}_n = \begin{bmatrix} h_{0-n} & h_{1-n} & \dots & h_{N-n} \end{bmatrix}^T$$

where  $h_i = 0$  for  $i < 0$ . Multiplying with  $\mathbf{G}$  gives

$$\mathbf{GH}_n = \begin{bmatrix} \mathbf{0}_{1,\Delta} & h_{\Delta-n+1} & \dots & h_{\Delta+\nu-n+1} & \mathbf{0}_{1,\Delta} \end{bmatrix}^T$$

where  $\mathbf{0}_{1,\Delta}$  denotes a row vector consisting of  $\Delta$  zeros. Then the elements of  $\mathbf{Y}$  are

$$Y_{m,n} = (\mathbf{GH}_m)^T (\mathbf{GH}_n) = \sum_{k=\Delta}^{\Delta+\nu} h_{k-m} h_{k-n} \quad (5.10)$$

From (5.10),

$$Y_{m+1,n+1} = \sum_{k=\Delta-1}^{\Delta+\nu-1} h_{k-m} h_{k-n}$$

which gives the following recursive formula on the diagonals of  $\mathbf{Y}$

$$Y_{m+1,n+1} = Y_{m,n} - h_{\Delta+\nu-m} h_{\Delta+\nu-n} + h_{\Delta-1-m} h_{\Delta-1-n} \quad (5.11)$$

To calculate  $\mathbf{Y}$ , I first use (5.10) to calculate the first column directly, which takes  $N_w(\nu + 1)$  MACs. Then, I use the recursion in (5.11) to fill out the lower triangular part of  $\mathbf{Y}$ . This takes  $N_w(N_w - 1)$  MACs. Since  $\mathbf{Y}$  is symmetric, the upper triangular part does not need to be calculated. Therefore, calculating  $\mathbf{Y}$  requires

$$N_w(\nu + N_w)\text{MACs}$$

### Calculating the Matrix $\mathbf{X}$

The matrix  $\mathbf{X}$  in (5.6) can be written in the form

$$\mathbf{X} = (\mathbf{DH})^T \mathbf{V} (\mathbf{DH}) \quad (5.12)$$

where

$$\mathbf{V} = \sum_{i \in \mathcal{S}} \left( \mathbf{q}_i \left( \frac{|H_i|^2 S_{x,i}}{S_{n,i}} \right) \mathbf{q}_i^H \right) \quad (5.13)$$

$\mathbf{V}$  is an  $N \times N$  Hermitian matrix with its first column equal to the  $N$ -point IFFT of  $(|H_i|^2 S_{x,i}/S_{n,i})$  for  $i = 0, 1, \dots, N - 1$  with a scaling difference of  $N$ :

$$\mathbf{V} = \begin{bmatrix} v_0 & v_{N-1} & \cdots & v_2 & v_1 \\ v_1 & v_0 & \cdots & v_3 & v_2 \\ \vdots & \vdots & \ddots & \vdots & \vdots \\ v_{N-2} & v_{N-3} & \cdots & v_0 & v_{N-1} \\ v_{N-1} & v_{N-2} & \cdots & v_1 & v_0 \end{bmatrix} \quad (5.14)$$

Calculating  $\mathbf{V}$  requires one  $N$ -point IFFT. The product  $\mathbf{DH}$  does not require any multiplications because  $\mathbf{D}$  is a diagonal matrix consisting only of ones and zeros. Hence, multiplying with  $\mathbf{D}$  is equivalent to selecting elements of  $\mathbf{H}$ . With the assumption that  $N_w < \Delta$  only for representation purposes, the

product in expanded form becomes

$$\mathbf{DH} = \begin{bmatrix} h_0 & 0 & 0 & \cdots & 0 \\ h_1 & h_0 & 0 & \cdots & 0 \\ \vdots & \vdots & \vdots & \ddots & \vdots \\ h_{N_w-1} & h_{N_w-2} & h_{N_w-3} & \cdots & h_0 \\ h_{N_w} & h_{N_w-1} & h_{N_w-2} & \cdots & h_1 \\ \vdots & \vdots & \vdots & \ddots & \vdots \\ h_{\Delta-1} & h_{\Delta-2} & h_{\Delta-3} & \cdots & h_{\Delta-N_w} \\ 0 & 0 & 0 & \cdots & 0 \\ \vdots & \vdots & \vdots & \vdots & \vdots \\ 0 & 0 & 0 & \cdots & 0 \\ h_{\Delta+\nu} & h_{\Delta+\nu-1} & h_{\Delta+\nu-2} & \cdots & h_{\Delta+\nu-N_w+1} \\ \vdots & \vdots & \vdots & \ddots & \vdots \\ h_{N-1} & h_{N-2} & h_{N-3} & \cdots & h_{N-N_w} \end{bmatrix} \quad (5.15)$$

Using (5.14) and (5.15), the elements of  $\mathbf{X}$  can be written as

$$\begin{aligned}
X_{m,n} &= \sum_{k=0}^{\Delta-1} \sum_{l=0}^{\Delta-1} h_{k-m} h_{l-n} v_{|k-l|} \\
&+ \sum_{k=0}^{\Delta-1} \sum_{l=\Delta+\nu}^{N-1} h_{k-m} h_{l-n} v_{|k-l|} \\
&+ \sum_{k=\Delta+\nu}^{N-1} \sum_{l=0}^{\Delta-1} h_{k-m} h_{l-n} v_{|k-l|} \\
&+ \sum_{k=\Delta+\nu}^{N-1} \sum_{l=\Delta+\nu}^{N-1} h_{k-m} h_{l-n} v_{|k-l|} \\
&= X_{m,n}^1 + X_{m,n}^2 + X_{m,n}^3 + X_{m,n}^4 \quad (5.16)
\end{aligned}$$

The double sums in (5.16) allow us to decompose  $\mathbf{X}$  into the sum of



four matrices, each of the form

$$P_{m,n} = \sum_{k=a}^b \sum_{l=c}^d h_{k-m} h_{l-n} v_{|k-l|} \quad (5.17)$$

Then,

$$P_{m+1,n+1} = \sum_{k=a-1}^{b-1} \sum_{l=c-1}^{d-1} h_{k-m} h_{l-n} v_{|k-l|} \quad (5.18)$$

From (5.18), I find the following recursive formula for the diagonals of  $\mathbf{P}$

$$\begin{aligned} P_{m+1,n+1} &= P_{m,n} - h_{b-m} h_{d-n} v_{|b-d|} \\ &\quad - h_{b-m} f(c, d, b, n) \\ &\quad - h_{d-n} f(a, b, d, m) \\ &\quad + h_{a-1-m} h_{c-1-n} v_{|a-c|} \\ &\quad + h_{a-1-m} f(c, d, a-1, n) \\ &\quad + h_{c-1-n} f(a, b, c-1, m) \end{aligned} \quad (5.19)$$

where

$$f(\alpha, \beta, \gamma, \delta) = \sum_{k=\alpha}^{\beta-1} h_{k-\delta} v_{|k-\gamma|} \quad (5.20)$$

The first three parameters are constant for each occurrence of the function  $f$  in (5.19). The last parameter is either  $m$  or  $n$ . Since there are only  $N_w - 1$  possible values of  $m$  or  $n$  there are only  $4(N_w - 1)$  different values of  $f$ . Half of these values will require  $b - a$  MACs each, and the other half will require  $d - c$  MACs each, so in total  $2(N_w - 1)(b - a + d - c)$  MACs are required to compute all possible values of  $f$ . The possible values of  $f$  can be precomputed and stored in memory. In the special case that  $a = c$  and  $b = d$  we only have  $2(N_w - 1)$  different function evaluations, thus needing only  $2(N_w - 1)(b - a)$  MACs to compute all values of  $f$ . Once all possible values of  $f$  is calculated, only 8 MACs are needed to move from  $P_{m,n}$  to  $P_{m+1,n+1}$ ,

which has to be repeated  $N_w(N_w - 1)/2$  times totaling  $4N_w(N_w - 1)$  MACs. To calculate  $X_{m,n}$ , the recursion in (5.19) has to be applied to all four terms in (5.16). This results in a total of  $4(N_w - 1)(N + 3N_w - \nu - 2)$  MACs.

The first column of  $\mathbf{X}$  needs to be calculated in order to use the recursion in (5.19). One solution is to reformulate the matrix equation for  $\mathbf{X}$  in (5.12)

$$\mathbf{X}_0 = (\mathbf{D}\mathbf{H})^T \mathbf{V}\mathbf{D}\mathbf{H}_0 \quad (5.21)$$

where  $\mathbf{X}_0$  denotes the first column of  $\mathbf{X}$ .  $\mathbf{V}$  is a FFT-domain weighting matrix which can be implemented with one FFT,  $N$  complex multiplications, and one IFFT. Therefore, computing  $\mathbf{X}_0$  requires 2  $N$ -point FFTs and  $4N + N_w(N - \nu - 1)$  MACs. With the additional complexity of calculating the first column, the total number of computations needed to compute  $\mathbf{X}$  is  $4(N_w - 1)(N + 3N_w - \nu - 2) + 4N + N_w(N - \nu - 1) + 8N \log_2 N$ . Adding the complexity of calculating  $\mathbf{Y}$  yields 2  $N$ -point FFTs and  $4(N_w - 1)(N + 3N_w - \nu - 2) + N_w(N + N_w - 1) + 4N$  MACs.

## 5.7 Conclusion

The near-optimal min-ISI TEQ design method generalizes the MSSNR method by weighting ISI in the frequency domain. ISI in high SNR subchannels can reduce the SNR dramatically, while in low SNR subchannels, it is dominated by channel noise. A frequency domain weighting can push the residual ISI power into the low SNR subchannels to optimize the channel capacity. The near-optimal min-ISI TEQ performs as well as the optimal MCC TEQ yet it does not require a nonlinear optimization method.

The key difference between the MSSNR and min-ISI methods is that

<i>step</i>	<i>description</i>	$\times$ and $+$	$\div$
1	Calculate $\mathbf{X}$ using (5.16)	$4(N_w - 1)(N + 3N_w - \nu - 2) + 4N + N_w(N - \nu - 1) + 8N \log_2 N$	0
2	Calculate $\mathbf{Y}$ using (5.11)	$N_w(\nu + N_w)$	0
3	Decompose $\mathbf{X}$ into LU components	$\frac{1}{6}(2N_w - 1)N_w(N_w - 1)$	$\frac{1}{2}N_w(N_w - 1)$
4	Iterate the following until convergence		
4.1	$\mathbf{y}^{(k)} = \mathbf{Y}\mathbf{w}^{(k-1)}$	$N_w^2$	0
4.2	Backward and forward substitution to solve $\mathbf{z}^{(k)}$ from $\mathbf{X}\mathbf{z}^{(k)} = \mathbf{y}^{(k)}$	$(N_w - 1)N_w$	$2N_w$
4.3	$\mathbf{w}^{(k)} = \frac{\mathbf{z}^{(k)}}{\ \mathbf{z}^{(k)}\ }$	$N_w$	$N_w$

Table 5.1: The recursive min-ISI TEQ design algorithm. The total complexity of the algorithm is  $15N_w^2 + N_w(5N - 4\nu - 21) + 4(\nu + 2) + \frac{1}{6}(2N_w - 1)N_w(N_w - 1) + 8N \log_2 N$  MACs and  $\frac{1}{2}N_w(N_w + 5)$  divisions.

the MSSNR method minimizes the ISI path impulse response itself while the min-ISI method minimizes its output. That means that the min-ISI method does not minimize the ISI path in the subchannels with no input energy while the MSSNR method does. This gives the min-ISI method an additional degree of freedom to achieve optimal performance.

The computational complexity of the min-ISI method can further be reduced by using a generalized power iteration for the generalized eigenvalue decomposition. Most of the computational complexity, however, is in the calculation of the matrices in the objective function and constraint. The computation required for these matrices is dramatically reduced by using recursive

algorithms that exploit the symmetry properties of the matrices. The dominant factor in the computational complexity of the fast recursive min-ISI method is  $N N_w$ . Considering that  $N$  is 512 and  $N_w$  is either 17 – 32 taps in commercial ADSL modems or  $N_w$  is as small as two taps with the MCC and min-ISI methods, the fast min-ISI algorithm is a significant improvement over a naive implementation of the min-ISI method, which would have a dominant factor of  $N^2 N_w$ .

# Chapter 6

## Performance Evaluation

This chapter compares the achievable channel capacity using the proposed MCC and min-ISI TEQs with that of the MMSE, MGSNR, and MSSNR TEQs as well as with the MFB bound on channel capacity. The comparison is based on MATLAB simulations using the eight standard CSA loops as test channels. Results show that the proposed MCC and min-ISI methods outperform all of the previously reported methods in terms of achievable channel capacity for any length equalizer and any target channel length. In addition, the proposed MCC and min-ISI TEQs require only two taps to deliver the same channel capacity of 10-17 tap TEQs designed by previous methods. As a side benefit of testing the TEQ design methods, I developed a MATLAB DMTTEQ toolbox. The toolbox combines ten TEQ design methods. It has a graphical user interface which enables the user to select the TEQ design method and DMT simulation parameters, and see the results as a table as well as graphics.

## 6.1 Introduction

This chapter compares the achievable channel capacity using the proposed MCC and min-ISI TEQ design methods with that of the MMSE, MGSNR, and MSSNR TEQ design methods as well as with the MFB bound on channel capacity. Section 6.2 describes ADSL line characteristics. Section 6.3 highlights sources of noise in ADSL systems. Section 6.4 and 6.5 present simulation results to compare the performance of the proposed MCC and min-ISI design methods, as well as the MMSE, MGSNR, and MSSNR methods described in Chapter 2, to the MFB performance. Section 6.6 describes a new MATLAB DMTTEQ Toolbox. The toolbox can be used to design and test performance of TEQs designed with ten different design methods. More details about the DMTTEQ toolbox are given in Appendix A. Section 6.7 concludes this chapter.

## 6.2 Digital Subscriber Line Characteristics

The transmission characteristics of DSL loops determine the performance of DSL systems. DSL loops are based on existing analog telephone subscriber loops which were originally developed for voice communication. A subscriber loop consists of twisted pair cables that connect a local central office to customer premises. Two subscribers are connected to each other through central offices. Analog voice is digitized and time division multiplexed with other voice channels at the central office. The resulting digital voice/data stream is transmitted through central offices to the central office at the other end.

A subscriber loop can consist of several sections of copper twisted pairs

with different gauge cables. Each subscriber line section is either aerial, buried (without a conduit), or underground (protected within a dedicated conduit). Cables are grouped together to form bundles. Grouping of cables is an important factor resulting in crosstalk noise.

Because loop plant construction usually occurs ahead of customer service request, distribution cables are usually made available to all potential customer sites. It is common practice to have extra twisted pairs from the feeder to reach more potential customers. The unused distribution cables result in bridged taps. Loop plant design rules such as “resistance design” and “carrier serving area” limit the total bridged tap length to minimize magnitude loss and spectrum distortion in plain old telephone system (POTS) transmission.

Extending central office serving distances for voice channels is accomplished through a procedure of installing load coils. Load coils are typically installed for cables with a total length exceeding 15 kft. Although load coils flatten the frequency response in the voice band they cause attenuation in higher frequency bands.

The Carrier Serving Area (CSA) engineering guidelines were introduced in the early 1980s to shorten subscriber loop length, which reduces loop deployment cost and supports all future digital services. The CSA is roughly defined as a serving distance of 9 kft for 26 gauge loops and 12 kft for 24 gauge loops from the remote terminal. CSA design guidelines are [44]:

- All loops are unloaded.
- For loops with 26-gauge cable, the maximum allowable loop length, including bridged taps, is 9 kft.
- If all cable is coarser than 26 gauge, then the maximum allowable loop

length, including bridged taps, is 12 kft.

- Any single bridged tap is limited to 2 kft maximum length, and the total length of all bridged taps is limited to 2.5 kft maximum length.
- The total length of multi-gauge cable containing 26 gauge cable must not exceed  $12 - (3 \times L_{26}) / (9 - L_{BTAP})$  kft, where  $L_{26}$  is the total length of 26-gauge cable excluding bridged tap and  $L_{BTAP}$  is the total length of all bridged taps.
- It is suggested that no more than two gauges of cable should be used.

The eight standard CSA loops [1] are used as test channels in all of the simulations in this chapter. All channel impulse responses consist of 512 samples sampled at a rate of 2.208 MHz.

### 6.3 Channel Noise

Sources of digital subscriber loop noise can be classified into three groups: crosstalk noise, impulse noise, and background noise [44]. Crosstalk noise is caused by adjacent subscriber loops transmitting data. It can be further divided into two groups called near-end crosstalk (NEXT) and far-end crosstalk (FEXT). NEXT noise occurs when the adjacent loop transmits data in the same direction and a part of the power couples into the loop of interest. The noise is generated at the near end of the channel. Similarly, FEXT is caused by adjacent subscriber loops receiving data at the same time when the loop of interest transmits data. Since the power level of the signal attenuates due to the channel, FEXT noise is generally less powerful than NEXT noise.



NEXT noise can be the strongest noise source in a subscriber loop. It cannot be overcome by increasing the power level of the transmitted signal because that will cause crosstalk in the adjacent loop which will adapt by increasing its power level. The increase in the power level of the adjacent loop will increase the crosstalk noise in the loop of interest. Crosstalk noise, especially NEXT noise, is often the limiting factor in the capacity of subscriber loops for high-speed communications [44].

Crosstalk noise is generally modeled as a coupling filter fed by a random signal [1]. The random signal has the same bandwidth and statistical properties of a signal modulated with the modulation method being used by the adjacent loops. For example, if the adjacent loops are using ADSL, then the random signal should be a multicarrier modulated random signal. In modeling the electromagnetic coupling between two copper wires, the coupling filter is generally a highpass filter with increasing gain as frequency increases.

Impulse noise consists of impulses occurring at random times. Impulse noise causes detection errors at the receiver. It could be caused by low-quality hardware such as switches as well as natural sources such as lightning. The amplitude of the impulse noise is generally several times higher than that of the background noise.

Background noise is partially caused by the electromagnetic signals picked up by the subscriber loop acting like an antenna. Another source of this type of noise is semiconductor devices generating thermal noise. The combination of the various sources of background noise is generally modeled as white Gaussian noise. In subscriber loops without crosstalk, background noise is the limiting factor of channel capacity. If crosstalk exists, then the performance in high-frequency bands is generally dominated by crosstalk, but the performance

in low-frequency bands in generally dominated by background noise.

In the simulations in this chapter, the channel noise is modeled as a  $-114$  dBm AWGN distributed over the entire bandwidth plus near-end-cross-talk (NEXT) noise. The NEXT noise is modeled with the transfer function  $|H_{\text{NEXT}}|^2 = k_{\text{NEXT}} f^{1.5}$  where  $k_{\text{NEXT}} = \left(\frac{10}{49}\right)^{0.6} \times \frac{1}{1.134 \times 10^{13}}$ , which corresponds to 10 ADSL disturbers [1]. The input signal power is 14 dBm and the FFT size is set to  $N = 512$  (as used in the ANSI and G.DMT standards). Delay optimization has been applied to all of the TEQ design methods.

## 6.4 Number of equalizer taps and length of cyclic prefix

This section analyzes the performance of ten TEQ design methods with respect to the number of equalizer taps  $N_w$  and the length of the cyclic prefix  $\nu$ . First, the cyclic prefix length is set according to the ANSI and G.DMT standards, and the number of taps in the TEQ is varied. This analysis gives insight on how many taps are needed to obtain high performance for the various methods. The results are shown in Fig. 6.1

Given a cyclic prefix length of 32, the MMSE method and the geometric TEQ method require about 20 taps to achieve the best performance, based on Fig. 6.1. Current TEQ implementations in ADSL transceivers use 17-32 taps, which supports the results. The MCC and min-ISI method as well as the MSSNR method, however, achieve within 99% of upper-bound performance even with two taps. That means, it is possible to achieve better performance with a dramatically smaller equalizer. Fig. 6.1(b) shows that the MCC and

min-ISI methods give virtually equal performance and outperform the MSSNR method.

From Fig. 6.1, the MCC method does not require a cyclic prefix of 32 samples. Since long cyclic prefixes reduce channel throughput, one would like to find the smallest cyclic prefix length for which the upper bound on channel capacity can be achieved (that is, within 99.99% of maximum channel capacity). So, I set  $N_w = 17$  and vary  $\nu$  from 2 to 32. The results are shown in Fig. 6.2.

The MCC and min-ISI methods essentially reach maximum channel capacity for  $\nu = 5$  (Fig. 6.2(b)). This shows that a cyclic prefix length of 5 is enough to achieve upper bound performance when a 17-tap equalizer is used. Although not designed for maximum channel capacity, the MSSNR method performs close to the upper bound. Because the MSSNR design method requires  $N_w < \nu$ , the MSSNR method requires a cyclic prefix of a length of at least 18. The MMSE and geometric TEQ methods approach the upper bound performance only for  $\nu > 30$ . The slope in the performance of the upper bound is caused by the bit rate reduction with the factor  $\frac{N}{N+\nu}$  due to the increase in the cyclic prefix length.

Fig. 6.1 suggests that a two-tap equalizer can effectively shorten a channel. The objective of Fig. 6.3 is to find the smallest possible cyclic prefix length given a two-tap equalizer. With a two-tap equalizer, the MCC and min-ISI methods achieve the upper bound for  $\nu = 24$ . Using the proposed min-ISI method, a two-tap equalizer and a cyclic prefix length of 24 can outperform all previously reported methods with up to 21 taps and a cyclic prefix length smaller than 32. As expected, the MMSE and geometric TEQ methods cannot compete with the other methods for small  $N_w$ .

loop	achievable percentage of MFB bit rate					bit rate (bps)
	MMSE	geometric	MSSNR	min-ISI	MCC	MFB
1	92.79%	93.32%	98.57%	99.95%	99.95%	1,071,981
2	96.80%	97.39%	97.70%	99.87%	99.87%	1,150,606
3	93.77%	94.57%	98.18%	99.98%	99.98%	1,118,265
4	91.33%	91.82%	99.58%	99.98%	99.98%	916,545
5	92.53%	93.35%	99.77%	99.90%	99.90%	1,092,975
6	93.04%	93.32%	98.66%	99.97%	99.97%	987,836
7	93.07%	94.36%	99.95%	99.99%	100.00%	1,064,619
8	92.74%	94.04%	99.83%	99.99%	100.00%	1,060,797

Table 6.1: Achievable bit rates for the eight CSA loops equalized with the MMSE [6], geometric TEQ [12], MSSNR [11], the proposed min-ISI, and the proposed MCC methods, as a percentage of the maximum achievable bit rate in the case of no ISI or equivalently with an SNR equal to the matched filter bound (MFB).  $N_w = 17$ ,  $\nu = 32$ ,  $N = 512$ , coding gain = 4.2 dB, margin = 6 dB, input power = 14 dBm, AWGN power  $-113$  dBm/Hz, NEXT noise modeled as 10 ADSL disturbers.

## 6.5 Achievable bit rates for the CSA loops

The bit rate results for all ten TEQ design methods on all eight CSA test channels are listed in Table 6.1 for  $N_w = 17$  and  $\nu = 32$  and Table 6.2 for  $N_w = 2$  and  $\nu = 32$ . All results are obtained by averaging 100 simulation runs for each case.

Table 6.1 suggest that given a 17-tap equalizer, the bit rate loss is up to 10% for the MMSE and geometric TEQ methods, 2% for the MSSNR method, and less than 1% for the proposed MCC and min-ISI methods. The results given in Table 6.2 suggest that a two-tap equalizer can perform within 2% capacity loss provided that either the MSSNR, min-ISI, or MCC method is used to design it. The MMSE and geometric TEQ methods can only achieve

loop	achievable percentage of MFB bit rate					bit rate (bps)
	MMSE	geometric	MSSNR	min-ISI	MCC	MFB
1	29.40%	29.55%	98.47%	98.84%	98.84%	1,071,981
2	30.84%	29.49%	98.26%	99.22%	99.22%	1,150,606
3	32.50%	29.41%	99.17%	99.52%	99.52%	1,118,265
4	21.81%	22.66%	98.67%	99.07%	99.07%	916,545
5	28.68%	28.35%	99.15%	99.51%	99.51%	1,092,975
6	28.63%	28.35%	98.70%	98.93%	98.93%	987,836
7	26.68%	25.84%	98.77%	99.22%	99.22%	1,064,619
8	28.41%	28.56%	97.76%	99.05%	99.05%	1,060,797

Table 6.2: Achievable bit rates for the eight CSA loops equalized with the MMSE [6], geometric TEQ [12], MSSNR [11], the proposed min-ISI, and the proposed MCC methods, as a percentage of the maximum achievable bit rate in the case of no ISI or equivalently with an SNR equal to the matched filter bound (MFB).  $N_w = 2$ ,  $\nu = 32$ ,  $N = 512$ , coding gain = 4.2 dB, margin = 6 dB, input power = 14 dBm, AWGN power  $-113$  dBm/Hz, NEXT noise modeled as 10 ADSL disturbers.

30% of the achievable bit rate.

The poor performance of the MMSE method can be explained as follows. The MMSE method minimizes the difference between the TIR and the SIR. It minimizes both the difference inside the target window and outside the target window. Since the TIR is zero outside the window, minimizing the difference outside of the target window means forcing the SIR to lie inside the target window. However, the difference between the SIR and TIR inside the target window does not cause any ISI. Furthermore, the TIR and SIR has larger magnitude inside the target window than outside which means that difference between them inside the window causes the major part of the error. This means that the MMSE method primarily tries to minimize the difference inside the window, which does not cause ISI, instead of outside the window, which

causes ISI. A TEQ which has larger MSE caused by the difference inside the target window could give better performance than one that gives smaller MSE only caused by difference outside the target window. Therefore, minimizing the MSE is a less desirable approach for designing TEQs. The geometric TEQ method is the first approach to include a channel capacity maximization into the TEQ design procedure. However, with all of the approximations in formulating the GSNR, a constraint on the MSE is required to achieve good performance. This constraint forces the method to converge to a solution close to that of the MMSE method. Therefore, the geometric TEQ method cannot achieve much higher performance than the MMSE method.

Since ISI is caused only by the part of the SIR lying outside the target window, minimizing only the part outside would be a better approach than the MMSE approach. The MSSNR method gives the optimal solution in the sense of minimizing the energy of the SIR outside the target window. This solves the problem with the MMSE method, but is still not optimal in terms of achievable channel capacity as demonstrated by the simulations. It is, in general, not possible to force the SIR to lie entirely inside a target window with a finite length FIR equalizer. The part outside of the target window acts as an equivalent ISI path impulse response. The frequency response of the ISI path determines which frequency bins are going to carry the ISI power and by what amount. The distribution of this ISI power changes the SNR distribution, which in turn changes the channel capacity. The MSSNR method, however, does not consider the shape of the SIR lying outside the target window but only the energy.

Although the derivation of our min-ISI method is based on maximizing the channel capacity, it is a generalization of the MSSNR method. The pri-

mary difference between the two methods is that the proposed min-ISI method weights the residual ISI in frequency to penalize ISI in high SNR subchannels. This is accomplished by minimizing the output of the ISI path impulse response instead of the impulse response itself as in the MSSNR method. Weighting the energy lying outside the target window is no longer necessary. The MCC TEQ is not practical due to its computational complexity it gives good insight into the TEQ design problem. The MCC TEQ is also useful as a benchmark since it gives the optimal TEQ.

## 6.6 MATLAB DMTTEQ Toolbox

The MATLAB DMTTEQ Toolbox is a collection of MATLAB functions to design and test the following time domain equalizer design methods:

- Minimum mean squared error – unit-energy constraint [19],
- Minimum mean squared error – unit-tap constraint [19],
- Maximum shortening signal to noise ratio method [12],
- Maximum geometric SNR method [15],
- Divide and conquer – cancellation (designed and implemented by Biao Lu) [38],
- Divide and conquer – minimization (designed and implemented by Biao Lu) [38],
- Maximum channel capacity method [46],
- Minimum intersymbol interference method [46],

- Matrix pencil design method (designed and implemented by Biao Lu) [38],
- Modified matrix pencil design method (designed and implemented by Biao Lu) [38].

The toolbox is available at

<http://signal.ece.utexas.edu/~arslan/dmtteq/dmtteq.html>

The toolbox has a graphical user interface (GUI) which enables the design of a TEQ by one of the methods above and testing of its performance. A snapshot of the GUI is shown in Fig. 6.4. In the upper right of the control window is a pulldown menu from which a design method can be chosen. Below this pulldown menu are the following editable text windows which are used to set the design and simulation parameters:

- Shortened impulse response (SIR) length. This is the desired length of the channel after equalization. For example, it should be set to 33 (one plus the cyclic prefix length) for the ANSI and G.DMT ADSL standards.
- Time domain equalizer (TEQ) length. Defines the number of taps of the TEQ.
- Fast Fourier transform (FFT) size. Sets the FFT size used in DMT modulation. It is twice the number of subchannels.
- Coding gain (dB). Defines a coding gain in dB which is used during capacity calculations [39].
- Margin (dB). Sets the desired system margin in dB. This is also used in capacity calculations [39].



- Dmin and Dmax. The interval of  $\Delta \in [D_{min} D_{max}]$  in which to search for the optimal delay value.
- Input power (dBm). Defines the input signal power in dBm.
- AWGN power (dBm/Hz). Sets the amount of additive white Gaussian noise in dBm/Hz. AWGN is added to the near-end crosstalk noise.
- CSA loop # (1-8). Selects the desired ADSL channel on which to run the simulation. Currently the eight standard CSA loops are supported [1].

Below the editable text windows is another pull-down menu which is used to select the desired graph to be displayed. The following graphics can be selected:

- Target & shortened channel. Displays the shortened channel impulse response and the target channel impulse response for the MMSE and geometric SNR methods. For all other methods, the location of the target window is displayed instead of a target impulse response.
- TEQ impulse response. Shows the impulse response of the TEQ.
- TEQ frequency response. Shows the frequency response of the TEQ.
- SNR & MFB. The SNR and matched filter bound to the SNR is displayed as a function of frequency (subchannels).
- Original & shortened channel. Displays the channel impulse response before and after equalization.

- Noise power spectrum. Shows the power spectrum of the noise which consists of NEXT noise plus AWGN.
- Delay plot. Displays the performance measure (i.e., MSE, SSNR, channel capacity) of the method with respect to the delay.
- Equalized channel frequency response. Displays the frequency response of the channel after equalization.

The two remaining buttons in the control frame are

- Info. Displays information on how to use the GUI.
- Calculate. Starts the calculation and performance evaluation of the TEQ.

The following performance measures are calculated and listed in the table:

- Rate. Gives the achievable bit rate with the given channel and TEQ settings.
- SNR. Shows the SNR at the output of the equalizer in dB.
- SSNR. Shows the shortening SNR in dB. This is defined as the ration of the energy of the shortened channel impulse response in the target window the energy outside the target window.
- MSE. Gives the MSE for the MMSE and geometric SNR methods.
- Delay. Shows the optimal delay for the system.
- Max Rate. Shows the absolute maximum achievable bit rate given the channel and equalizer settings. It is calculated from the MFB.

Once all of the design and simulation parameters are set to the desired values and the design method is chosen, the user hits the “Calculate” button to start the calculations. The simulator first loads the channel information and generates the channel noise according to the parameter values. Then, it will generate a transmit sequence and pass it through the channel to obtain a received signal. In the next step, the simulator estimates the power spectra of the transmitted signal and channel noise. It also estimates the magnitude square of the channel frequency response. Based on these estimates, the SNR in each subchannel is estimated.

The simulator then calls the desired TEQ design function to calculate the equalizer taps, target impulse response (if it exists for that method), and optimal delay. All of the results are then passed to a performance evaluation function which returns the six performance measures. The selected graph is plotted and the results are written in the table. For different graphs the simulations does not need to be run again, all results are saved. Appendix A covers the DMTTEQ toolbox in more detail.

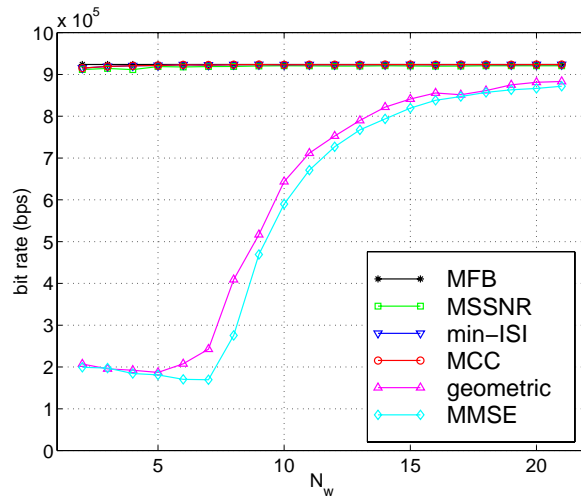
## 6.7 Conclusion

The proposed MCC and min-ISI TEQ design methods outperform all of the previous design methods in bit rate yet require fewer taps. Better performance during data transmission is obtained with lower computational complexity. The design complexity of the proposed methods is higher than the previous design methods, but the design method is used only once at the initialization and can be off-line. For the same TEQ length, the bit rate difference between the proposed design methods and the MMSE and MGSNR methods is up to

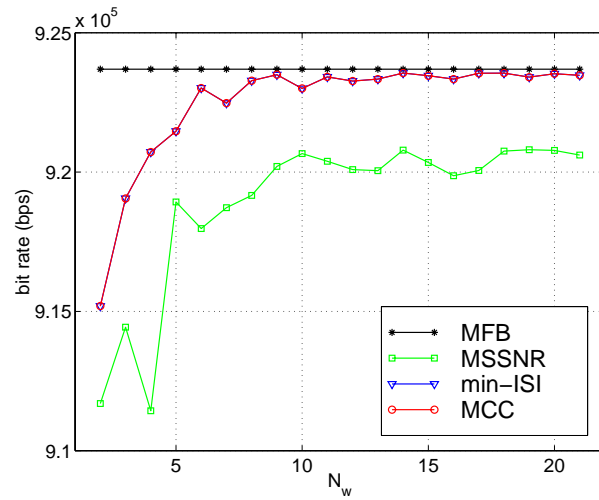
400%. Or for the same performance, the proposed methods require 10% of the TEQ taps of the MMSE and MGSNR methods. Although the proposed design methods also outperform the MSSNR method, the performance difference is not as dramatic. The computation complexity of the min-ISI method is slightly higher than the MSSNR method.

The min-ISI design method generalizes the MSSNR design method. The fundamental difference is that the MSSNR method minimizes the energy of ISI path impulse response while the min-ISI minimizes the output power of the ISI path impulse response. The min-ISI TEQ can outperform the MSSNR TEQ only if the latter leaves considerable residual ISI or in the case where not all available bandwidth is used for data transmission. Otherwise, their performance is equal.

In the simulations given in this chapter, it is assumed that all subchannels are used for data transmission; hence, the min-ISI cannot use the additional degree of freedom given by unused subchannels for higher performance. The residual ISI is the only source of performance difference in the results given in this chapter.

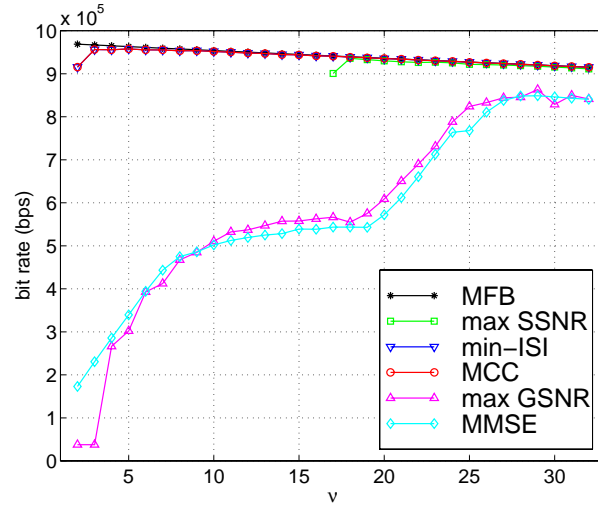


(a)

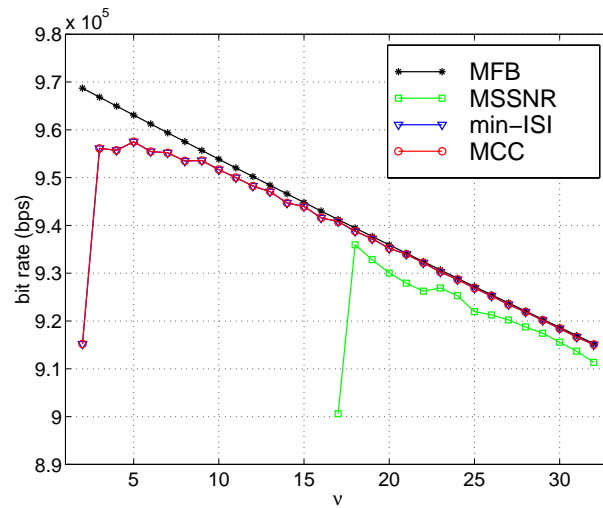


(b)

Figure 6.1: Achievable bit rate vs. the number of equalizer taps for CSA loop 4,  $\nu = 32$ ,  $N = 512$ , coding gain = 4.2 dB, margin = 6 dB, input power = 14 dBm, AWGN power  $-113$  dBm/Hz, NEXT noise modeled as 10 ADSL disturbers. (a) all methods and (b) zoom plot into the proposed and MSSNR methods.

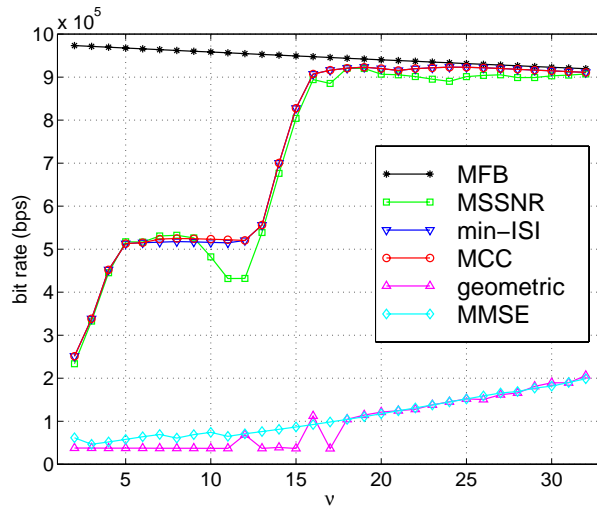


(a)

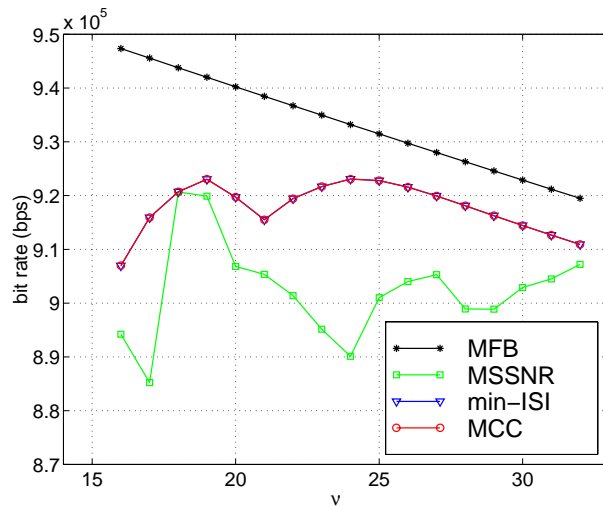


(b)

Figure 6.2: Achievable bit rate vs. the cyclic prefix length  $\nu$  for CSA loop 4,  $N_w = 17$ ,  $N = 512$ , coding gain = 4.2 dB, margin = 6 dB, input power = 14 dBm, AWGN power  $-113$  dBm/Hz, NEXT noise modeled as 10 ADSL disturbers. (a) all methods, and (b) zoom plot into the proposed and MSSNR methods.



(a)



(b)

Figure 6.3: Achievable bit rate vs. cyclic prefix length  $\nu$  for CSA loop 4,  $N_w = 2$ ,  $N = 512$ , coding gain = 4.2 dB, margin = 6 dB, input power = 14 dBm, AWGN power  $-113$  dBm/Hz, NEXT noise modeled as 10 ADSL disturbers. (a) all methods, and (b) zoom plot into the proposed and MSSNR methods.

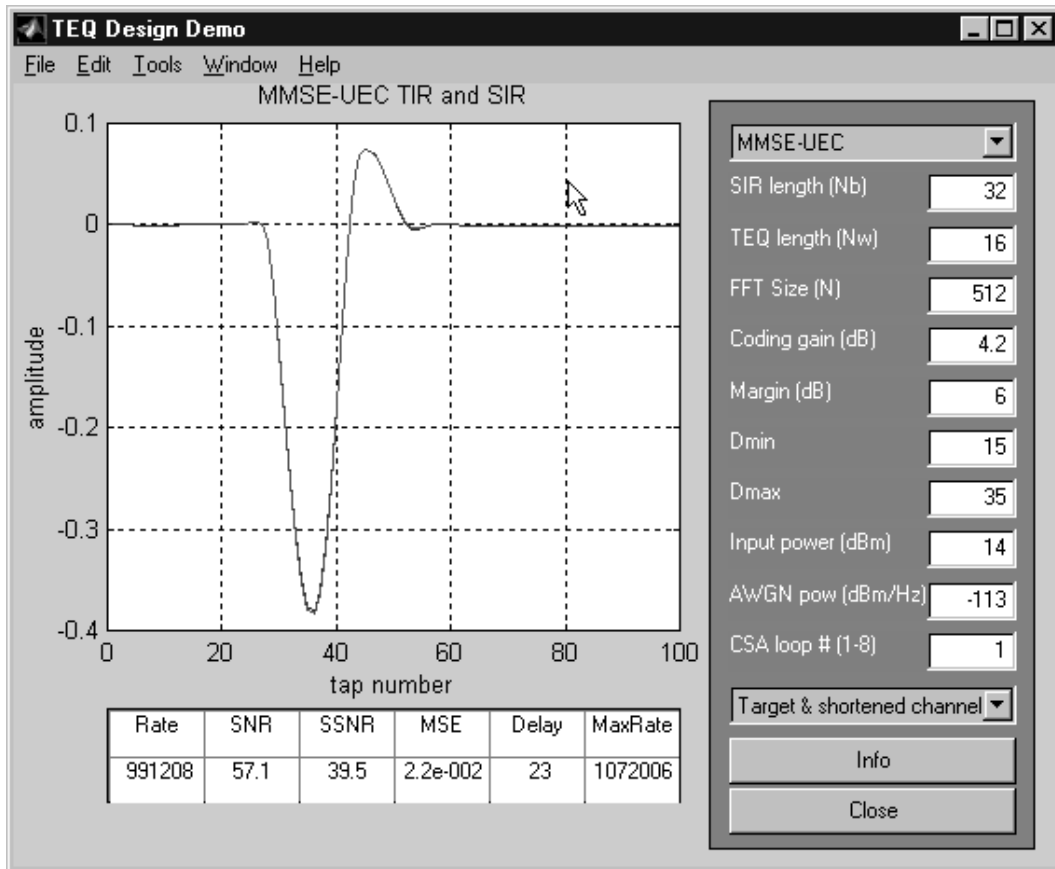


Figure 6.4: TEQ designed with the MMSE-Unit Energy Constraint (UEC) design method in the MATLAB DMTTEQ toolbox.



# Chapter 7

## Conclusion

### 7.1 Summary

Multicarrier modulation is one of the most prominent modulation techniques for high-speed communications. Discrete Multitone Modulation (DMT) and Orthogonal Frequency Division Multiplexing (OFDM) are two widely used versions of multicarrier modulation based on the fast Fourier transform (FFT). DMT has been standardized for Asymmetric Digital Subscriber Lines (ADSL) and is proposed for Very-high-speed Digital Subscriber Lines (VDSL) as well as for digital audio/video broadcasting.

Research and development is continuing to improve the performance of DMT systems for current and future applications and standards. Improvement in time-domain equalizer (TEQ) design methods has a potential to increase the achievable bit rates in DMT systems. Combining a TEQ with a guard period (cyclic prefix) is used to prevent inter-symbol interference in DMT transceivers. The TEQ shortens the channel to the length of the guard period

so that two adjacent symbols do not interfere with each other.

Many different TEQ design methods have been proposed. Among them, those based on the Minimum Mean Squared Error (MMSE) are the most commonly used in commercial ADSL modems [1]. MMSE design methods are relatively easier to implement with adaptive algorithms and are efficient in the sense of computational complexity. However, MMSE design methods are not optimal in the sense of maximizing channel capacity.

Of the many previously reported TEQ design methods, only one method attempts to optimize channel capacity – the maximum geometric SNR (GSNR) method. The maximum GSNR (MGSNR) method optimizes an approximation to the GSNR which is measure directly related to channel capacity. However, the inaccurate assumptions and approximations used in the derivation of the method prevent this design method to generate optimal TEQs in the sense of achievable channel capacity.

In this dissertation, I defended the following thesis statement:

DMT TEQ design that minimizes frequency weighted ISI power to push ISI into low SNR frequency bands gives equivalent performance to optimal DMT TEQ design that maximizes channel capacity.

My first step in defending this statement was to derive a new model for sub-channel SNR that was used in deriving the channel capacity optimal TEQ – the MCC TEQ. The behavior of the MCC method showed that the capacity is maximized when the ISI power is minimized and the residual ISI is pushed into low SNR frequency bands. Instead of using a nonlinear optimization with the MCC method, I derived a suboptimal design method, the min-ISI method,

to implement the idea of pushing ISI into low SNR subchannel. Simulation results show that the performance, measured as achievable channel capacity, is essentially equivalent for both methods. Although the min-ISI and the MCC methods are not optimizing the same cost function, they give equivalent performance.

The goal of this research was develop a method to design optimal TEQs in the sense of maximum channel capacity. The first challenge was to derive the channel capacity in terms of the TEQ taps, which included modeling the effect of ISI caused by an imperfect TEQ. A previous solution to this problem classifies ISI as additive noise and incorporates it into the SNR definition along with the channel noise. Instead, in Chapter 3, I propose a subchannel SNR model that defines SNR in a subchannel as the ratio of signal power to noise plus ISI power.

In order to write the SNR in this form, however, the received signal must be partitioned into noise, signal, and ISI components. I achieve this by partitioning the equalized channel impulse response into equivalent signal, noise, and ISI paths. The signal path impulse response is defined as the portion of the equalized channel impulse response lying inside a target window. The ISI path impulse response is defined as the portion lying outside the target window. The target window is a rectangular window of length equal to the target length of the equalized channel impulse response. In the ideal case, in which the TEQ shortens the channel perfectly to the target length, the equalized channel lies entirely inside the target window. Then, the signal path impulse response would be equivalent to the equalized channel impulse response, and the ISI path impulse response would be zero, so there would be no ISI as expected. The noise path impulse response is simply the impulse

response of the TEQ since the channel noise passes only through the TEQ. By using the signal, noise, and ISI paths, it is possible to partition the received signal into signal, noise, and ISI components.

Naturally, all equivalent paths are related to the TEQ taps. Therefore, the proposed SNR definition is a function of the TEQ taps, which enables the channel capacity to be expressed as a function of TEQ taps. Chapter 4 derives the channel capacity as a nonlinear function of the TEQ taps. The nonlinearity is a result of the channel capacity equation which is defined as a sum of capacities of all additive white Gaussian noise subchannels. By applying an unconstrained nonlinear optimization method, I develop the optimal Maximum Channel Capacity (MCC) TEQ design method.

Unlike the MGSNR design method, the MCC design method does not require constrained nonlinear optimization, but instead unconstrained nonlinear optimization, which requires lower computational complexity. The constraints in the MGSNR method arise from the fact that the method is based on the MMSE method. The MGSNR method constrains the MSE to be smaller than a certain threshold. Therefore, the method is essentially relying on the MMSE method for the shortening of the channel since the GSNR definition used in the derivations does not include any ISI information. That means, maximizing the GSNR does not minimize ISI, hence shorten the channel, but only maximizes an approximation of signal to channel noise ratio.

Nonlinear programming is computationally too complex for a low-cost real-time implementation. To avoid the need for a nonlinear optimization method, I propose the near-optimal minimum-ISI (min-ISI) method in Chapter 5. Instead of maximizing the channel capacity directly, this method minimizes the total ISI power over all subchannels. The ISI power is written as

a quadratic function of TEQ taps. A constraint is required to prevent the trivial all-zero solution. I propose to constrain the equalized channel gain to one, which is also a quadratic function of the TEQ taps. In this case, the min-ISI TEQ design is a generalized eigenvalue problem which can be solved with the iterative power method as described in Chapter 5. Simulation results in Chapter 6 show that the min-ISI TEQ performs as well as the MCC TEQ.

The min-ISI TEQ method is a generalization of the maximum SSNR (MSSNR) method with the addition of frequency domain weighting. The MSSNR method minimizes the energy of the ISI path impulse response while constraining the signal path impulse response to one. The min-ISI method, in contrast, minimizes the ISI caused by the ISI path impulse response with additional frequency domain weighting. In other words, the min-ISI method minimizes the output energy of the ISI path impulse response while the MSSNR method minimizes the ISI path impulse response itself. The difference can be seen if some subchannels are not used and no power is assigned to these subchannels. In this case, the min-ISI method does not attempt to minimize the gain of the ISI path frequency response at those subchannels. The MSSNR method cannot use this information and minimizes the gain in these subchannels even though they are not contributing to the ISI.

The frequency domain weighting of the min-ISI method is another improvement over the MSSNR method. By analyzing the results obtained from the optimal MCC method, the optimal TEQs try to push the residual ISI power into frequency bands with high channel noise. Having some ISI power in these frequency bands does not affect the SNR in these bands dramatically because the ISI power is generally dominated by the channel noise power. However, if we had the same amount of ISI power in a frequency band with low

channel noise, the ISI would be significant relative to the channel noise and the SNR in this frequency band would drop dramatically. In summary, having minimum ISI power does not mean higher channel capacity. It is important how the ISI power is distributed over frequency.

The min-ISI design method does not require nonlinear optimization, but it is still computationally complex. Calculating the cost matrices in the objective function is the most computationally intensive part of the design method. To reduce complexity, I derive recursive methods to calculate the entries of these matrices in collaboration with Mr. Jeff Wu. The generalized eigenvalue problem can be solved in the same way as in the MSSNR method or by using the iterative power method.

A comparison of all TEQ design methods mentioned in this dissertation are summarized in Table 7.1. The only method that really maximizes channel capacity is the proposed MCC method. However, the MCC method requires the solution of nonlinear optimization problem. The min-ISI method prevents nonlinear optimization but still requires an eigenvalue decomposition which can be solved with the power method iteratively. The min-ISI method has all of the advantages but only one disadvantage the complexity of the required eigenvalue decomposition.

During the research on TEQ design methods, I implemented six different TEQ design methods in MATLAB. With the additional four methods programmed by Ms. Biao Lu, we form a MATLAB Toolbox for TEQ design called the DMTTEQ Toolbox. Currently the toolbox supports the following ten TEQ design methods:

- Minimum mean squared error – unit-energy constraint [19],

Advantages							Disadvantages						
1. Adaptive or iterative 2. Off-line (initialization) 3. Maximizes channel capacity 4. Minimizes directly ISI causing tail 5. Frequency weighting 6. Subchannel optimization							1. Deep notches in frequency 2. SIR-TIR difference inside window 3. Slow or uncertain convergence 4. Requires eigendecomposition 5. Requires nonlinear optimization 6. Narrowband frequency response 7. Numerical instabilities possible						
Methods	Advantages						Disadvantages						
	1	2	3	4	5	6	1	2	3	4	5	6	7
<i>MMSE methods</i>													
Chow <i>et al.</i> [9]		✓					✓	✓				✓	✓
Chow <i>et al.</i> [10, 11]	✓						✓	✓	✓			✓	✓
Al-Dhahir <i>et al.</i> [19]		✓					✓	✓		✓		✓	✓
Kerckhove <i>et al.</i> [26]		✓			✓		✓	✓		✓		✓	✓
Nafe <i>et al.</i> [30]	✓	✓		✓			✓						
Strait [29]	✓						✓	✓				✓	
Wang <i>et al.</i> [21, 22]		✓			✓		✓	✓		✓		✓	✓
Lashkarian <i>et al.</i> [32]	✓	✓					✓	✓		✓		✓	
Acker <i>et al.</i> [27, 28]	✓	✓			✓	✓			✓				
Boroujeny <i>et al.</i> [33]		✓						✓		✓		✓	✓
Wang <i>et al.</i> [25]		✓			✓					✓		✓	✓
<i>MSSNR methods</i>													
Melsa <i>et al.</i> [12]		✓		✓						✓			✓
Yin <i>et al.</i> [35]		✓		✓						✓			✓
Chiu <i>et al.</i> [37]	✓	✓		✓					✓				
Wang <i>et al.</i> [36]		✓		✓	✓					✓			✓
Lu <i>et al.</i> [38]	✓	✓		✓									
<i>MGSNR methods</i>													
Al-Dhahir <i>et al.</i> [15]		✓	✓ <sup>†</sup>			✓	✓	✓			✓	✓	✓
Lashkarian <i>et al.</i> [42]	✓	✓	✓ <sup>†</sup>			✓	✓		✓			✓	✓
Milisavljević <i>et al.</i> [43]	✓	✓	✓ <sup>†</sup>			✓			✓		✓		
<i>Proposed methods</i>													
MCC		✓	✓	✓	✓	✓					✓		
min-ISI	✓	✓	✓ <sup>‡</sup>	✓	✓	✓				✓			

<sup>†</sup>Maximizes an approximate geometric SNR, not the true channel capacity.

<sup>‡</sup>Not optimal but gives equivalent performance to that of the optimum method.

Table 7.1: Advantage/disadvantages of TEQ design methods.

- Minimum mean squared error – unit-tap constraint [19],
- Maximum shortening signal to noise ratio method [12],
- Maximum geometric SNR method [15],
- Divide and conquer – cancellation (implemented by Ms. Biao Lu) [38],
- Divide and conquer – minimization (implemented by Ms. Biao Lu) [38],
- Maximum channel capacity method [46],
- Minimum intersymbol interference method [46],
- Matrix pencil design method (implemented by Ms. Biao Lu) [38],
- Modified matrix pencil design method (implemented by Ms. Biao Lu) [38].

The toolbox has a graphical user interface which enables the design of a TEQ by one of the methods above and testing of its performance.

## 7.2 Future research

- *Joint optimization of bit loading and TEQ*: Bit loading is the task to assign bits and power to each subchannel using the SNR information in each subchannel [47]. The bit loading problem can be posed as an optimization problem where the goal is either to maximize the system margin given a target bit rate and available power, or to maximize the number of bits to be transmitted given the available power and desired



system margin. Generally, the bit loading problem is solved independently from the TEQ design problem. That is, first the TEQ is designed and the bit loading algorithm is run using the equalized channel.

The TEQ design method does not use any information from the bit loading result which might be useful. For example, it is possible that the bit loading algorithm decides that some of the subchannels do not have high enough SNR to carry any bits and shuts those subchannels off. These unused subchannels could be used to improve the performance of the TEQ if this information would be available during the TEQ design. One of the results in this dissertation is that the residual ISI power should be placed according to the SNR distribution. However, the SNR distribution changes with bit loading. This change might degrade the performance of the TEQ. To prevent this, bit loading and TEQ design could be combined into one optimization problem. Such a combined procedure could be implemented within the current ADSL standard.

The simplest way of doing this is to iterate back and forth between the TEQ design and the bit loading algorithm. After the initial TEQ design and bit loading, the new SNR information is used to redesign the TEQ. Then, by using the new TEQ, the bit loading algorithm can be used to determine the new bit allocation. This procedure might converge to an optimal TEQ and bit allocation solution.

A better approach would be to derive a cost function, such as the channel capacity, as a function of TEQ taps and bit allocation. This combined cost function could then be optimized for the joint optimal TEQ and bit allocation.

- *Taking into account the noise floor*: One practical problem which is not taken into account in any of the TEQ design methods mentioned in this dissertation is the noise floor. All practical systems have a noise floor which is determined by the quality of the data converters and analog hardware. In the digital domain, it is not possible to suppress the noise below this level.

This could cause a difference between theoretical and practical performance of a TEQ. For example, theoretically, a TEQ cannot change the signal to channel noise ratio since both the signal and channel noise are filtered by the same frequency response of the TEQ. The only exception is when the TEQ has a zero gain at a certain frequency. In this case, there is no signal and no noise at that frequency; hence, SNR really has no meaning. In general, however, the TEQ amplifies or attenuates the signal the same way it does the channel noise. If we do not take into account the noise floor, the SNR would not change by adding a TEQ into the system.

If the TEQ attenuates the signal and noise so much that after the TEQ, the noise is below the noise floor at some frequencies, then the SNR would change. The signal is attenuated more than the noise and the SNR is lower after the TEQ. If a TEQ design method does not incorporate the noise floor into its design procedure, then there is no guarantee that the practical system achieves the capacity obtained by calculations or simulations.

One way to incorporate the noise floor into the design is to refine the

SNR definition as follows:

$$\text{SNR} = \frac{\text{signal power}}{\text{noise power} + \text{ISI power} + \text{noise floor}} \quad (7.1)$$

The noise floor is a small constant which dominates over the noise power and ISI power if they become smaller than the noise floor. Both the MCC design method can easily be modified to incorporate the noise floor by using the above definition of SNR.

- *Adaptation of TEQ taps:* In many practical systems, it is desirable that the equalizer is adaptive so that it can track changes in the channel impulse response. The min-ISI design method could be made adaptive by combining the channel estimation into the TEQ design. In most DMT systems, the channel is estimated with a periodic training signal in the FFT domain. The updated channel FFT coefficients can be transformed to the time domain to obtain an updated channel impulse response. The cost and constraint matrices can then be updated according the changes of the channel. An iteration of the power method would bring the TEQ taps closer to the desired solution.

One full iteration would require a channel update in the DFT domain, an IFFT to obtain the channel impulse response, two matrix updates, and a power method iteration. The most challenging part is the update of the two matrices. There may be a way to omit that step if one could derive an update for the dominant eigenvector given a small change in the matrices.

- *Perturbation analysis:* Both the MCC and min-ISI design methods assume perfect knowledge about the channel impulse response. In practice,

the channel impulse response is not known and can only be estimated with an estimation error. Eigendecomposition-based algorithms, such as the min-ISI method, are sensitive to such errors. A perturbation analysis would give some insight on how the proposed methods react to errors in the channel impulse response.

The perturbation analysis can be performed by introducing some random error into the real channel impulse response and recalculating the TEQ taps with this modified impulse response. By repeating this experiment, the average performance loss due to channel estimation error can be calculated. A better approach would be to simulate the channel estimation procedure along with the TEQ design simulations and compare the performance with the simulations where perfect channel knowledge is assumed.

- *Smooth windowing*: The subchannel SNR model proposed in Chapter 3 uses a rectangular window in the calculation of the signal and ISI path impulse responses. This can result in signal and ISI paths with sudden changes around the window boundaries. Sudden changes can degrade the frequency response of the signal and ISI paths. Performance analysis using a different window (e.g., Hamming, Hanning, or Kaiser) is another direction for further research on the proposed model as well as design methods.
- *Fixed-point analysis*: No TEQ design method would be implemented in practical systems before analyzing its performance under fixed-point arithmetic. The first algorithm for min-ISI method in Chapter 5 is a good place to start. A fixed-point analysis should show whether or not it is

possible to implement the algorithm in fixed point and what precision is required for each part of the design method. A first step in this direction might be a floating-point to fixed-point converter to the C code [48].

- *Modifications on the model for subchannel SNR:* The subchannel SNR model proposed in Chapter 3 assumes that all of the samples outside the target window is causing ISI/ICI. With some modifications some of these samples could be considered as a part of the signal. I use the motivating example of Chapter 3 to explain this claim. Let us rewrite (3.2) by ignoring the left-hand side of the equation and the noise term,

$$\begin{array}{|l}
 \hline
 \tilde{h}_1 a_4 \\
 \hline
 \tilde{h}_1 a_1 + \tilde{h}_2 a_4 \\
 \hline
 \tilde{h}_1 a_2 + \tilde{h}_2 a_1 + \tilde{h}_3 a_4 + \tilde{h}_4 a_3 - \tilde{h}_4 a_3 \\
 \tilde{h}_1 a_3 + \tilde{h}_2 a_2 + \tilde{h}_3 a_1 + \tilde{h}_4 a_4 \\
 \tilde{h}_1 a_4 + \tilde{h}_2 a_3 + \tilde{h}_3 a_2 + \tilde{h}_4 a_1 \\
 \tilde{h}_1 a_1 + \tilde{h}_2 a_4 + \tilde{h}_3 a_3 + \tilde{h}_4 a_2 + \tilde{h}_1 b_4 - \tilde{h}_1 a_1 \\
 \hline
 \tilde{h}_1 b_1 + \tilde{h}_2 b_4 + \tilde{h}_3 a_4 + \tilde{h}_4 a_3 \\
 \hline
 \tilde{h}_1 b_2 + \tilde{h}_2 b_1 + \tilde{h}_3 b_4 + \tilde{h}_4 b_3 + \tilde{h}_4 a_4 - \tilde{h}_4 b_3 \\
 \tilde{h}_1 b_3 + \tilde{h}_2 b_2 + \tilde{h}_3 b_1 + \tilde{h}_4 b_4 \\
 \tilde{h}_1 b_4 + \tilde{h}_2 b_3 + \tilde{h}_3 b_2 + \tilde{h}_4 b_1 \\
 \tilde{h}_1 b_1 + \tilde{h}_2 b_4 + \tilde{h}_3 b_3 + \tilde{h}_4 b_2 - \tilde{h}_1 b_1 \\
 \hline
 \tilde{h}_3 b_4 + \tilde{h}_4 b_3 \\
 \hline
 \text{desired part} \quad \tilde{h}_4 b_4 \\
 \hline
 \end{array} \tag{7.2}$$

By adding and subtracting some terms to the samples of the symbols, one can obtain a new structure. In this form, each sample of each symbol is allowed to have four terms with which the circular convolution property

holds. Therefore, the desired part of the received samples is now the four elements in each row and is shown in the oval box. Everything outside the box is causing ISI/ICI.

Compared with the model in Chapter 3, the undesired part has fewer elements and probably has lower power. That means the distortion is smaller than the model in Chapter 3 suggests. In this modified model, the received symbols are the circular convolution of the transmitted symbols  $\tilde{\mathbf{a}}$  and  $\tilde{\mathbf{b}}$  with the channel  $[\tilde{h}_1 \tilde{h}_2 \tilde{h}_3 \tilde{h}_4]$ . In the original model, the received symbols were the circular convolution of the transmitted symbols  $\tilde{\mathbf{a}}$  and  $\tilde{\mathbf{b}}$  with the channel  $[0 \tilde{h}_2 \tilde{h}_3 0]$ .

In summary, the undesired part of the received signal may be overestimated by the original model. The problem with the modified model is that the equalized channel impulse response cannot be partitioned as easily into signal and ISI paths as it can with the original model. To use the modified model, we need to write the distortion (ISI/ICI) as a filtered version of the transmitted samples.

- *Effect of analog filters on TEQ:* In all of the simulations in this dissertation, I assume that there is no additional filtering in the channel. In practice, however, several filters are placed before and after data conversions. In frequency domain multiplexing based ADSL systems, the upstream and downstream is filtered out with a sharp filter. Similarly, the POTS bands, which consist of the first six subchannels in the G.DMT standard, are filtered out. These filters change the effective channel impulse response and make the design of the TEQ more difficult. The performance of the proposed methods might be tested with different

combination of transmit, receive, and masking filters.

- *Optimal frequency domain weighting:* The derivations of the min-ISI design method results in a weighting function which is the signal power spectrum divided by the noise power spectrum. Simulation results suggest that multiplying this weighting function with the magnitude squared of the channel frequency response improves the performance of the TEQ. The weighting function after this multiplication is the SNR as seen at the receiver just before the TEQ. Weighting the ISI with the SNR distribution forces the ISI power to be located in low SNR bands where it is dominated by the channel noise. However, there is no theoretical background to this choice of weighting and it might be possible a better weighting function exists. Further research could result in an optimal weighting function for the min-ISI method.

# Appendix A

## MATLAB DMTTEQ Toolbox

It is possible to load the equalizer taps, target impulse response, and optimal delay as well as other results into MATLAB workspace by typing “load teqresults”. The variables used to pass parameters and get the results are listed in Table A.1

### A.1 TEQ Design Functions

#### UTC.M

*Description:* Minimum mean-squared error time domain equalizer design using the unit-tap constraint

*Usage:*  $[B, W, D, MSE, I, Dv] = UTC(X, Y, N, H, Nb, Nw, Dmin, Dmax)$

Returns the optimal target impulse response  $B$ , the time domain equalizer  $W$ , the delay  $D$ , and the unit tap index  $I$ . Optimal is in the sense of minimum mean-squared error under the constraint of a unit-tap.  $MSE$  is the resulting mean-squared error and  $Dv$  is a vector containing the mean-squared error for delay values between  $Dmin$  and  $Dmax$ .



Variable	Content
TEQequalizerTaps	equalizer taps
TEQtargetImpulseResp	target impulse response
TEQoptimalDelay	optimal delay
TEQoriginalChannel	original channel impulse response
TEQequalizedChannel	equalized channel impulse response
TEQmatchedFilterBoundPerChannel	matched filter bound in subchannels
TEQSNRperChannel	SNR in subchannels
TEQoriginalChannelFreqResp	channel frequency response
TEQequalizerFreqResp	equalizer frequency response
TEQequalizedChannelFreqResp	equalized channel frequency response
TEQchannelNoisePowerSpecAfterEqual	noise power spectrum after equalization
TEQchannelNoisePowerSpecBeforeEqual	noise power spectrum before equalization
TEQperformanceVersusDelay	performance for various delays
TEQDmin	minimum delay
TEQDmax	maximum delay
TEQNb	desired equalized channel length
TEQNw	number of taps in the TEQ
TEQN	FFT size of the DMT modulation

Table A.1: Global variable names used in the DMTTEQ Toolbox

X is the transmitted data vector. Y is the received data vector (without channel noise). N is the channel noise vector. H is channel impulse response. Nb is the number of taps in the target impulse response and Nw the number of taps in the time domain equalizer. Dmin and Dmax define the search interval for the optimal delay.

### **UEC.M**

*Description:* Minimum mean-squared error time domain equalizer design using the unit-energy constraint.

*Usage:* [B, W, D, MSE, Dv] = UEC(X, Y, N, H, Nb, Nw, Dmin, Dmax)

Returns the optimal target impulse response B, the time domain equalizer W, and the delay D. Optimal is in the sense of minimum mean-squared error under the unit-energy constraint. MSE is the resulting mean-squared error and Dv is a vector containing the mean-squared error for delay values between Dmin and Dmax.

X is the transmitted data vector. Y is the received data vector (without channel noise). N is the channel noise vector. H is channel impulse response. Nb is the number of taps in the target impulse response and Nw the number of taps in the time domain equalizer. Dmin and Dmax define the search interval for the optimal delay.

### **MINISI.M**

*Description:* Minimum-ISI TEQ design.

*Usage:* [W, D, Dv] = MINISI(Sx, Sn, Sh, H, N, Nb, Nw, Dmin, Dmax, M)

Returns the time domain equalizer in W and the delay in D. Dv is a vector containing the remaining ISI power for delay values between Dmin and Dmax.

Sx is the input data frequency spectrum. Sn is the channel noise fre-

quency spectrum.  $S_h$  is the magnitude square of the channel frequency response.  $H$  is the channel impulse response.  $N$  is the FFT size in the discrete multitone modulation.  $N_b$  is target window size (target length of the equalized channel).  $N_w$  is the number of taps in the time domain equalizer.  $D_{\min}$  and  $D_{\max}$  define the search interval for the optimal delay.  $M$  is a string defining what method to be used for the generalized eigenvalue decomposition. Choices are:

- 'AUTOMATIC' automatic selection of best method
- 'GENEIGEND' direct generalized eigenvalue decomposition
- 'CHOLESKYD' Cholesky decomposition based method
- 'MINEIGEND' convert to normal minimum eigenvalue decomposition
- 'MAXEIGEND' convert to normal maximum eigenvalue decomposition

## **GEO.M**

*Description:* Geometric TEQ design.

*Usage:*  $[B, W, D, MSE, Dv] = \text{GEO}(X, Y, N, N_b, N_w, D_{\min}, D_{\max}, \text{MSE}_{\max}, U)$

Returns the optimal target impulse response  $B$ , time domain equalizer  $W$ , and delay  $D$ . Optimal is in the sense of maximizing the approximate geometric SNR.  $MSE$  is the resulting mean-squared error.  $Dv$  is a vector containing the mean-squared error for delay values between  $D_{\min}$  and  $D_{\max}$ .

$X$  is the transmitted data vector.  $Y$  is the received data vector (without channel noise).  $N$  is the channel noise vector.  $N_b$  is the number of taps in the target impulse response and  $N_w$  the number of taps in the time domain

equalizer.  $D_{\min}$  and  $D_{\max}$  define the search interval for the optimal delay.  $MSE_{\max}$  the upperbound on the mean-squared error.  $U$  is a binary vector of size  $N/2+1$  with 1s for used subchannels and 0s for unused ones.

Optimization Toolbox Version 1.5.1 has been used in this function

### **MCC.M**

*Description:* Maximum channel capacity TEQ design.

*Usage:*  $[W, D, Dv] = \text{OPT}(S_x, S_n, H, N, N_b, N_w, D_{\min}, D_{\max}, W_o, G, I)$

Returns the optimal time domain equalizer  $W$ , and delay  $D$ . Optimal is in the sense of maximum channel capacity.  $Dv$  is a vector containing the objective value for delays between  $D_{\min}$  and  $D_{\max}$ .  $I$  is a scalar which is multiplied with  $N_w$  to determine the number of iterations to be run for the optimization.

$S_x$  is the transmitted signal power spectrum.  $S_n$  is the channel noise power spectrum.  $H$  is the channel impulse response.  $N$  is the FFT size in the discrete multitone modulation.  $N_b$  is the target length of the equalized channel.  $N_w$  is the number of taps in the time domain equalizer.  $D_{\min}$  and  $D_{\max}$  define the interval over which the delay is being searched.  $W_o$  is the initial starting point for the optimization.  $G$  is the SNR gap (not in dB).  $I$  is the number of iteration to be used in the optimization procedure.

### **MELS.M**

*Description:* Maximum shortening signal-to-noise ratio TEQ design.

*Usage:*  $[W, D, Dv] = \text{MELS}(H, N_b, N_w, D_{\min}, D_{\max})$

Returns the optimal time domain equalizer, and delay. Optimal in the sense of maximizing the shortening signal to noise ratio.  $Dv$  is a vector containing the remaining tail power for delay values between  $D_{\min}$  and  $D_{\max}$ .

$H$  is the channel impulse response.  $N_b$  is the target length of the short-

ened impulse response.  $N_w$  is the number of taps in the TEQ.  $D_{\min}$  and  $D_{\max}$  define the search interval for the optimal delay.

## A.2 Performance Evaluation Functions

### PERFORM.M

*Description:* Evaluate the performance of an TEQ in terms of SSNR, SNR, geometric SNR, and channel capacity.

*Usage:* [SS, S, Si, Sg, Mg, Bf, Bm, Rf, Rm, Hw, Fh, Fw, Nc, Phw] =  
PERFORM(W, B, H, D, Nb, NN, X, N, Ph, Px, Pn, M, C, Fs, Mi)

Returns the shortening SNR in SS, the SNR at the output of the equalizer in S, the SNR distribution over the subchannels in the vector Si. Sg is the real geometric SNR achieved with the TEQ and Mg is the geometric SNR that can be achieved in the case of zero ISI (Mg is calculated using the MFB distribution while Sg is calculated with the SNR distribution.). Bf is the number of bits per symbol achievable with the TEQ and Bm is the upperbound on bits per symbol. Rf is the channel capacity achieved with the TEQ and Rm is the upperbound on the channel capacity. Hw is a vector containing the equalized channel impulse response. Fh is a vector containing the frequency response of the original channel and Fw is vector containing the equalizer. Nc is a vector of the power spectrum of the channel noise after equalization and Phw is a vector containing the magnitude square of the frequency response of the equalized channel.

W is TEQ impulse response. B is the target impulse response (for MMSE based techniques). H is the channel impulse response. D is the optimal delay with TEQ. Nb is the target window size. NN is the FFT size used in

the DMT modulation.  $X$  is the transmitted signal.  $N$  the channel noise.  $P_h$  is the magnitude square of the channel frequency response.  $P_x$  is the power spectrum of the transmitted signal.  $P_n$  is the power spectrum of the channel noise.  $M$  is the desired system margin in dB which is used for channel capacity calculations.  $C$  is the coding gain in dB assumed for channel capacity calculations.  $F_s$  is the sampling frequency.  $M_i$  is the matched filter bound distribution over frequency.

### **GEOSNR.M**

*Description:* Geometric SNR, bit per symbol, and bit rate.

*Usage:*  $[G, B, R] = \text{GEOSNR}(\text{SNR}, M, C, N, N_b, F_s)$

Returns the geometric SNR in  $G$  (dB), bit per symbol in  $B$ , and bit rate in  $R$ .

$\text{SNR}$  is a vector containing the SNRs in each used subchannel.  $M$  is the system margin in dB.  $C$  is the coding gain of any code applied in dB.  $N$  is the FFT size in the discrete multitone modulation.  $N_b$  is the cyclic prefix length.  $F_s$  is the sampling frequency.

## **A.3 Utility Functions**

### **TEQDEMO.M**

*Description:* Demonstrates time-domain equalizer design using the DMTTEQ Toolbox.

*Usage:* `TEQDEMO`

### **SETPROGBAR.M**

*Description:* Setup a progress bar.

*Usage:*  $[H_f, H_s] = \text{SETPROGBAR}(S)$

Sets up a progress bar with the title given in the string S.

Hf is the handle to the figure and Hs is the handle to the status of the progress bar.

#### **UPDATEPROGBAR.M**

*Description:* Update progress bar by increasing it one step.

*Usage:* UPDATEPROGBAR(H,S,M)

Updates the progress bar with handle H by an amount of 1/M. So that in M steps the progress bar is full (100%).

#### **SPECESTIM.M**

*Description:* Frequency spectrum estimation.

*Usage:* [Sx, Sn, Sh] = SPECESTIM(X, N, H, NN)

Returns the frequency spectrum of the transmitted data in Sx, the channel noise in Sn and the magnitude square frequency response of the channel in Sh.

X is the transmitted data vector. N is the channel noise vector. H is the channel impulse response. NN is the FFT size in the discrete multitone modulation.

#### **OBJECTIVE.M**

*Description:* Objective function to maximize approximate geometric signal-to-noise ratio.

*Usage:* [F, G] = OBJECTIVE(B, D, N, Rd, MSE, MSEmax, U)

Returns the negative of the approximate geometric SNR in F. G returns a negative number when the constraints are satisfied, non-negative otherwise.

B is the target impulse response. D is the delay. N is the FFT size of the discrete multitone modulation. Rd is the MSE matrix. MSEmax the upperbound on the mean-squared error. U is a binary vector of size N/2+1

with 1s for used subchannels and 0s for unused ones.

### **OBJ.M**

*Description:* Objective function to be minimized to maximize channel capacity.

*Usage:*  $F = \text{OBJ}(W, N, A, B, G)$

Returns the objective value which is the negative of the bit rate.

$W$  is a vector containing the tap values of the time domain equalizer.  $N$  is the number of used subchannels.  $A$  and  $B$  are 3 dimensional arrays containing  $N$  matrices.  $A$  contains the signal matrices and  $B$  the distortion matrices.  $G$  is the SNR gap (not in dB).

### **DSL.M**

*Description:* Simulate a standard digital subscriber line.

*Usage:*  $[Y, H, N] = \text{DSL}(X, \text{channelName}, P, S, U)$

Returns the received signal  $Y$  (without channel noise), channel impulse response in  $H$ , and channel noise in  $N$ . The channel noise consists of NEXT noise of  $U$  users and AWGN of power  $P$ .

$X$  is the transmitted signal.  $\text{channelName}$  is a string containing the channel name. The channel data should be in a subdirectory "channel". Currently supported channels are the CSA loops from 1 to 8. The name format is "csaloop#" where # = 1,2,...,8.  $P$  is the AWGN power.  $S$  is a subsampling factor. The default length of  $H$  is 512 samples. A shorter channel can be generated by subsampling  $H$  by a factor of  $S$ .  $U$  is the number of users causing NEXT noise.

### **MINEIG.M**

*Description:* Minimum eigenvalue and the corresponding eigenvector.

*Usage:*  $[L, Q] = \text{MINEIG}(A)$

Returns the minimum eigenvalue  $L$  and the corresponding eigenvector



Q of the square matrix A. Minimum is in the sense of absolute value if complex eigenvalues exist.

*Usage:* [L, Q] = MINEIG(A, B)

Returns the minimum generalized eigenvalue L and the corresponding generalized eigenvector Q of the square matrix A. Minimum is in the sense of absolute value if complex eigenvalues exist.

### **MAXEIG.M**

*Description:* Maximum eigenvalue and the corresponding eigenvector.

*Usage:* [L, Q] = MAXEIG(A)

Returns the maximum eigenvalue L and the corresponding eigenvector Q of the square matrix A. Maximum is in the sense of absolute value if complex eigenvalues exist.

*Usage:* [L, Q] = MAXEIG(A, B)

Returns the maximum generalized eigenvalue L and the corresponding generalized eigenvector Q of the square matrix A. Maximum is in the sense of absolute value if complex eigenvalues exist.

### **EIGEN.M**

*Description:* Solves the eigenvalue problem in design of the unit-energy constrained minimum mean-squared error time domain equalizer.

*Usage:* [B, W, D, MSE, R, Dv] = EIGEN(RXX, RYY, RXY, Dmin, Dmax, Nb, Nw, L)

Returns the optimal target impulse response B, the time domain equalizer W, and the delay D. Optimal is in the sense of minimum mean-squared error under the unit-energy constraint. MSE is the resulting mean-squared error. R is the input-output cross-correlation matrix obtained with the optimum delay D, and Dv is a vector containing the mean-squared error for

delay values between  $D_{\min}$  and  $D_{\max}$ .

$R_{XX}$  is the input autocorrelation matrix.  $R_{YY}$  is the output autocorrelation matrix.  $R_{XY}$  is the input-output cross-correlation vector used to generate the input-output cross-correlation matrix depending on the current delay.  $D_{\min}$  and  $D_{\max}$  define the search interval for the optimal delay.  $N_b$  is the number of taps in the target impulse response and  $N_w$  the number of taps in the time domain equalizer.

# Bibliography

- [1] T. Starr, J. M. Cioffi, and P. J. Silverman, *Understanding Digital Subscriber Line Technology*. Prentice-Hall PTR, 1999.
- [2] G. Held, *Next-Generation Modems*. New York, NY: John Wiley & Sons, Inc., 2000.
- [3] A. Azzam and N. Ranson, *Broadband Access Technologies*. New York, NY: McGraw-Hill, 1999.
- [4] ANSI T1.413-1995, “Network and customer installation interfaces: Asymmetrical digital subscriber line (ADSL) metallic interface,” 1995. ADSL Forum System Reference Model.
- [5] ETS 300 401, “Radio broadcast systems; digital audio broadcasting (DAB) to mobile, portable and fixed receivers,” 1994. European Telecommunications Standards Institute (ETSI).
- [6] ETS 300 744, “Digital broadcasting systems for television, sound and data services; framing structure, channel coding and modulation for digital terrestrial television,” 1997. European Telecommunications Standards Institute (ETSI).

- [7] C. Shannon, “A mathematical theory of communication,” *Bell System Technical J.*, vol. 27, pp. 379–423 and 623–656, 1948.
- [8] J. A. C. Bingham, “Multicarrier modulation for data transmission: An idea whose time has come,” *IEEE Comm. Magazine*, vol. 28, pp. 5–14, May 1990.
- [9] J. S. Chow and J. M. Cioffi, “A cost-effective maximum likelihood receiver for multicarrier systems,” in *Proc. IEEE Int. Conf. Comm.*, vol. 2, (Chicago, IL), pp. 948–952, June 1992.
- [10] J. S. Chow, J. M. Cioffi, and J. A. Bingham, “Equalizer training algorithms for multicarrier modulation systems,” in *Proc. IEEE Int. Conf. Comm.*, vol. 2, (Geneva, Switzerland), pp. 761–765, May 1993.
- [11] J. Chow and J. M. Cioffi, “Method for equalization a multicarrier signal in a multicarrier communication system.” U.S. Patent Number: 5,285,474, 1994.
- [12] P. J. W. Melsa, R. C. Younce, and C. E. Rohrs, “Impulse response shortening for discrete multitone transceivers,” *IEEE Trans. on Comm.*, vol. 44, pp. 1662–1672, Dec. 1996.
- [13] P. J. W. Melsa, C. E. Rhors, and R. C. Younce, “Joint optimal impulse response shortening,” in *Proc. IEEE Int. Conf. Acoust., Speech, and Signal Processing*, vol. 3, (Atlanta, GA), pp. 1763–1766, May 1996.
- [14] P. J. W. Melsa and R. C. Younce, “Joint impulse response shortening,” in *Proc. IEEE Global Telecommunications Conf.*, vol. 1, (London, UK), pp. 209–213, Nov. 1996.

- [15] N. Al-Dhahir and J. M. Cioffi, "Optimum finite-length equalization for multicarrier transceivers," *IEEE Trans. on Comm.*, vol. 44, pp. 56–63, Jan. 1996.
- [16] N. Al-Dhahir and J. Cioffi, "The combination of finite-length geometric equalization and bandwidth optimization for multicarrier transceivers," in *Proc. IEEE Int. Conf. Acoust., Speech, and Signal Processing*, vol. 2, (Detroit, MI), pp. 1201–1204, May 1995.
- [17] D. D. Falconer and F. R. Magee, "Adaptive channel memory truncation for maximum likelihood sequence estimation," *Bell System Technical J.*, vol. 52, pp. 1541–1562, Nov. 1973.
- [18] E. A. Lee and D. G. Messerschmitt, *Digital Communication*. Kluwer Academic Publishers, 1994.
- [19] N. Al-Dhahir and J. M. Cioffi, "Efficiently computed reduced-parameter input-aided MMSE equalizers for ML detection: A unified approach," *IEEE Trans. on Info. Theory*, vol. 42, pp. 903–915, May 1996.
- [20] M. Webster and R. Roberts, "Adaptive channel truncation for FFT detection in DMT systems - error component partitioning," in *Proc. IEEE Asilomar Conf. on Signals, Systems, and Computers*, vol. 1, (Pacific Grove, CA), pp. 669–673, Nov. 1997.
- [21] B. Wang and T. Adali, "A frequency-domain eigenfilter approach for equalization in discrete multitone systems," in *Proc. IEEE Asilomar Conf. on Signals, Systems, and Computers*, vol. 2, (Pacific Grove, CA), pp. 1058–1062, Nov. 1999.

- [22] B. Wang and T. Adalı, “Joint impulse response shortening for discrete multitone systems,” in *Proc. IEEE Global Telecommunications Conf.*, vol. 5, (Rio de Janeiro, Brazil), pp. 2508–2512, Dec. 1999.
- [23] B. Wang and T. Adalı, “Time-domain equalizer design for discrete multitone systems,” in *Proc. IEEE Int. Conf. Comm.*, vol. 2, (New Orleans, LA), pp. 1080–1084, June 2000.
- [24] B. Wang and T. Adalı, “A weighted frequency-domain least squares approach for equalization in discrete multitone systems,” in *Proc. IEEE Int. Conf. Comm.*, vol. 2, (New Orleans, LA), pp. 1054–1058, June 2000.
- [25] X. F. Wang, W.-S. Lu, and A. Antoniou, “Equalization for partially bandwidth-occupied multicarrier transceivers,” in *Proc. IEEE Pacific RIM Conf. on Comm., Computers, and Signal Processing*, (Victoria, BC), pp. 568–571, Aug. 1999.
- [26] J.-F. V. Kerckhove and P. Spruyt, “Adapted optimization criterion for FDM-based DMT-ADSL equalization,” in *Proc. IEEE Int. Conf. Comm.*, vol. 3, (Dallas, TX), pp. 1328–1334, June 1996.
- [27] K. V. Acker, G. Leus, M. Moonen, O. V. D. Wiel, and T. Pollet, “Per tone equalization for DMT receivers,” in *Proc. IEEE Global Telecommunications Conf.*, vol. 5, (Rio de Janeiro, Brazil), pp. 2311–2315, Dec. 1999.
- [28] K. V. Acker, G. Leus, M. Moonen, and T. Pollet, “Frequency domain equalization with tone grouping in DMT/ADSL-receivers,” in *Proc. IEEE*

- Asilomar Conf. on Signals, Systems, and Computers*, vol. 2, (Pacific Grove, CA), pp. 1067–1070, Nov. 1999.
- [29] J. C. Strait, “Performance enhanced adaptive equalizers for multicarrier channels,” in *Proc. Sym. on Circuits and Systems*, vol. 2, (Sacramento, CA), pp. 750–753, Aug. 1997.
- [30] M. Nafie and A. Gatherer, “Time-domain equalizer training for ADSL,” in *Proc. IEEE Int. Conf. Comm.*, vol. 2, (Montreal, Canada), pp. 1085–1089, June 1997.
- [31] G. H. Golub and C. F. V. Loan, *Matrix Computations*. Baltimore, MA: The Johns Hopkins University Press, 3 ed., 1996.
- [32] N. Lashkarian and S. Kiaei, “Fast algorithm for finite-length MMSE equalizers with application to discrete multitone modulation,” in *Proc. IEEE Int. Conf. Acoust., Speech, and Signal Processing*, vol. 5, (Phoenix, AR), pp. 2753–2756, Mar. 1999.
- [33] B. Farhang-Bouroujeny and M. Ding, “An eigen-approach to the design of near-optimum time domain equalizer for DMT transceivers,” in *Proc. IEEE Int. Conf. Comm.*, vol. 2, (Vancouver, Canada), pp. 937–941, June 1999.
- [34] B. Farhang-Bouroujeny and M. Ding, “Channel classification and time-domain equalizer design for ADSL transceivers,” in *Proc. IEEE Int. Conf. Comm.*, vol. 2, (New Orleans, LA), pp. 1059–1063, June 2000.

- [35] C. Yin and G. Yue, "Optimal impulse response shortening for discrete multitone transceivers," *IEE Electronics Letters*, vol. 34, pp. 35–36, Jan. 1998.
- [36] B. Wang, T. Adalı, Q. Liu, and M. Vlaynic, "Generalized channel impulse response shortening for discrete multitone transceivers," in *Proc. IEEE Asilomar Conf. on Signals, Systems, and Computers*, vol. 1, (Pacific Grove, CA), pp. 276–280, Nov. 1999.
- [37] W. Chiu, W. K. Tsai, T. C. Liau, and M. Troulis, "Time-domain channel equalizer design using the inverse power method," in *Proc. IEEE Int. Conf. Comm.*, vol. 2, (Vancouver, Canada), pp. 973–977, June 1999.
- [38] B. Lu, L. D. Clark, G. Arslan, and B. L. Evans, "Divide-and-conquer and matrix pencil methods for discrete multitone equalization," *IEEE Trans. on Signal Processing*, submitted.
- [39] J. M. Cioffi, *A Multicarrier Primer*. Amati Communication Corporation and Stanford University, T1E1.4/91-157, Nov. 1991.
- [40] N. Al-Dhahir and J. M. Cioffi, "Bandwidth-optimized reduced-complexity equalized multicarrier transceiver," *IEEE J. on Selected Areas in Comm.*, vol. 45, pp. 948–956, Aug. 1997.
- [41] W. H. Press, S. A. Teukolsky, W. T. Vetterling, and B. P. Flannery, *Numerical Recipes in C*. New York, NY: Cambridge University Press, 2 ed., 1992.



- [42] N. Lashkarian and S. Kiaei, "Optimum equalization of multicarrier systems via projection onto convex set," in *Proc. IEEE Int. Conf. Comm.*, vol. 2, (Vancouver, Canada), pp. 968–972, June 1999.
- [43] M. Milisavljevic and E. I. Verriest, "Fixed point algorithm for bit rate optimal equalization in multicarrier systems," in *Proc. IEEE Int. Conf. Acoust., Speech, and Signal Processing*, vol. 5, (Phoenix, AZ), pp. 2515–2518, Mar. 1999.
- [44] W. Y. Chen, *DSL Simulation Techniques and Standards Development for Digital Subscriber Line Systems*. Indianapolis, Indiana: McMillan Technical Publishing, 1998.
- [45] N. Al-Dhahir, A. H. Sayed, and J. M. Cioffi, "Stable pole-zero modeling of long FIR filters with application to the MMSE-DFE," *IEEE J. on Selected Areas in Comm.*, vol. 45, pp. 508–513, May 1997.
- [46] G. Arslan, B. L. Evans, and S. Kiaei, "Equalization for discrete multi-tone transceivers to maximize channel capacity," *IEEE Trans. on Signal Processing*, submitted.
- [47] P. S. Chow, J. M. Cioffi, and J. A. C. Bingham, "A practical discrete multitone transceiver loading algorithm for data transmission over spectrally shaped channels," *IEEE J. on Selected Areas in Comm.*, vol. 43, pp. 773–775, Feb./Mar./Apr 1995.
- [48] K.-I. Kum, J. Kang, and W. Sung, "AUTOSCALAR for C: An optimizing floating-point to integer C program converter for fixed-point digital signal

- processors,” *IEEE Trans. on Circuits and Systems II– Analog and Digital Signal Processing*, vol. 47, pp. 840–848, Sept. 2000.
- [49] I. Djokovic, “Cyclic prefix extension in DMT systems,” in *Proc. IEEE Asilomar Conf. on Signals, Systems, and Computers*, vol. 1, (Pacific Grove, CA), pp. 65–69, Nov. 1998.
- [50] D. Pal, G. N. Iyengar, and J. Cioffi, “A new method of channel shortening with application to discrete multi tone (DMT) systems,” in *Proc. IEEE Int. Conf. Comm.*, vol. 2, (Atlanta, GA), pp. 763–768, June 1998.
- [51] I. Djokovic, “MMSE equalizers for DMT systems with and without crosstalk,” in *Proc. IEEE Asilomar Conf. on Signals, Systems, and Computers*, vol. 1, (Pacific Grove, CA), pp. 545–549, Nov. 1998.
- [52] ADSL Forum TR-001, “ADSL forum system reference model,” 1996. ADSL Forum System Reference Model.
- [53] ADSL Forum TR-003, “Framing and encapsulation standards for ADSL: Packet mode,” 1997. ADSL Forum System Reference Model.
- [54] ADSL Forum TR-007, “Interfaces and system configurations for ADSL: Customer premises,” 1998. ADSL Forum System Reference Model.
- [55] I. Lee, J. S. Chow, and J. M. Cioffi, “Performance evaluation of a fast computation algorithm for the DMT in high-speed subscriber loop,” *IEEE J. on Selected Areas in Comm.*, vol. 13, pp. 1564–1570, Dec. 1995.
- [56] S. V. Ahamed, P. L. Gruber, and J.-J. Werner, “Digital subscriber line (HDSL and ADSL) capacity of the outside loop plant,” *IEEE J. on Selected Areas in Comm.*, vol. 13, pp. 1540–1549, Dec. 1995.

- [57] J. S. Chow, J. C. Tu, and J. M. Cioffi, "A computationally efficient adaptive transceiver for high-speed digital subscriber lines," in *Proc. IEEE Int. Conf. Comm.*, vol. 4, (Atlanta, GA), pp. 1750–1754, Apr. 1990.
- [58] J. T. Aslanis and J. M. Cioffi, "Capacity and cutoff rate of the digital subscriber loop with near end crosstalk noise," in *Proc. IEEE Int. Conf. Comm.*, vol. 2, (Boston, MA), pp. 1075–1079, June 1989.
- [59] J. C. Tu, J. S. Chow, G. P. Dudevoir, and J. M. Cioffi, "Crosstalk-limited performance of a computationally efficient multichannel transceiver for high rate digital subscriber lines," in *Proc. IEEE Global Telecommunications Conf.*, vol. 3, (Dallas, TX), pp. 1940–1944, Nov. 1989.
- [60] P. S. Chow, J. C. Tu, and J. M. Cioffi, "Performance evaluation of a multichannel transceiver system for ADSL and VHDSL services," *IEEE J. on Selected Areas in Comm.*, vol. 9, pp. 909–919, Aug. 1991.
- [61] P. S. Chow, J. C. Tu, and J. M. Cioffi, "A multichannel transceiver system for asymmetric digital subscriber line service," in *Proc. IEEE Global Telecommunications Conf.*, vol. 3, (Phoenix, AR), pp. 1992–1996, Dec. 1991.
- [62] ADSL Forum TR-009, "Channelization for DMT and CAP ADSL line codes: Packet mode," 1998. ADSL Forum System Reference Model.
- [63] K. Sistanizadeh, *Study of the Feasibility and Advisability of Digital Subscriber Lines Operating at Rates Substantially in Excess of the Basic Access Rate*. Bellcore, T1E1.4 Technical Subcommittee Working Group T1E1.4/92-026, Feb. 1992.

- [64] W. Walkoe and T. J. J. Starr, "High bit rate digital subscriber line: A copper bridge to the network of the future," *IEEE J. on Selected Areas in Comm.*, vol. 9, pp. 765–768, Aug. 1991.
- [65] J.-J. Werner, "The HDSL environment," *IEEE J. on Selected Areas in Comm.*, vol. 9, pp. 785–800, Aug. 1991.
- [66] J. T. Aslanis, Jr., and J. M. Cioffi, "Achievable information rates on digital subscriber loops: Limiting information rates with crosstalk noise," *IEEE Trans. on Comm.*, vol. 40, pp. 361–372, Feb. 1992.
- [67] J. A. C. Bingham, *Design of Multitone Transceivers*. Amati Communication Corporation, T1E1.4 Technical Subcommittee Working Group T1E1.4/92-198, Dec. 1992.
- [68] K. Sistanizdeh, P. S. Chow, and J. M. Cioffi, "Multi-tone transmission for asymmetric digital subscriber lines (ADSL)," in *Proc. IEEE Int. Conf. Comm.*, vol. 2, (Geneva, Switzerland), pp. 756–760, May 1993.
- [69] P. S. Chow, J. M. Cioffi, and J. A. C. Bingham, "DMT-based ADSL: Concept, architecture, and performance," in *IEE Colloquium on High Speed Access Technology And Services, Including Video-On-Demand*, (London, UK), pp. 3/1–3/6, Oct. 1994.
- [70] I. Kalet, "The multitone channel," *IEEE Trans. on Comm.*, vol. 37, pp. 119–124, Feb. 1989.
- [71] N. Al-Dhahir and J. M. Cioffi, "Optimum finite-length equalization for multicarrier transceivers," in *Proc. IEEE Global Telecommunications Conf.*, vol. 3, (San Francisco, CA), pp. 1884–1888, Nov. 1994.

- [72] H. V. D. Velde, T. Pollet, and M. Moeneclaey, "Effect of cable and system parameters on passband ADSL performance," *IEEE Trans. on Comm.*, vol. 43, pp. 1248–1251, Feb./Mar./Apr. 1995.
- [73] T. N. Zogakis and J. M. Cioffi, "The effect of timing jitter on the performance of a discrete multitone system," *IEEE Trans. on Comm.*, vol. 44, pp. 799–808, July 1996.
- [74] B. R. Saltzberg, "Comparison of single-carrier and multitone digital modulation for ADSL applications," *IEEE Comm. Magazine*, vol. 36, pp. 114–121, Nov. 1998.
- [75] A. Leke and J. M. Cioffi, "Multicarrier systems with imperfect channel knowledge," in *Proc. IEEE Int. Sym. Personal, Indoor and Mobile Radio Comm.*, vol. 2, (Boston, MA), pp. 549–553, Sept. 1998.
- [76] B. S. Krongold, K. Ramchandran, and D. L. Jones, "Computationally efficient optimal power allocation algorithm for multicarrier communication systems," in *Proc. IEEE Int. Conf. Comm.*, vol. 2, (Atlanta, GA), pp. 1018–1022, June 1998.
- [77] A. Leke and J. M. Cioffi, "Impact of imperfect channel knowledge on the performance of multicarrier systems," in *Proc. IEEE Global Telecommunications Conf.*, vol. 2, (Sydney, Australia), pp. 951–955, Nov. 1998.
- [78] B. S. Krongold, K. Ramchandran, and D. L. Jones, "Computationally efficient optimal power allocation algorithms for multicarrier communication systems," *IEEE Trans. on Comm.*, vol. 48, pp. 23–27, Jan. 2000.

- [79] M. Hawryluck, A. Yongacoglu, and M. Kavehrad, "Simulation of a FFT based multi-carrier system for ADSL and VDSL transmission," in *Proc. IEEE Sym. Computers and Comm.*, vol. 2, (Atlanta, GA), pp. 537–542, June 1998.
- [80] D. Veithen, P. Spruyt, T. Pollet, M. Peeters, S. Braet, O. V. de Wiel, and H. V. D. Weghe, "A 70 Mb/s variable-rate DMT-based modem for VDSL," in *Proc. IEEE Int. Solid-State Circuits Conf.*, vol. 42, (San Francisco, CA), pp. 248–249, Feb. 1999.
- [81] X. Wang and K. J. R. Liu, "Adaptive channel estimation using cyclic prefix in multicarrier modulation system," *IEEE Comm. Letters*, vol. 10, pp. 291–293, Oct. 1999.
- [82] J. M. Cioffi, "Very high-speed digital subscriber lines (VDSL)," in *Proc. IEEE Int. Sym. Circuits and Systems*, vol. 2, (Monterey, CA), pp. 590–594, May 1998.
- [83] J. M. Cioffi, V. Oksman, J.-J. Werner, T. Pollet, P. M. P. Spruyt, C. Jacky S., and K. S. Jacobsen, "Very-high-speed digital subscriber lines," *IEEE Comm. Magazine*, vol. 37, pp. 72–79, Apr. 1999.
- [84] J. Fijoleck, M. Kuska, V. C. Majeti, and K. Sriram, *Cable Modems: Current Technologies and Applications*. Piscataway, NJ: IEEE Press, 1999.
- [85] N. M. W. Al-Dhahir, *Optimized-Transmitter Reduced-Complexity MMSE-DFE Under Finite-Length Constraints*. PhD thesis, Stanford University, Stanford, CA, June 1994.

- [86] J. Dixon, G. Beene, and R. Baker, *ADSL Line Interface Issues: Design, Simulation, and Lab Measurements*. Bellcore, T1E1.4 Technical Subcommittee Working Group T1E1.4/92-152, Aug. 1992.
- [87] J. Cioffi, J. Aslanis, and M. Ho, *Performance of Enhanced (6 Mbps) ADSL*. Amati Communication Corporation, T1E1.4 Technical Subcommittee Working Group T1E1.4/92-205, Dec. 1992.
- [88] K. Maxwell and J. Bingham, *Why DMT Should be Chosen for ADSL Now*. Amati Communication Corporation, T1E1.4 Technical Subcommittee Working Group T1E1.4/93-018, Mar. 1993.
- [89] R. Gross and D. Veeneman, *Measured Performance of the Amati-Northern Telecom ADSL II System Operating at 6.3 Mb/s*. GTE Laboratories, Inc., T1E1.4 Technical Subcommittee Working Group T1E1.4/93-048, Mar. 1993.
- [90] J. M. Cioffi, J. S. Chow, and J. T. Aslanis, *Detailed DMT Transmitter Description for ADSL*. Amati Communication Corporation, T1E1.4 Technical Subcommittee Working Group T1E1.4/93-084, Apr. 1993.
- [91] J. M. Cioffi and J. S. Chow, *Recommended Training Sequence for SNR Computation for DMT ADSL*. Amati Communication Corporation, T1E1.4 Technical Subcommittee Working Group T1E1.4/93-087, Apr. 1993.
- [92] J. A. C. Bingham and P. S. Chow, *Recommended Procedures for Exchange of DMT Loading Information in ADSL*. Amati Communication Corpo-

- ration, T1E1.4 Technical Subcommittee Working Group T1E1.4/93-088, Apr. 1993.
- [93] N. Knudsen, *Proposed Parameters for the Characterization of Test Loops*. Consultronics Ltd., T1E1.4 Technical Subcommittee Working Group T1E1.4/93-132, May 1993.
- [94] M. Elder, *Effects of NEXT and FEXT in the Same Cable*. Northern Telecom Inc., T1E1.4 Technical Subcommittee Working Group T1E1.4/93-220, Aug. 1993.
- [95] J. A. C. Bingham and E. Arnon, *ADSL Performance in the Presence of T1 NEXT and Vice Versa*. Amati Communication Corporation, T1E1.4 Technical Subcommittee Working Group T1E1.4/93-248, Oct. 1993.
- [96] R. A. McDonald, *Performance Margin Issues in DSLs*. Bellcore, T1E1.4 Technical Subcommittee Working Group T1E1.4/95-133, Nov. 1995.
- [97] D. C. Jones, *Achievable Downstream Rates over Distribution Area Loops Using Remotely-Deployed ATU-Cs*. US WEST Advanced Technologies, T1E1.4 Technical Subcommittee Working Group T1E1.4/95-135, Nov. 1995.



# Vita

Güner Arslan was born in Pinneberg, Germany in 1973. He moved to his home country, Turkey, in 1984. He graduated from a business high school (Bakırkoy Ticaret Lisesi) where he decided to become an electrical engineer. He graduated as Valedictorian with B.S. in Electronics and Telecommunication Engineering degree from Yıldız University at Kocaeli, Kocaeli, Turkey in July 1994. He joined the Dept. of Electronics and Telecommunication Engineering of Yıldız Technical University in Istanbul as a Research Assistant in 1995 where he worked on DTMF detection, stereophonic acoustic echo cancellation, SAR image processing, and speech recognition. He received his MS in Electronics and Telecommunication Engineering from Yıldız Technical University, Istanbul, Turkey in July 1996.

While taking classes for his Ph.D. at Yıldız Technical University he received a full scholarship from the Turkish Government in 1998 to continue his graduate education abroad. He received his Ph.D.E.E degree in the area of Telecommunications and Information Systems Engineering from The Dept. of Electrical and Computer Engineering at the University of Texas at Austin, Austin, TX. His current research interests are digital signal processing for communications, audio/speech applications, and learning systems (neural net-

works, genetic algorithms, adaptive filters).

Permanent Address: Kazim Karabekir Mah. 1. Cad. No:51/8  
34600 Esenler, Istanbul, TURKEY

This dissertation was typeset with L<sup>A</sup>T<sub>E</sub>X 2<sub>ε</sub><sup>1</sup> by the author.

---

<sup>1</sup>L<sup>A</sup>T<sub>E</sub>X 2<sub>ε</sub> is an extension of L<sup>A</sup>T<sub>E</sub>X. L<sup>A</sup>T<sub>E</sub>X is a collection of macros for T<sub>E</sub>X. T<sub>E</sub>X is a trademark of the American Mathematical Society. The macros used in formatting this dissertation were written by Dinesh Das, Department of Computer Sciences, The University of Texas at Austin.